



저작자표시-비영리-변경금지 2.0 대한민국

이용자는 아래의 조건을 따르는 경우에 한하여 자유롭게

- 이 저작물을 복제, 배포, 전송, 전시, 공연 및 방송할 수 있습니다.

다음과 같은 조건을 따라야 합니다:



저작자표시. 귀하는 원저작자를 표시하여야 합니다.



비영리. 귀하는 이 저작물을 영리 목적으로 이용할 수 없습니다.



변경금지. 귀하는 이 저작물을 개작, 변형 또는 가공할 수 없습니다.

- 귀하는, 이 저작물의 재이용이나 배포의 경우, 이 저작물에 적용된 이용허락조건을 명확하게 나타내어야 합니다.
- 저작권자로부터 별도의 허가를 받으면 이러한 조건들은 적용되지 않습니다.

저작권법에 따른 이용자의 권리는 위의 내용에 의하여 영향을 받지 않습니다.

이것은 [이용허락규약\(Legal Code\)](#)을 이해하기 쉽게 요약한 것입니다.

[Disclaimer](#)

공학석사 학위논문

Control of Corrosion and Biofouling in Seawater Pipe

해수 배관 내부의 부식 및 생물오손 제어에 관한 연구



지도교수 정진아

2019년 2월

한국해양대학교 대학원
기관시스템공학과

김문수

본 논문을 김문수의 공학석사 학위논문으로 인준함

위원장 : 이 명 훈



위원 : 윤 용 섭



위원 : 정 진 아



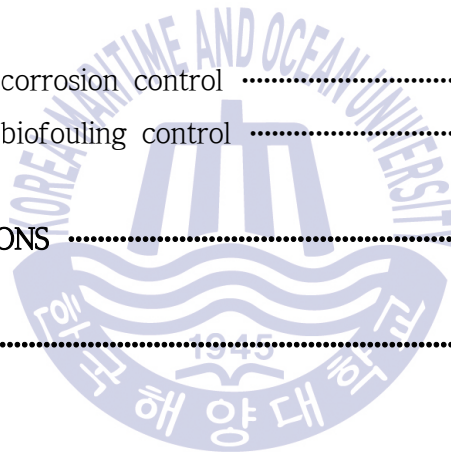
2018 년 12 월 20 일

한국해양대학교 대학원

TABLE OF CONTENTS

Table of Contents	i
List of Tables	iii
List of Figures	iv
Abstract	xi
Chapter I INTRODUCTION	1
1.1 Study background and objective	1
1.2 Study contents	3
Chapter II LITERATURE REVIEW	4
2.1 Corrosion	4
2.1.1 Background theory	4
2.1.2 Corrosion control in seawater	22
2.1.3 Review of previous study on corrosion control in seawater pipe	29
2.2 Biofouling	33
2.2.1 Background theory	33
2.2.2 Biofouling control	36
2.2.3 Review of previous study on biofouling control by electrochlorination	44
2.3 Technology to control corrosion and biofouling	50
2.3.1 Current technology to control corrosion and biofouling	50
2.3.2 Hybrid technology for cathodic protection and electrochlorination	53

Chapter III EXPERIMENTAL METHOD	54
3.1 Test outlines	54
3.2 Laboratory tests	55
3.2.1 Materials and specimens	55
3.2.2 Test apparatus	58
3.2.3 Procedures	62
3.3 Field test	67
 Chapter IV RESULTS & DISCUSSION	 75
4.1 Test results of corrosion control	75
4.2 Test results of biofouling control	104
 Chapter V CONCLUSIONS	 112
 References	 114



List of Tables

Table 2.1	Potential of reference electrodes compared with SHE	10
Table 2.2	Selected dissolved materials in 3.5 ‰ seawater	23
Table 2.3	Electric resistance of seawater with temperature	24
Table 2.4	Comparison of the pros and cons for ICCP and SACP	26
Table 2.5	Characteristic according to free and total chlorine measuring method	41
Table 2.6	Comparison of common analytical methods for free and total chlorine in water	42
Table 2.7	Ratings of common chlorine analytical methods vs. the ideal method	42
Table 2.8	Effect of chlorination on inactivating selected bacteria	45
Table 2.9	Effect of chlorination on inactivating selected protozoa	45
Table 2.10	Mortality of adult and juvenile zebra mussels exposed to continuous low-level chlorination	49
Table 3.1	Chemical composition of specimen	55
Table 3.2	Symbol list of electrochemical polarization test according to conditions	62
Table 3.3	Experimental set up of electrochemical polarization test	63
Table 3.4	Experimental set up of cathodic protection test in beaker	64
Table 3.5	Experimental set up of cathodic protection test in cistern	66
Table 3.6	Arrangement of installed specimen and anode	66
Table 3.7	Specification of chlorine sensor	73
Table 3.8	Experimental set up of cathodic protection and electrochlorination	74

List of Figures

Fig. 2.1	The corrosion cycle of steel	4
Fig. 2.2	Coupled electrochemical reactions occurring at different sites on the same metal surface	6
Fig. 2.3	Anodic and cathodic reactions between steel and copper in seawater	8
Fig. 2.4	Summary diagram of standard hydrogen electrode	10
Fig. 2.5	Graphical scheme to compare potentials of the most commonly used reference electrodes	11
Fig. 2.6	Half-cell reaction existing simultaneously on the surface of zinc	14
Fig. 2.7	Polarization of half-cell of zinc in the acid solution	14
Fig. 2.8	Experimental set-up to measure the corrosion potential of a specimen	15
Fig. 2.9	Schematic representation of anodic polarization for an anode	17
Fig. 2.10	Schematic representation of cathodic polarization for a cathode	18
Fig. 2.11	Activation polarization curve for the anodic reaction of iron and ferrous ions	20
Fig. 2.12	Activation polarization curve for the cathodic reaction of hydrogen ions and hydrogen gas	20
Fig. 2.13	Combined diagram of an anodic reaction and a cathodic reaction with activation polarization	21

Fig. 2.14	Major dissolved components in seawater	22
Fig. 2.15	Graph for calculation of seawater resistivity as a function of salinity and temperature	24
Fig. 2.16	Pourbaix diagram of iron in seawater	26
Fig. 2.17	Typical polarization curve of ICCP	28
Fig. 2.18	Typical polarization curve of SACP	28
Fig. 2.19	Cathodic polarization results of specimen in seawater with and without agitation	30
Fig. 2.20	Galvanostatic polarization results of specimen in seawater without agitation	30
Fig. 2.21	Test results of cathodic protection current measurement flowed from a ribbon type MMO anode to the specimens by setting potentials	32
Fig. 2.22	Test results of cathodic protection current measurement in comparison of the galvanic corrosion test	32
Fig. 2.23	Different phases of marine biofouling: Time-line evolution and respective roughness increase	35
Fig. 2.24	Biofouling process and the formation of biofilm	35
Fig. 2.25	Diagram of anti-biofouling strategy/technology	37
Fig. 2.26	Principle of hypochlorous acid generation	40
Fig. 2.27	Graph of available chlorine present as HClO varying with pH value	40
Fig. 2.28	Pocket colorimeter and Test kit	43
Fig. 2.29	The results of pathogen culture for each solution	44
Fig. 2.30	Effect of chlorine concentration and exposure time on the growth of mono-species (Amphora and Navicula) and natural biofilms	47

Fig. 2.31 Effect of chlorine concentration and exposure time on concentration of chlorophyll ‘a’ in mono-species and natural biofilms	47
Fig. 2.32 Principle of the ICCP for ship’ s hull corrosion protection	50
Fig. 2.33 Schematic drawing of the MGPS	51
Fig. 2.34 Schematic piping diagram of the chlorination type MGPS	52
Fig. 2.35 Schematic piping diagram of hybrid technology for cathodic protection and HClO generation	53
Fig. 3.1 Photograph and schematic diagram of specimen for electrochemical polarization test	56
Fig. 3.2 Photograph and schematic diagram of carbon steel specimen for cathodic protection test in the beaker	56
Fig. 3.3 Photograph and schematic diagram of specimen for cathodic protection test in the cistern	57
Fig. 3.4 Test apparatus for electrochemical polarization test, (a): Schematic diagram, (b): Overall appearance	58
Fig. 3.5 Test apparatus for cathodic protection in the beaker, (a): Schematic diagram, (b): Overall appearance	59
Fig. 3.6 Test apparatus for cathodic protection in the cistern, (a): Schematic diagram, (b): Overall appearance	60
Fig. 3.7 Drawing of cistern for cathodic protection test in the cistern	61
Fig. 3.8 Auxiliary test apparatus for cathodic protection in the cistern, (a): Silver-silver/chlorine electrode, (b): Rod type MMO anode	61
Fig. 3.9 Pipe specimens for cathodic protection and electrochlorination, (a): Pipe with flange, (b): Insulation flange with hole, (c): Elbow with flange	68

Fig. 3.10 Schematic diagram and appearance of anode installed in the pipe	68
Fig. 3.11 Configuration of test apparatus connected to seawater pipe in engine room of T/S Hanbada	69
Fig. 3.12 Photograph of test apparatus for cathodic protection and electrochlorination, (a): Appearance of pipe, (b): Appearance of flexible hose connected with seawater pipe	70
Fig. 3.13 Auxiliary test apparatus for cathodic protection and electrochlorination, (a): Flow meter for measuring flow rate, (b): Power supply for cathodic protection and electrochlorination, (c): Fluke multi meter, (d): Portable chlorine tester made by Hach	71
Fig. 3.14 Appearance of free chlorine meter	72
Fig. 3.15 Photograph and schematic diagram of chlorine sensor	72
Fig. 4.1 Polarization resistance test results of carbon steel specimen in fresh water and seawater with the range of ± 20 mV/SSCE ..	75
Fig. 4.2 Comparison of corrosion rate and corrosion current density calculated from polarization resistance test result in fresh water and seawater, (a): Corrosion rate, (b): Corrosion current density	77
Fig. 4.3 Variation of anodic polarization as a function of different solutions and temperatures	78
Fig. 4.4 Variation of cathodic polarization as a function of different solutions and temperatures	80
Fig. 4.5 Polarization curve for carbon steel specimens as a function of different solutions and temperatures	80

Fig. 4.6 Variation of potentiostatic polarization as a function of various environments of fresh water	81
Fig. 4.7 Variation of potentiostatic polarization as a function of various environments of seawater	82
Fig. 4.8 Variation of potentiostatic polarization as a function of fresh water and seawater in different flow rates and temperatures ..	83
Fig. 4.9 Variation curves of open-circuit potential with time and different solutions and flow rates	86
Fig. 4.10 Current density maintaining $-1,100$ mV/SSCE for 7 days in each condition of the beaker	86
Fig. 4.11 Comparison of photographs between corroded specimens and protected specimens in different solutions and flow rates for 7 days	88
Fig. 4.12 Macro-photographs of protected specimens' surface in each condition over time	89
Fig. 4.13 Macro-photographs of corroded and protected specimen after scrubbing in fresh water with different flows	90
Fig. 4.14 Current density maintaining $-1,100$ mV/SSCE for 7 days in general corrosion condition	93
Fig. 4.15 Current density maintaining $-1,100$ mV/SSCE for 7 days in galvanic corrosion condition	93
Fig. 4.16 Comparison of photographs between corroded specimens and protected specimens in fresh water without flow	95
Fig. 4.17 Comparison of photographs between corroded specimens and protected specimens in fresh water with flow	96
Fig. 4.18 Macro-photographs of corroded and protected specimen after test in fresh water with different flows	97

Fig. 4.19	Comparison of photographs between corroded specimens and protected specimens in seawater without flow	99
Fig. 4.20	Comparison of photographs between corroded specimens and protected specimens in seawater with flow	100
Fig. 4.21	Macro-photographs of corroded and protected specimen after test in seawater with different flows	101
Fig. 4.22	Current density at each cathodic protection potential in various flow rates	102
Fig. 4.23	Comparison of photographs between pipes after test, (a): Protected pipe, (b): Partially protected pipe, (c): Corroded pipe	103
Fig. 4.24	Test results of cathodic protection current and HClO concentration as a function of cathodic protection potential setting	104
Fig. 4.25	Test results of total applied current and HClO concentration at -1,200 mV/SSCE of cathodic protection potential in 3 m ³ /h ..	107
Fig. 4.26	Test results of total applied current and HClO concentration at -1,200 mV/SSCE of cathodic protection potential in 6 m ³ /h ..	107
Fig. 4.27	Test results of total applied current and HClO concentration at -1,200 mV/SSCE of cathodic protection potential in 15 m ³ /h ..	108
Fig. 4.28	Comparisons of total applied current and HClO concentration at -1,200 mV/SSCE of cathodic protection potential in each flow rate	108
Fig. 4.29	Difference of concentration between DPD and FCL calibrated at 0.5 mg/L	110

Fig. 4.30 Difference of concentration between DPD and FCL
calibrated at 2.0 mg/L110

Fig. 4.31 Difference of concentration between DPD and FCL
calibrated at 4.0 mg/L111



해수 배관 내부의 부식 및 생물오손 제어에 관한 연구

김문수

한국해양대학교 대학원
기관시스템공학과

초록

최근 기술의 발달로 해양 관련 산업은 급속한 성장을 거듭하고 있다. 이에 따라 선박, 해양플랜트 및 발전소와 같은 설비는 고부가가치화, 장수명화가 요구되고 있다. 이러한 설비들은 운항 및 시스템 가동을 위해서 해수를 냉각수로 사용하고 있기 때문에 배관 내부에 부식문제와 해양생물의 번식에 의한 냉각 불량 문제가 생긴다. 부식과 해양생물의 번식이 냉각계통에 영향을 미치면 결과적으로 선박의 운항 불능, 플랜트 설비의 시스템 중단과 같은 사태가 발생한다. 그럼에도 불구하고, 해수 배관 내면에서의 방지 및 방오 기술과 관련된 연구개발은 미비한 상태이다. 배관 내면의 부식방지 기술에는 코팅하는 방법이 사용되고 있으나, 이는 결함이 생기면 부식이 진행되는 것을 막을 수 없다. 또한 해양생물의 번식 억제 기술로 해수 전해설비를 사용하고 있으나 비전문가에 의해 운용되어 전류량에 따라 해양생물의 번식을 억제하지 못해 냉각관이 막히거나 고농도의 배출수에 의해 배수구 주변 생태계가 파괴되는 문제가 발생하고 있다. 따라서 배관 내면의 부식을 예방함과 동시에 해양생물의 부착을 억제하기 위한 연구개발이 필요한 상황이다.

본 연구에서는 음극 방지와 해수 전해를 배관 내면에 적용하여 배관 내부에서 발생하는 부식을 막고, 동시에 해양생물을 사멸하는 산화제인 차아염소산의

농도를 조절하는 실험을 수행하였다.

배관 내면의 음극 방식 실험결과 청수보다 해수에서, 정지중인 환경보다 유속이 존재하는 환경에서 높은 방식 전류가 공급되었고 탄소강 시험편과 배관의 표면 확인 시, 방식을 시행한 시험편은 표면의 보호가 이루어짐을 확인하였다. 음극방식을 하면서 만들어지는 차아염소산 농도의 측정 결과, 낮은 방식전위를 유지할 수록 방식전류에 의해 생성되는 차아염소산 농도가 증가하는 것을 확인하였다. 또한, 해수전해설비에서 전류를 추가적으로 제어할 경우 해양생물을 사멸시킬 수 있는 차아염소산 농도범위로 조절이 가능함을 확인하였다.

KEY WORDS : 부식; 음극방식; 해수전해; 차아염소산; 생물오손



Control of Corrosion and Biofouling in Seawater Pipe

Mun Su, Kim

*Department of Marine System Engineering
Graduate School of Korea Maritime and Ocean University*

Abstract

In the present-day society, with the emergence of sophisticated technologies, shipbuilding and marine industries have been developed in a rapid and broad manner. This requires that ships and marine structures, such as offshore plants and power plants have not only high value, but also a long life-expectancy. In the case of the marine infrastructures including vessels, their system should be obligatorily cooled to navigate vessels and operate facilities in order to avoid system being overheated. Therefore, most facilities have used seawater as coolant. However, along with the advantages of using seawater as coolant, such as cost-efficiency and resource abundance, there are also disadvantages, including corrosion and biofouling. Thus, in the field of vessels and energy plants, a disaster-defined as the inability to navigate, stop of generating power, and malfunction of plant facility-could occur either due to poor cooling or pitting caused by corrosion.

Nevertheless, what aggravates the situation is that an effective and efficient technique that would enable control of corrosion and biofouling in seawater pipes is still lacking. Among relevant pipeline corrosion protection technologies, there is the method that is the inner surface coating of the

pipe. However, the shortcoming of this method is that it is no longer effective when the coated surface is cracked. In addition, in thermal power and nuclear plants, a widely used technique that enables restricting the growth of marine organisms is electrochlorination. However, the limitation of this technique is that it is manually operated and adjusted by non-experts. Depending on the amount of current, marine organisms would evolve too much in the pipe or HClO produced by electrochlorination devastates ecosystem. In this context, it is obvious that a thorough investigation of effective ways to control corrosion and biofouling in seawater pipes is urgently needed.

In the present study, cathodic protection and electrochlorination were experimentally tested for their effectiveness in the control of corrosion and biofouling.

As a result of the cathodic protection in the pipes, when inspecting the surface of specimen and pipe, we observed that the studied specimens were properly protected. Furthermore, as shown by the results of measuring hypochlorous acid produced by electrochlorination, the lower cathodic protection potential was maintained, the higher increase of the HClO concentration was observed. In addition, when adjusting additional current in the electrochlorination facility, we were also able to adjust the total HClO concentration, which could decimate marine organisms. From these results, we observe that the control of corrosion and biofouling would be possible by using cathodic protection and electrochlorination.

KEY WORDS : Corrosion; Cathodic protection; Electrochlorination;

Hypochlorous acid(HClO); Biofouling

Chapter I

INTRODUCTION

1.1 Study background and objective

In the present-day society, with the emergence of sophisticated technologies, shipbuilding and marine industries have been developed in a rapid and broad manner. This requires that ships and marine structures, such as offshore plants and power plants have not only high value, but also a long life-expectancy. In the case of the marine infrastructures including vessels, their system should be obligatorily cooled to navigate vessels and operate facilities in order to avoid system being overheated. Therefore, most facilities have used seawater as coolant. However, along with the advantages of using seawater as coolant, such as cost-efficiency and resource abundance, there are also disadvantages, including corrosion and biofouling. Specifically, corrosion accelerates damage in pipes, which leads to unexpected and frequent leaks. With regard to biofouling, it causes rapidly evolving blocks in the cooling system.

In the field of vessels and energy plants, a disaster—defined as the inability to navigate, stop of generating power, and malfunction of plant facility—could occur either due to poor cooling or pitting caused by corrosion. If a plant system ceases its operation, there is a risk of explosion caused by the increase of the boiler steam pressure and the difficulty to acquire a power source because of the stop of power generation. Furthermore, in the case of vessels, a dramatic accident can occur due to the loss of propulsion. Consequently, economic and social losses needed to recover the system are astronomical¹⁾.

From the past accidents, there are three representative cases of pipe damage by corrosion: (1) the accident at Ul-jin nuclear station in Dec, 1988; (2) the accident at Han-bit nuclear station in 2012; and (3) the accident at Wol-sung nuclear station in Jun, 2013. In all these accidents, the underlying reason was corrosion in the pipes. Similar cases have also occurred abroad: for instance, in 2004, an accident occurred at the MIHAMA nuclear station in Japan, and the reason was the seawater pipe being fractured by corrosion. As a result of this accident, four persons died, and five persons got severe injuries²⁾. With regard to biofouling, the experience of Marchwood (Southampton) showed that between 1957 and 1964, 4000 condenser tubes failed due to mussel fouling leading to leakage. Apart from the loss of generation, these leaks contaminated the feed water system and accelerated boiler water side corrosion, resulting in a failure of the boiler tube. In addition, an analysis of all tube failures at Kansai Electric Power Corporation (Japan) in 1982 and 1983 showed that 94 % of all tube failures were related to macro-fouling in the tubes³⁾. Despite the devastating consequences of such incidents, corrosion and biofouling in the cooling system of energy plants, vessels, and marine structures continue to be reported⁴⁾.

Nevertheless, what aggravates the situation is that an effective and efficient technique that would enable control of corrosion and biofouling in seawater pipes is still lacking. Among relevant pipeline corrosion protection technologies, there is the method of coating of the surface of the pipe. However, the shortcoming of this method is that it is no longer effective when the coated surface is cracked. In addition, in thermal power and nuclear plants, a widely used technique that enables restricting the growth of marine organisms is electrochlorination. However, the limitation of this technique is that it is manually operated and adjusted by non-experts. Therefore, if the current is too low, marine organisms would evolve too much in the cooling system. This phenomenon results in blocking of the cooling pipe. By contrast, if the current is

too high, fishes and shellfishes living near the discharge port of the cooling water would die. In this context, it is obvious that a thorough investigation of effective ways to control corrosion and biofouling in seawater pipe is urgently needed.

In the present study, cathodic protection and electrochlorination were experimentally tested for their effectiveness in the control of corrosion and biofouling. The major objective of this study was to achieve simultaneous and full control of corrosion and biofouling in seawater pipe.

1.2 Study contents

The remainder of this present thesis is structured as follows.

- (1) Study background and objectives are described in Chapter I .
- (2) The corrosion and biofouling control theory and relevant literature are reviewed in Chapter II .
- (3) Specimens, test apparatus, and experimental procedures for cathodic protection and electrochlorination are described in Chapter III .
- (4) The results of testing the effectiveness of cathodic protection and electrochlorination in various environments are reported in Chapter IV .
- (5) Conclusions and outlined directions of further research are drawn in Chapter V .

Chapter II

LITERATURE REVIEW

2.1 Corrosion

2.1.1 Background theory

Corrosion is a natural phenomenon. Just like water flows to the lowest level, all natural process tend toward the lowest possible energy states. For instance, iron and steel have a natural tendency to combine with other chemical elements to return to their lowest energy states. In order to return to their lowest energy states, iron and steel frequently combine with oxygen and water, both of which are present in the most natural environments, to form hydrated iron oxides (rust), similar in chemical composition to the original iron ore. Corrosion life cycle of a steel product is shown in Fig 2.1⁵⁾. Like this, corrosion is the destructive results of chemical reactions between metal or metal alloy and their environments⁶⁾.

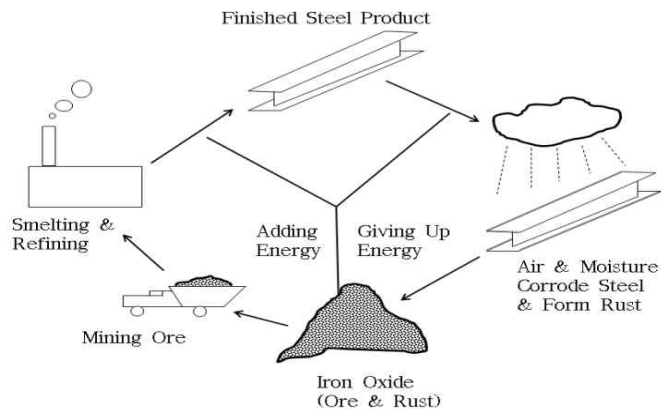


Fig 2.1 The corrosion cycle of steel

Corrosion of the metal in solution environments is proceeded by electrochemical reactions. Surface of metal which occur corrosion reaction act as mixed electrode and its couple of metal play a role as both anodic and cathodic reaction. At local anode site, oxidation reaction is occurred and metal atom is dissolved into solution in a form of ferrous ions. Liberated electrons move from anode to cathode and reduction reaction is occurred at local cathode site by consuming electrons. In corrosion reaction, the most general example of both anodic and cathodic reaction is as follows.

Anodic reaction:



Cathodic reaction:

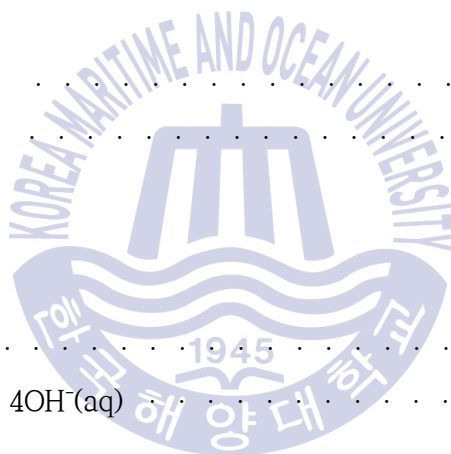


Fig 2.2 illustrates behavior for an iron surface immersed in acidic aqueous environment. At certain sites on the iron surface, iron atoms pass into solution as Fe^{2+} ions. The two electrons produced by this anodic half-cell reaction are consumed elsewhere on the surface to reduce two hydrogen ions to one H_2 molecule. The reason that two different electrochemical half-cell reactions can occur on the same metal surface lies in the heterogeneous nature of a metal surface. Polycrystalline metal surfaces contain an array of site energies due to the existence of various crystal faces (i.e. grains) and grain boundaries⁷.

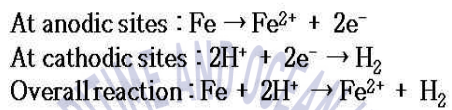
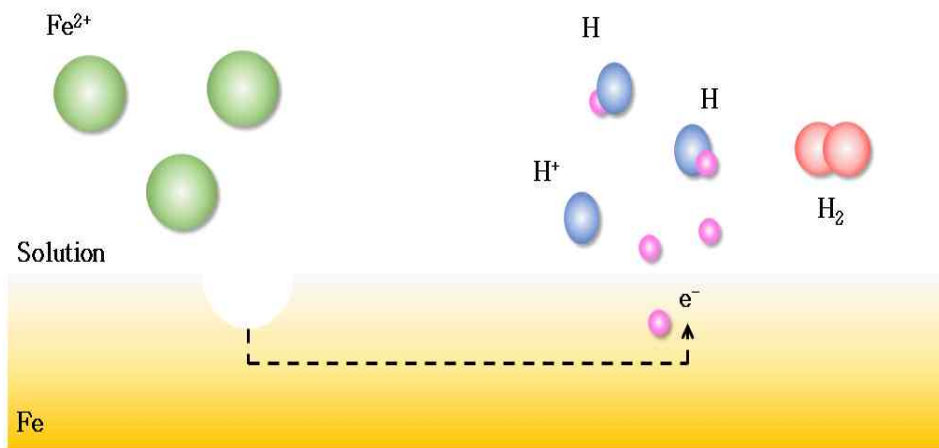
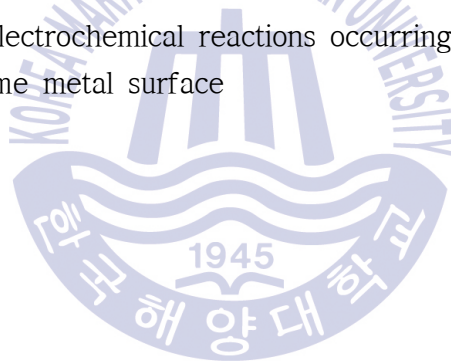
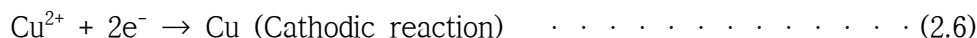


Fig 2.2 Coupled electrochemical reactions occurring at different sites on the same metal surface



(1) Electrode Potential

Reaction of each metal in this cell are expressed as follows:



Overall reaction is summarized as follows:



Metal Fe release electrons and produce Fe^{2+} ions. On the other hand, at Cu metal, Cu^{2+} ions are combined with electrons released from Fe metal. These reactions are called half cell reaction and each potential of two metals is called half cell potential.

It is expressed relation thermodynamically free energy change with electrochemical potential(E) as follows:

$$\Delta G = -nFE \quad \dots \dots \dots (2.8)$$

ΔG : Free energy change

n : The number of exchanged electrons during reaction

F : Faraday' s constant (96,500 Coulomb/equiv.)

E : Electrochemical potential

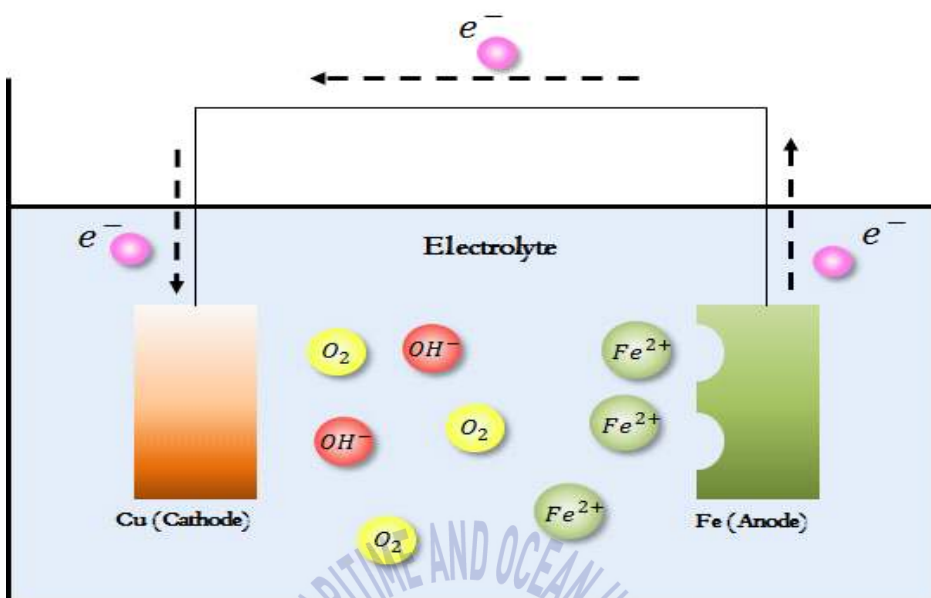


Fig 2.3 Anodic and cathodic reactions between steel and copper in seawater

Although equilibrium potential in each half-cell metal can be obtained, the absolute value of the equilibrium potential of each electrode cannot be measured. Each electrode has a higher or lower potential based on an electrolyte solution, but it is not possible to measure the difference with that electrolyte. This is because it is always necessary to contact with wires from the measuring device in order to measure the potential difference. Another electrode is made when the wires are in contact with the solution, and there is a potential difference between the electrodes and electrolyte. Therefore, measured potential is always the difference between the two electrodes. Consequently, reference electrodes, which can be a common potential reference, are used to measure and display potential. When H_2 gas is at 1 atm pressure and unit activity H^+ is at 1, This electrode is called Standard Hydrogen Electrode (SHE).

Fig 2.4 indicates that a platinum foil specimen is suspended in a sulfuric acid solution of unit activity H^+ , which is bubbled with purified hydrogen to remove dissolved oxygen and establish the standard state for H_2 gas at 1 atm pressure. The hydrogen electrode is connected to another half-cell through a solution bridge which contains a porous glass barrier to permit charge transfer and potential measurement but not mass transfer of the acid solution in the electrode⁶⁾. The Standard Hydrogen Electrode is normally used for laboratory because it requires careful caution. Except for Standard Hydrogen Electrode, there are various types of electrodes such as Copper-copper Sulphate Electrode (CSE), Saturated Calomel Electrode (SCE), Saturated Silver-silver Chloride Electrode (SSCE). Comparison of potential between standard hydrogen electrode and other standard electrode is represented in Table 2.1¹²⁾.

When reporting electrochemical potential measurements, it is always important to indicate which reference half-cell was used to carry out the work. This information is required to compare these measurements to similar data that could have been obtained using any other reference half-cell. The scheme presented in Fig 2.5 provides a graphical representation to help visualize some of the information between references which is mainly used³⁰⁾.

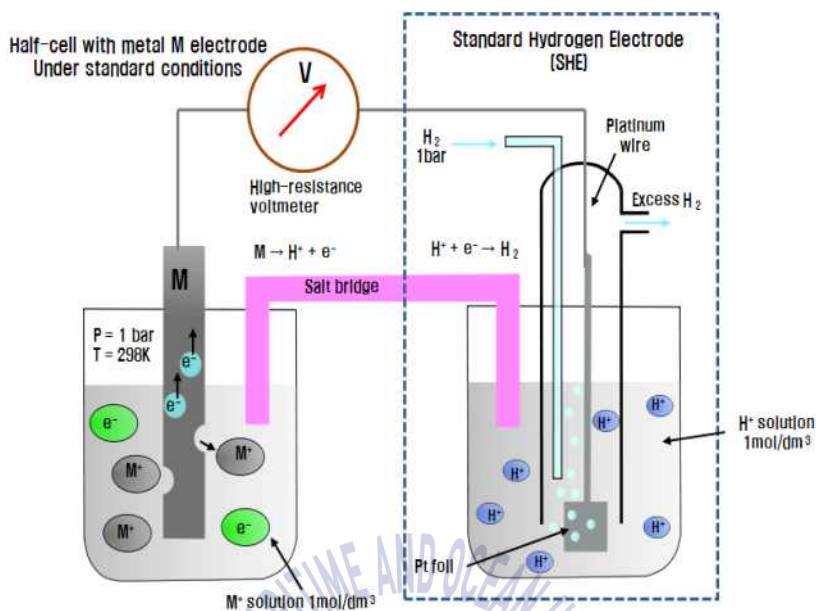


Fig 2.4 Summary diagram of standard hydrogen electrode

Table 2.1 Potential of reference electrodes compared with SHE

Type of electrode	E(V vs. SHE)
Saturated calomel electrode(SCE) Hg [Hg ₂ Cl ₂] sat KCl	0.241
1M calomel electrode : Hg [Hg ₂ Cl ₂] 1N KCl	0.280 ~ 0.283
0.1M calomel electrode : Hg [Hg ₂ Cl ₂] 0.1N KCl	0.333
Mercurous sulfate electrode : Hg [Hg ₂ SO ₄] Hg ₂ SO ₄ (aq)	0.615
Silver/Silver chloride electrode : (SSCE) Ag [AgCl] HCl (aq)	0.222
Mercuric oxide electrode : Hg [HgO] KOH(aq)	0.098
Copper/copper sulphate electrode (SCE) Cu [CuSO ₄] sat. 5H ₂ O	0.316

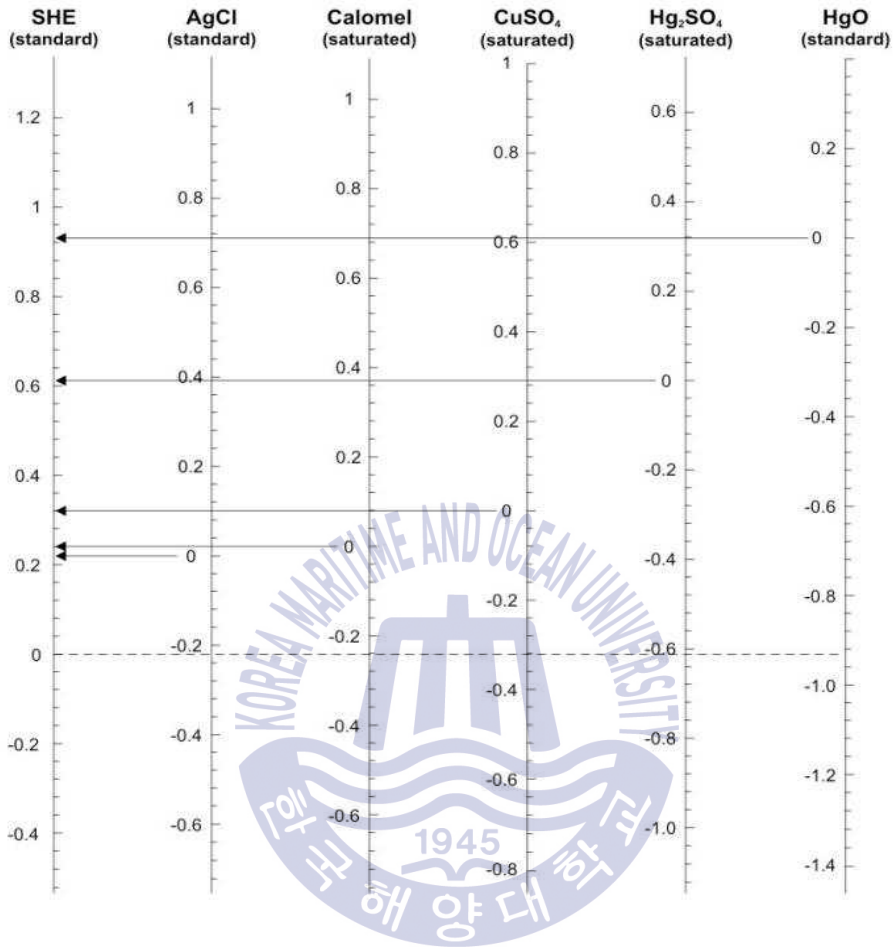


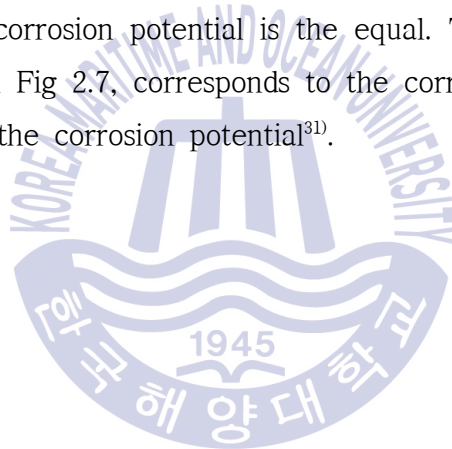
Fig 2.5 Graphical scheme to compare potentials of the most commonly used reference electrodes

Half-cell electrode potential polarized at the same surface changes until having a common value at corrosion potential (see Fig 2.7).

$$\eta_a = \beta_a \log \frac{i_a}{i_o} \quad \dots \dots \dots (2.11)$$

$$\eta_c = \beta_c \log \frac{i_c}{i_o} \quad \dots \dots \dots (2.12)$$

The speed of the positive reaction equation 2.11 and the negative reaction equation 2.12 at the corrosion potential is the equal. The positive dissolution speed (i_a), as shown in Fig 2.7, corresponds to the corrosion rate (i_{corr}) a term of current density at the corrosion potential³¹⁾.



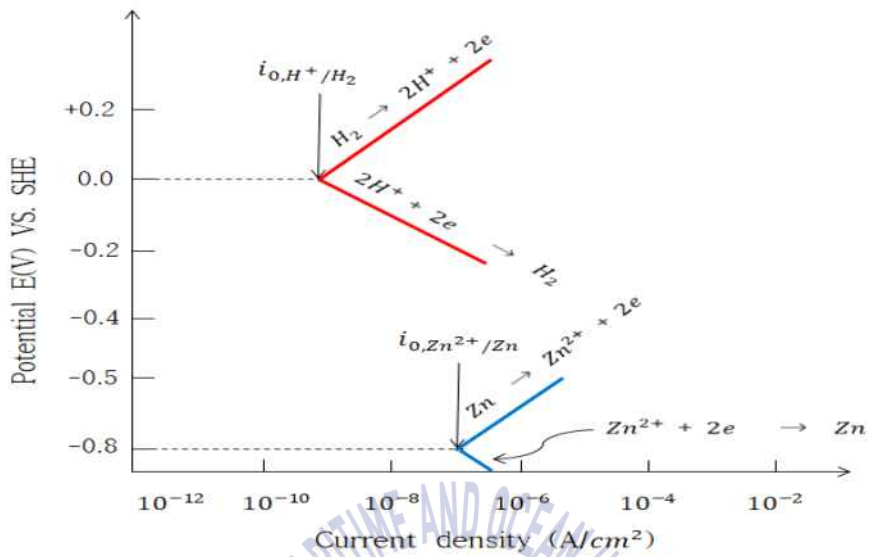


Fig 2.6 Half-cell reaction existing simultaneously on the surface of zinc

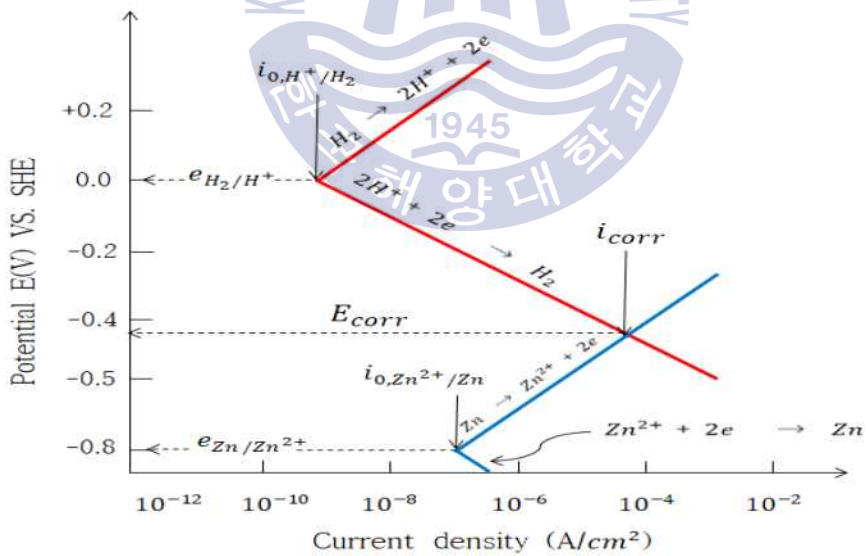


Fig 2.7 Polarization of half-cell of zinc in the acid solution

The potential of a corroding metal is readily measured by determining the voltage difference between a metal immersed in a given environment and an appropriate reference electrode. Fig 2.8 illustrates an experimental technique for measuring the corrosion potential of a metal using a laboratory cell. This is accomplished by measuring the voltage difference between the reference electrode and the metal using a high impedance voltmeter capable to accurately measure small voltages without drawing any appreciable current. In measuring and reporting corrosion potentials, it is necessary to indicate the magnitude of the voltage and its sign. In the example shown in Fig 2.8, the corrosion potential of metal M is -0.405 V . The minus sign indicates that the metal is negative with respect to the reference electrode³⁰.

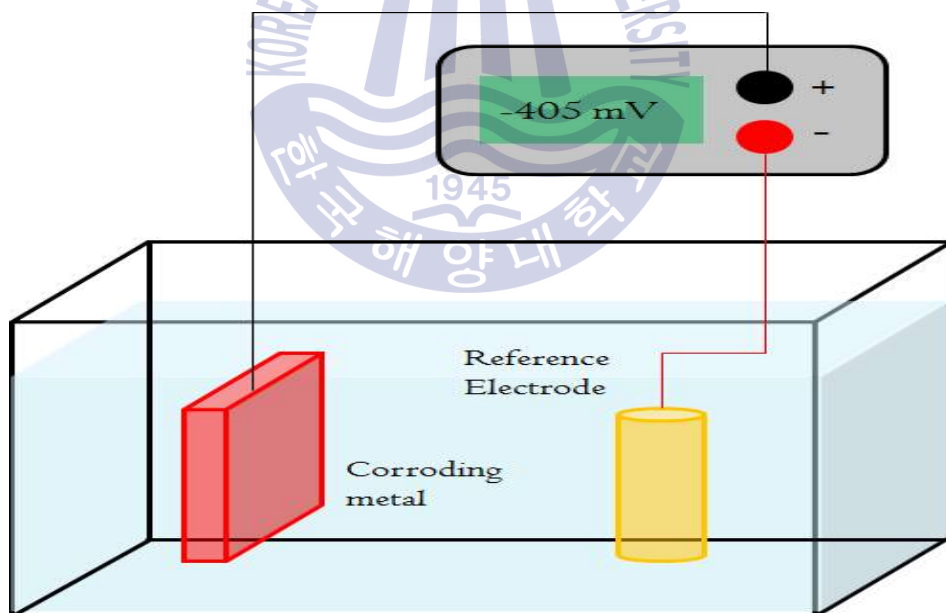


Fig 2.8 Experimental set-up to measure the corrosion potential of a specimen

(3) Polarization

When artificially changing the energy state of an electrode in equilibrium, the potential change is called polarization, and variation of potential is called overvoltage. Corrosion potential is that anode and cathode current indicate the same value, but at the polarization potential, there is difference in the magnitude of the positive current (i_a) and negative current (i_c) because of artificially supplied current. In other words, polarization potential is a condition in which it artificially changes the energy of metal by supplying electric current from outside.

Polarization is expressed as follows:

$$\eta = E - E_0 \quad \dots \dots \dots (2.13)$$

E : Electrode potential with current flow

E_0 : Electrode potential without current flow (=Corrosion potential)

We should consider the following anodic reaction to understand anodic polarization.



Suppose that the oxidation of Fe atoms to Fe^{2+} ions is slow. Then electrons exit the electrode faster than Fe atoms leave the metal matrix, as illustrated in Fig 2.9. This means that the electron concentration is decreased at the metal side of the interface. The electrode potential E thus

becomes more positive due to activation polarization. Also, suppose next that the products of the anodic reaction, i.e., Fe^{2+} ions, are slow to diffuse away from the metal surface (see Fig 2.9)⁷⁾. Then the surface becomes more positively charged due to the accumulation of Fe^{2+} ions. The electrode potential E again becomes more positive, but this time due to concentration polarization³⁴⁾.

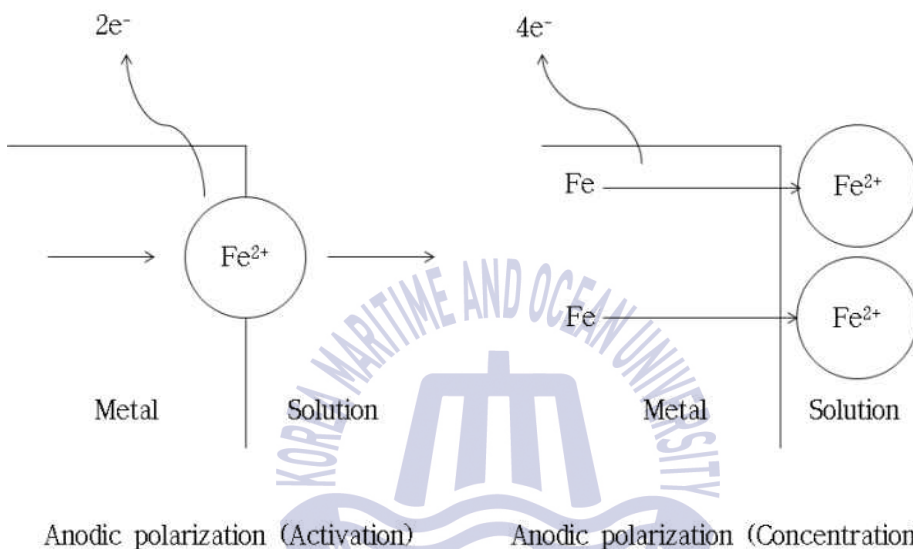
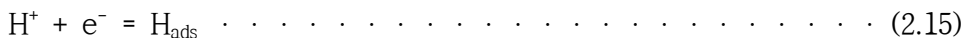
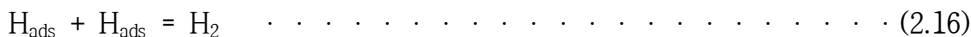


Fig 2.9 Schematic representation of anodic polarization for an anode

To understand cathodic polarization, we should consider the hydrogen evolution reaction occurring at a metal surface. First, hydrogen atoms are produced by the reduction reaction.



followed by their combination:



The process of activation polarization involves a slow step in the electrode reaction. Suppose that electrons are supplied to the metal electrode faster than they can react to form H atoms (see Fig 2.10)⁷⁾. Then the concentration of electrons is increased at the metal side of the interface. The result is that the electrode potential E becomes more negative, due to activation polarization.

Suppose instead that there are concentration effects near the electrode surface for the hydrogen reduction reaction. If reactant hydrogen ions H^+ are slow to diffuse to the electrode surface (see Fig 2.10), then electrons again could accumulate at the metal side of the interface. The result is that the electrode potential E again becomes more negative, but this time due to concentration polarization³⁴⁾.

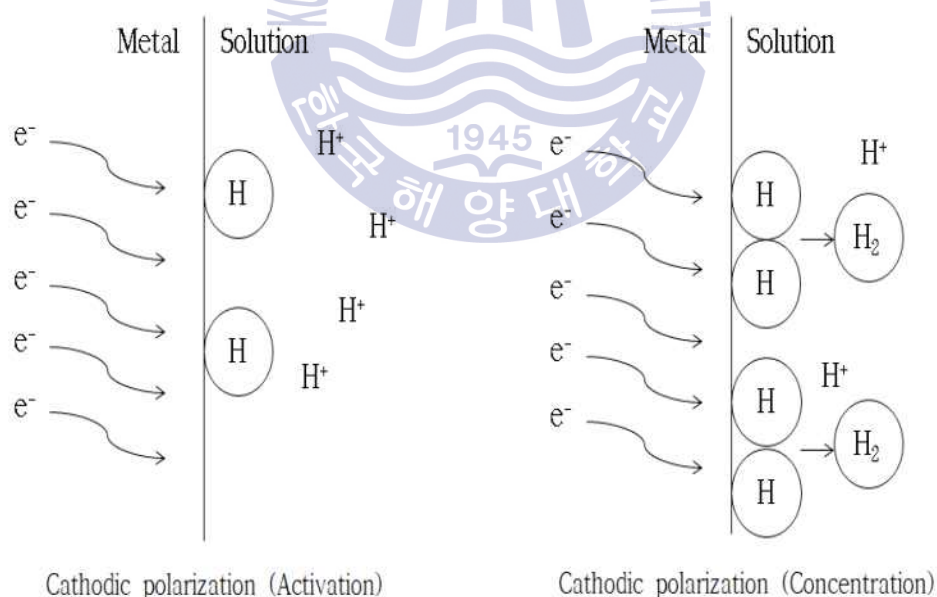


Fig 2.10 Schematic representation of cathodic polarization for a cathode

Fig 2.11 graphically illustrates relationship for the anodic reaction, which is the oxidation of iron atoms to soluble, ferrous ions. The activation polarization curve for this anodic reaction is a straight line extending from the lower left to the upper right. The slope of the line is given by the anodic Tafel slope, β_a . Fig 2.11 shows that a unit increase in the overpotential, E , results in an order of magnitude increase in the reaction rate. As the oxidizing potential becomes more positive, the rate of the corrosion or oxidation of iron increases, that is, the anodic overpotential increases. Ferrous ions are generated more rapidly, and more electrons are left at the metal surface⁵⁾.

The activation polarization curve for the cathodic reaction of hydrogen ions to form hydrogen gas is shown in Fig 2.12. The slope of the line is the cathodic Tafel slope, β_c . The reduction reaction increases as the oxidizing conditions become more reducing or the overpotential becomes more negative. As the potential becomes more reducing by a unit value, the rate of the reduction reaction increases by an order of magnitude. As the conditions become more reducing, hydrogen ions and electrons are consumed more rapidly at the metal surface and more hydrogen gas is generated.

It is important to note that the anodic current, i_a , is the rate of generation of electrons and that cathodic current, i_c , is the rate of consumption of electrons. In an operating electrochemical cell, oxidation current leaves the metal surface at the anode, and a cathodic current enters the metal surfaces at the cathode⁵⁾.

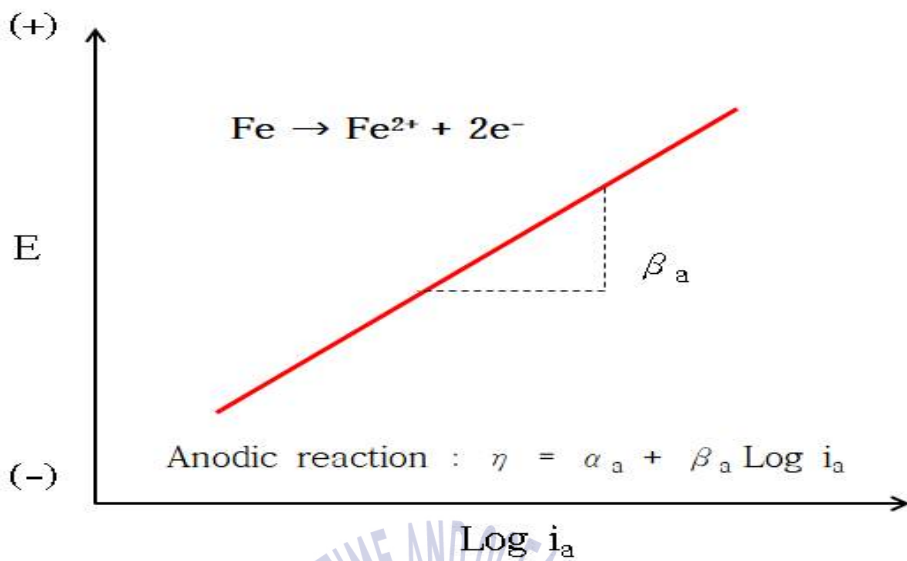


Fig 2.11 Activation polarization curve for the anodic reaction of iron and ferrous ions

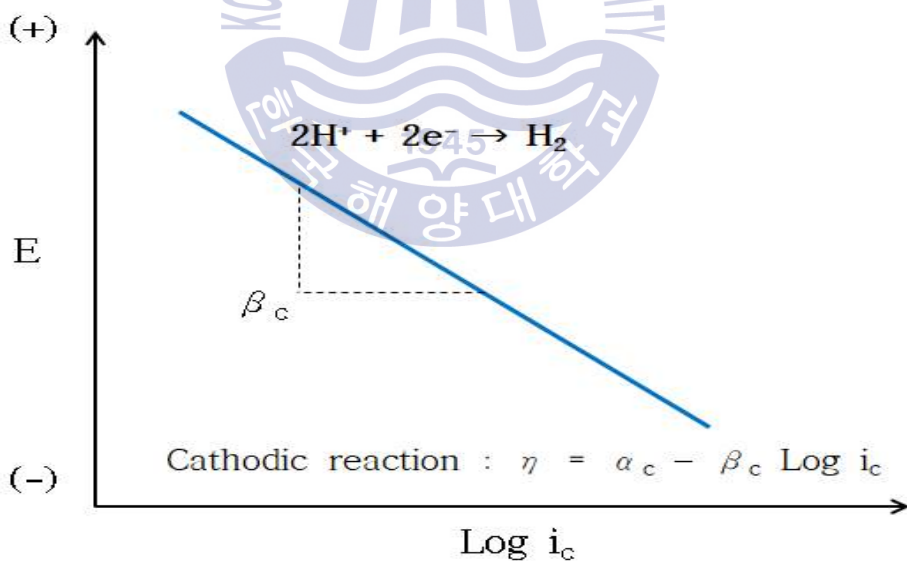


Fig 2.12 Activation polarization curve for the cathodic reaction of hydrogen ions and hydrogen gas

The anodic reaction and the cathodic reaction are combined on a single diagram in Fig 2.13. The requirements of mixed-potential theory are met at only a single point, that is, the point where the anodic and cathodic reaction curves cross. This is the only location at which the anodic reaction rate equals the cathodic reaction rate. The potential of this intersection is identified as E_{corr} , and the current at this intersection is defined as i_{corr} .

At potentials more positive or more oxidizing than the corrosion potential, the anodic current is greater than the cathodic current, and more electrons are generated than are consumed. At potentials more negative or more reducing than the corrosion potential, the cathodic current is greater than the anodic current, and more electrons are consumed than are generated. A steady state of no net consumption or generation of electrons is achieved only at the corrosion potential. In order to maintain a system away from the corrosion potential (E_{corr}), current must be supplied from an external source or other reactions. The slopes β_a and β_c are determined by the properties of both the metal surface and the electrolyte⁵).

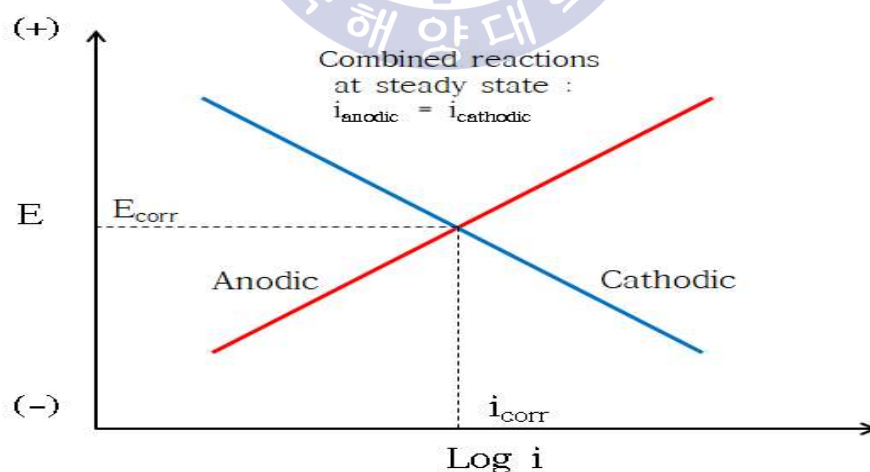


Fig 2.13 Combined diagram of an anodic reaction and a cathodic reaction with activation polarization

2.1.2 Corrosion control in seawater

It seems perplexing that our planet is called “*Earth*” when 70.8 % of its surface is covered by oceans. One of the most obvious differences is that seawater contains dissolved substances. These dissolved substances are not simply sodium chloride (table salt) – they include various other salts, metals, and dissolved gas.

The salinity of seawater is typically about 3.5%. It means that it also contains 96.5% pure water. Fig 2.14 and Table 2.2 show that the elements such as chlorine, sodium, sulfur (as the sulfate ion), magnesium, calcium, and potassium account for over 99% the dissolved solids in seawater⁸⁾.

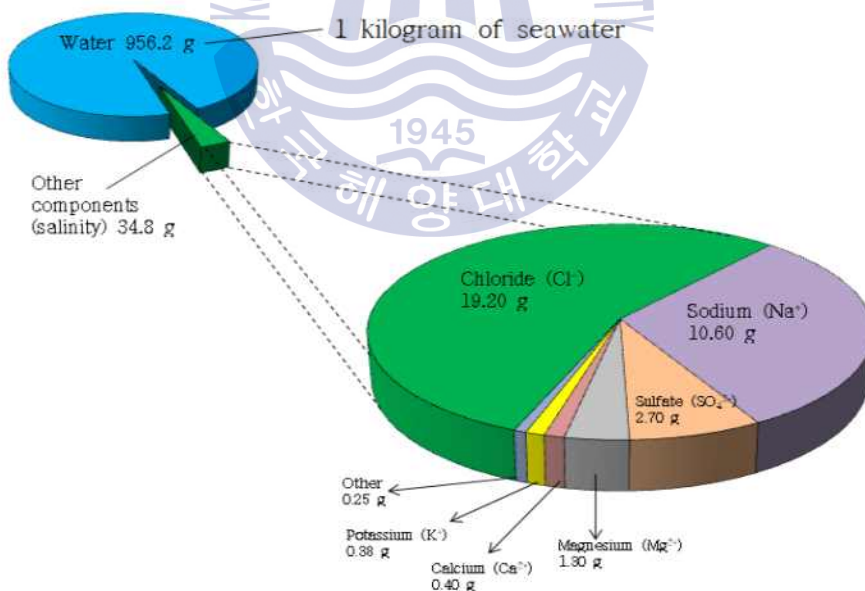


Fig 2.14 Major dissolved components in seawater

Table 2.2 Selected dissolved materials in 3.5 ‰ seawater

Major constituents (in parts per thousand)		
Constituent	Concentration (‰)	Ratio of constituent / total salts (%)
Chloride (Cl ⁻)	19.2	55.04
Sodium (Na ⁺)	10.6	30.61
Sulfate (SO ₄ ²⁻)	2.7	7.68
Magnesium (Mg ²⁺)	1.3	3.69
Calcium (Ca ²⁺)	0.40	1.16
Potassium (K ⁺)	0.38	1.10
Total	34.58 ‰	99.28 %

The seawater of 3.5 ‰ salinity contains from 6 to 9 ppm of dissolved oxygen in the temperature range between 0 and 30 °C. If the temperature of seawater increase to 60 °C, concentration of dissolved oxygen decrease to 3 ppm approximately. Specific resistance of seawater is 100 to 200 times less than that of fresh water. Although there is a little change by temperature, it varies in 20 to 30 Ω·cm range (see Table 2.3).

Fig 2.15 demonstrate states of specific resistance according to temperature and salinity of seawater. Range which is described as spotted line indicates range of general seawater condition. Seawater has a tendency to exist in alkalinity environment and range of pH is normally 8.1 to 8.3^{9),10)}.

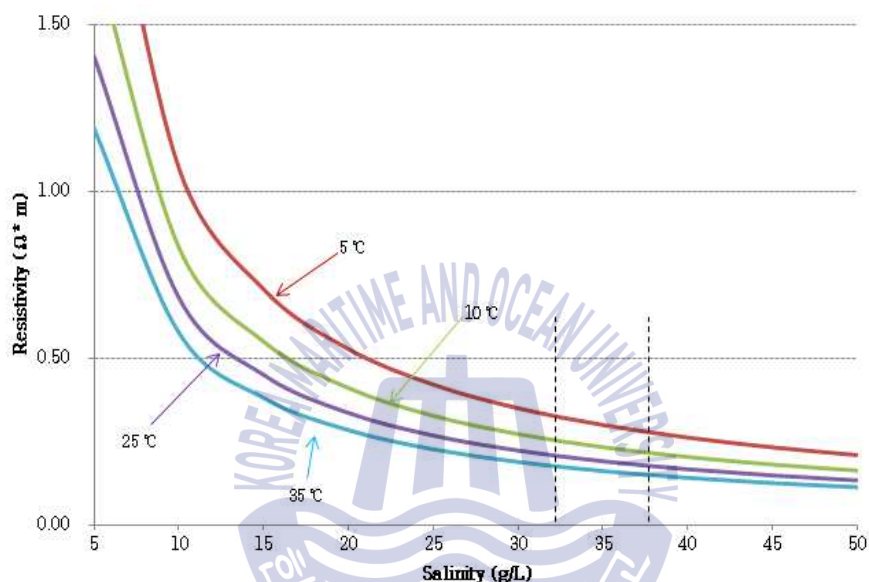


Fig 2.15 Graph for calculation of seawater resistivity as a function of salinity and temperature

Table 2.3 Electric resistance of seawater with temperature

Temperature (°C)	10	15	20	25
Conductivity [$\times 10^{-3} \Omega/\text{cm}$ (S/cm)]	37.4	42.2	47.1	52.1
Specific resistance ($\Omega \cdot \text{cm}$)	26.8	23.7	21.2	19.2

Because of these characteristics of seawater, seawater is known as the most aggressive agent to steel among all natural environments. Compared to fresh water, seawater is more corrosive atmosphere. That's because seawater containing chloride is electrolyte that easily provoke corrosion and such various factors as temperature, pH, contamination of water, velocity have an effect on corrosion additionally. For instance, although aluminium, chrome and stainless steel is the metal which is great stability by forming passivity in shore or fresh water, harsh corrosion derived from devastation of passivity is occurred on metal surface due to the effect of chlorine ion¹¹⁾.

Generally, there are a number of method to prevent corrosion; development of materials that have a resistivity, isolating metal surface with external environment by coating, and anodic & cathodic protection. Among them, cathodic protection that is one of the methods to prevent corrosion of structures exposed to marine environments is known as the most cost-efficient and effective device⁹⁾. Cathodic protection is an electrochemical method of corrosion prevention which could change potential of metallic structure which is to be protected to immunity region of the Pourbaix diagram described in Fig 2.16¹⁰⁾ by acting cathodic polarization in conjunction with either the supplying of external power source or the attaching of sacrificial anode. Generally, it is applied to such environments as buried pipe, marine atmosphere (pipe, ship's hull, marine structure, and submerged structure) and concrete structure. Method of cathodic protection is mainly used to ICCP (Impressed Current Cathodic Protection System) and SACP (Sacrificial Anode Cathodic Protection System). Cathodic protection by sacrificial anodes is obtained with any metal, provided its working potential is less noble than the protection potential of the metal to protect. In the ICCP system, current is provided by DC feeder through an anode which is able to apply current to the environment. Table 2.4¹³⁾ compares the pros and cons of both methods.

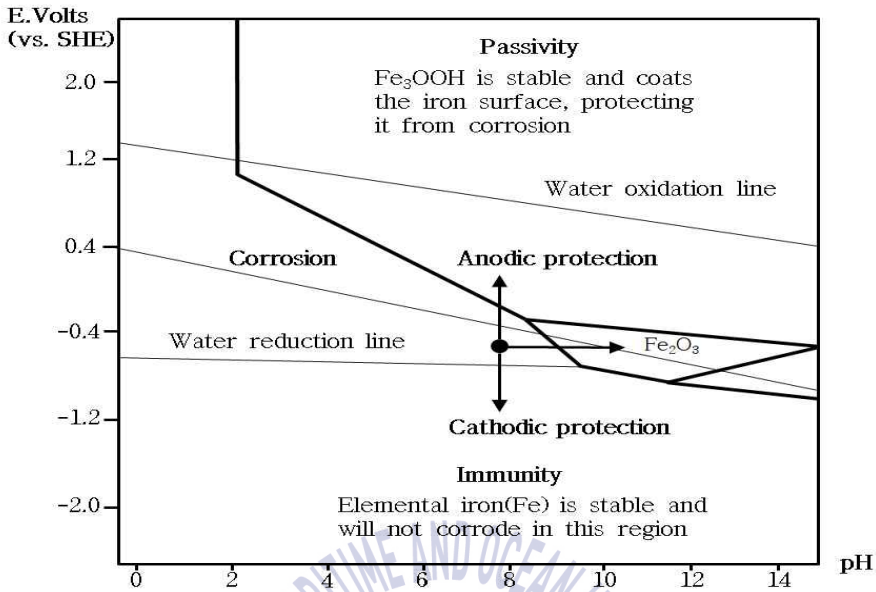


Fig 2.16 Pourbaix diagram of iron in seawater

Table 2.4 Comparison of the pros and cons for ICCP and SACP

ICCP	SACP
Advantages	
<ol style="list-style-type: none"> 1. Output control 2. Long life 3. Automatic monitoring 4. Application in both soil and marine environments 	<ol style="list-style-type: none"> 1. Almost no required maintenance 2. Easy to install 3. Unnecessariness of power supplier 4. Cost effective 5. Suitable for low resistivity region
Disadvantages	
<ol style="list-style-type: none"> 1. Power supply problem 2. Partial failure affects the whole system 3. Interference problem due to stray current 4. Expertise requirement to install and use 5. A lot of maintenance cost 	<ol style="list-style-type: none"> 1. Periodic replacement of anode due to its limited lifetime 2. Difficulty to apply in high-resistivity region 3. Formation of passivity in high alkaline environment

(1) ICCP (Impressed Current Cathodic Protection)

Alternative currents converted into direct power source at rectifier supply cathodic protection current to structure to be protected by insoluble anode. For cathodic protection of steel in seawater, metallic alloy such as Titanium (Ti), Lead (Pb), Niobium (Nb) have been used. Typical polarization curve of ICCP is shown in Fig 2.17⁴¹⁾. That is, corrosion proceed by forming corrosion potential (E_{corr}) and corrosion current density (i_{corr}) at point C in polarization curve due to polarization occurred by oxygen-reduction reaction at anode and cathode. If a power source apply external current through rectifier and insoluble anode for cathodic protection, Anodic polarization moves from C to B passing by B' and increase current by cathodic polarization. At this time, external current which is amount of $i_C - i_{B'} = \Delta i'$ flows at B' C' potential. When approaching BD potential, external current which is amount of $i_D - i_B = \Delta I'$ is applied from external power source and corrosion rate of structure is minimized.

(2) SACP (Sacrificial Anode Cathodic Protection)

SACP is a method that structure exposed to corrosive environment is protected by connecting with the anodic metal which have lower potential than protected structure. Consequently, structure exposed to corrosive environment is protected while anodic metal is corroding. At this time, cathodic protection current applied from sacrificial anode flow like arrow described in Fig 2.18. The materials of sacrificial anode are typically three metals (Zn, Al, Mg Alloy), and Zn and Al are used for cathodic protection in seawater. In terms of amount of electricity and economical aspects, Al alloy is preferred to the other alloys⁴¹⁾.

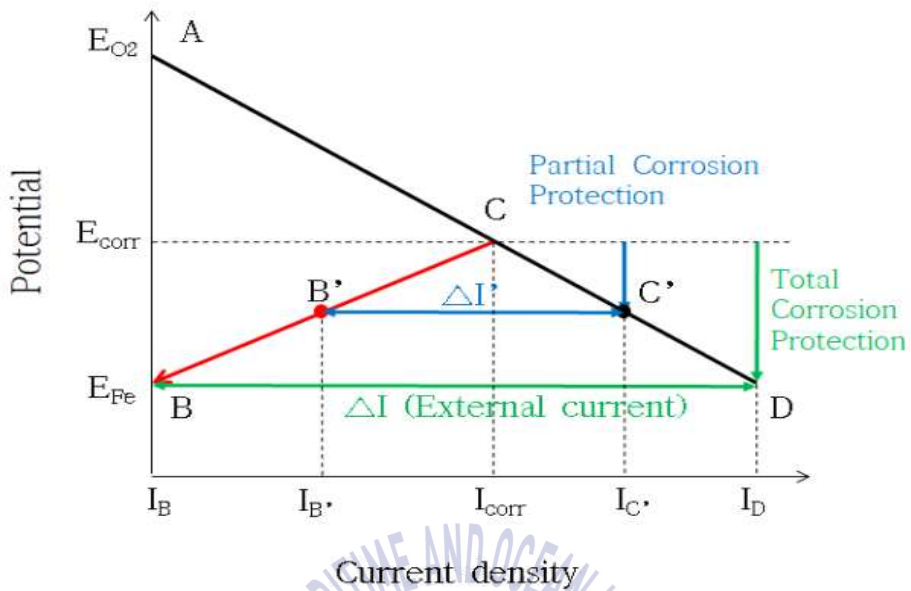


Fig 2.17 Typical polarization curve of ICCP

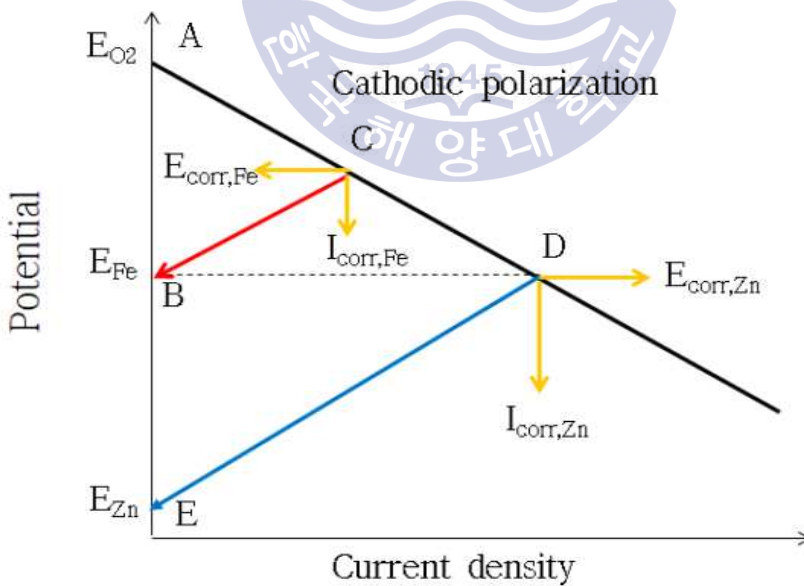


Fig 2.18 Typical polarization curve of SACP

2.1.3 Review of previous study on corrosion control in seawater pipe

In the marine industry, carbon steel pipes have been normally used for cooling pipes. By the way, accident of leak is occurred unexpectedly and frequently due to corrosion in welded area of cooling pipes and the defect areas inside of pipe. Nevertheless, in case of corrosion in the pipe, there is method such as coating on inner surface of pipe. However, this method have a shortcoming when coated surface is cracked. Hence, cathodic protection using external power source in the pipe has been investigated by a number of authors. The primary objective of these experiments was to determine both the feasibility and the performance of ICCP in practical field adopting to the seawater pipe.

Jeong, et al.,¹⁴⁾ conducted electrochemical polarization experiment of carbon steel which is material of piping system. Through this study, authors tried to find out ideal cathodic protection condition for preventing corrosion occurring in seawater pipe. In seawater environment with flow, limiting diffusion current density of approximately 7 to 20 mA/cm² was observed, and ideal cathodic protection potential was in range from -1,300 to -1,200 mV/SSCE (see Fig 2.19). As a result of galvanostatic cathodic polarization, the higher cathodic protection current applied, the lower cathodic protection potential maintained. Furthermore, to achieve cathodic protection in range of ideal cathodic protection potential, authors came to the conclusion that current density of 2 to 5 mA/cm² was generally needed to protect seawater pipe without flow rate (see Fig 2.20).

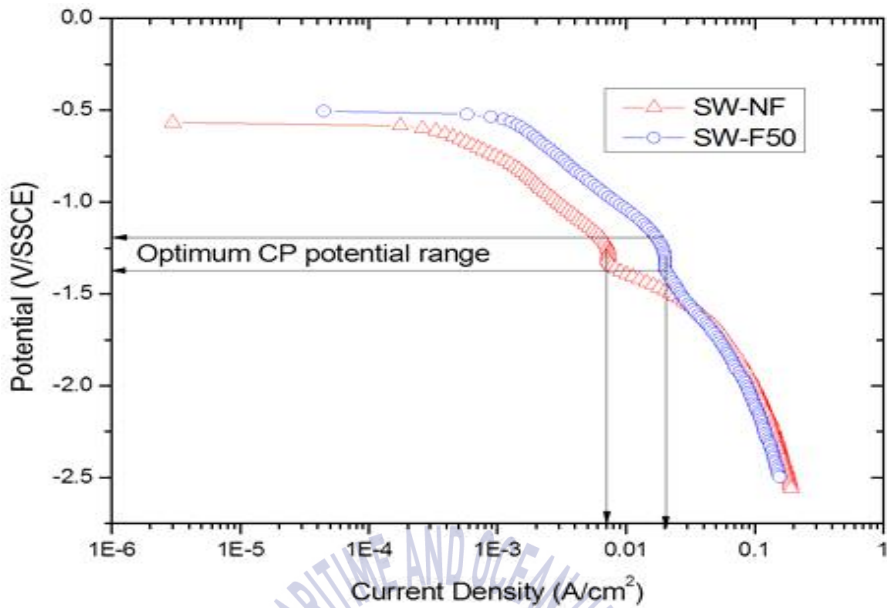


Fig 2.19 Cathodic polarization results of specimen in seawater with and without agitation

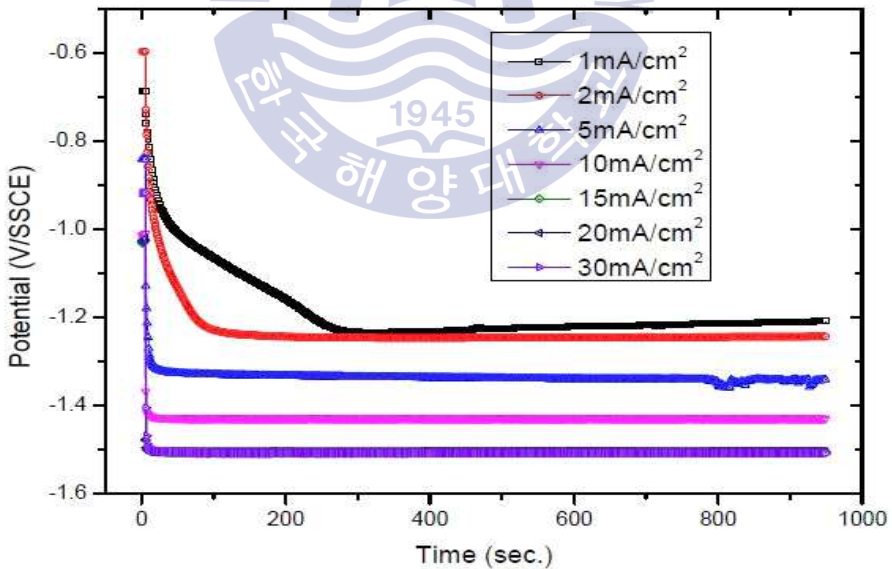
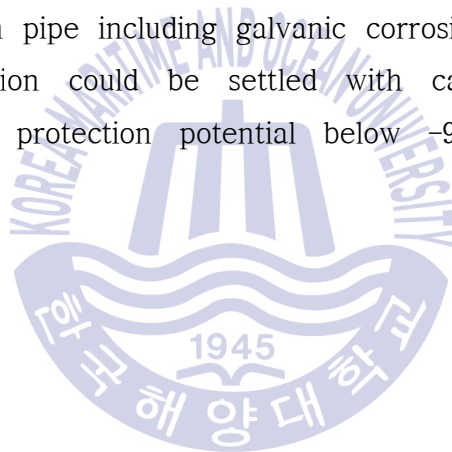


Fig 2.20 Galvanostatic polarization results of specimen in seawater without agitation

Jeong, et al.,¹⁵⁾ experimentally studied on the characteristic of cathodic protection by adopting external power supply to prevent the inner surface of pipe from corrosion. There was a tendency that the higher cathodic protection current applied, both the longer approaching distance of cathodic protection current and the lower cathodic protection potential. At this time, approaching distance of cathodic protection current was confined to 60 cm approximately. That is, to resolve a problem, corrosion of the inner surface of pipe, authors concluded that rod type anodes should be installed at intervals of up to 60 cm or ribbon type anodes should be placed along the pipe to be protected (see Fig 2.21). In addition, in the event of corrosion in pipe including galvanic corrosion, authors concluded that galvanic corrosion could be settled with cathodic protection by maintaining cathodic protection potential below -900 mV/SSCE (see Fig 2.22).



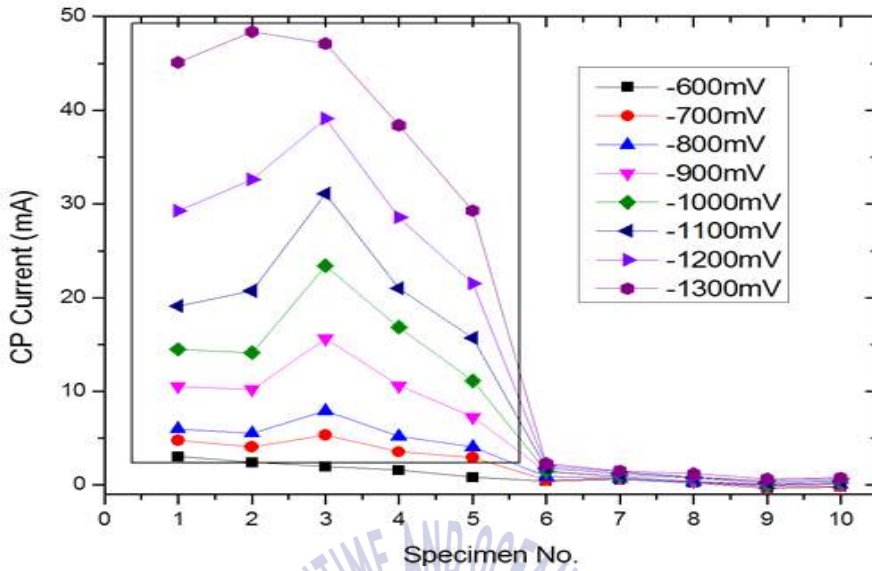


Fig 2.21 Test results of cathodic protection current measurement flowed from a ribbon type MMO anode to the specimens by setting potentials

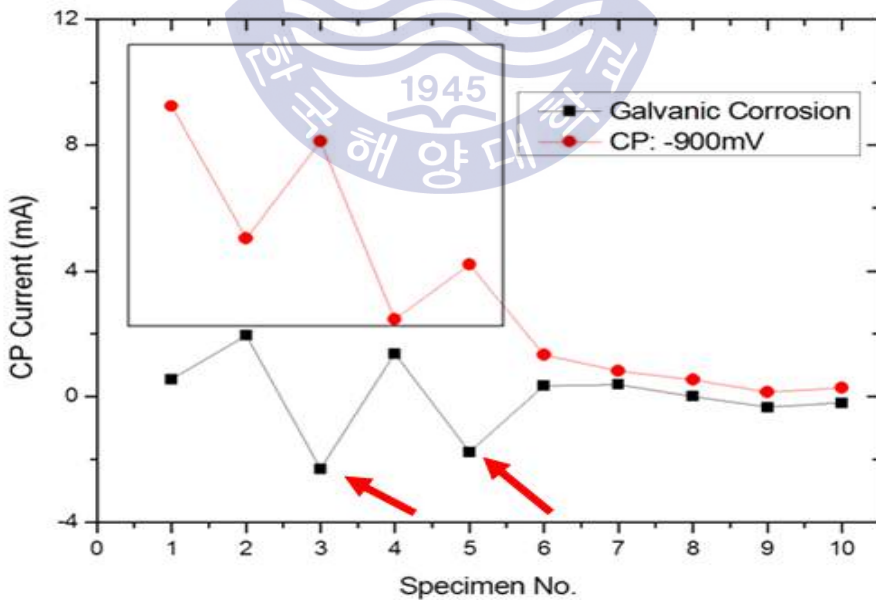


Fig 2.22 Test results of cathodic protection current measurement in comparison of the galvanic corrosion test

2.2 Biofouling

2.2.1 Background theory

Marine structures continually exposed to marine environments and facilities such as pipe for the sake of seawater cooling system are the best place to accumulate and grow marine organisms in a fast and easy manner owing to feeding both dissolved oxygen and prey for marine organisms ceaselessly. The phenomenon that artificial surface is contaminated by growth and adhesion of marine organisms is called biofouling. Representatively, biofouling is divided into macro-biofouling and micro-biofouling by size of species which compose of each fouling. Marine organisms causing biofouling are effortlessly adsorbed to any surface such as intake of cooling water for energy plant, condenser tube, surface of heat exchanger. Each marine organism have peculiarities according to various factors : habitat, season, the way to adhere to surface.

The organisms which take part in marine biofouling are primarily the attached or sessile forms occurring naturally in the shallower water along the coast. *“Marine Fouling and its Prevention”* reported that nearly 2000 species had been identified on fouled structures and later increased the number to more than 4000 species. Nevertheless, it still includes a very small proportion of the known marine species²⁰⁾. More than 4000 kinds of marine biofouling species have been reported globally, most of which live primarily in the shallower water along the coast and in harbors that provide abundant nutrients. In general, marine adhesion organisms can be divided into two major categories. The first of these includes the micro-biofouling or biofilm organisms, which are bacteria and diatoms. Biofilms are ubiquitous, as long as the surfaces are exposed to water. The other category includes macro-fouling organisms such as algae and barnacles. The most important macro-fouling species are barnacles, mussels, polychaete worms, bryozoans and seaweed²¹⁾.

Marine biofouling can be defined as the undesirable accumulation of microorganisms, algae and animals on artificial surfaces immersed in seawater. The fouling process starts from the moment when the surface is immersed in water and takes place in three main stages: formation of a conditioning film, micro-fouling and macro-fouling. The conditioning film, comprised of organic molecules (e.g. proteins) attached to the surface, forms within the first minutes and sets the scene for further attachments. In the next hours bacteria settle in, in two phases : first, by an instantaneous and reversible attachment via hydrodynamic and electrostatic interactions and second, via an irreversible attachment which occurs in the time scale of a few hours and involves covalent bonding between the bacteria and the substrate. The combination of the conditioning film and the slime of living and dead bacteria cells generates the first stage of micro-fouling, so called the primary film. Furthermore, diatoms colonies, macro-algae and protozoa spores settlement increases the micro-biofouling extent within the first 2-3 weeks, originating the secondary film. Finally, this micro-fouling stimulates the settlement of algae, spores and animal larvae, followed by the attachment of an adult marine organism, which is called macro-fouling. Biofouling in marine environments is therefore, a relatively fast, dynamic and cumulative process which spans over several sizes and time scales and constitutes a complex problem with several forefronts. Fig 2.23 indicates the formation of biofouling as evolving time and phase pass by²²⁾. The process of biofouling occurs by both physical reactions and biochemical reactions as illustrated in Fig 2.24. The physical reactions are governed by factors such as electrostatic interaction and water flow, leading to formation of the conditioning biofilm and adsorption of microorganisms. The biochemical reactions include EPS (Extracellular polymeric substances) secretion, movement and secondary adhesion of microorganisms, formation of the biofilm, and adhesion of macro-foulers. Whereas the physical reactions are usually reversible, the biochemical reactions are effectively irreversible²¹⁾.

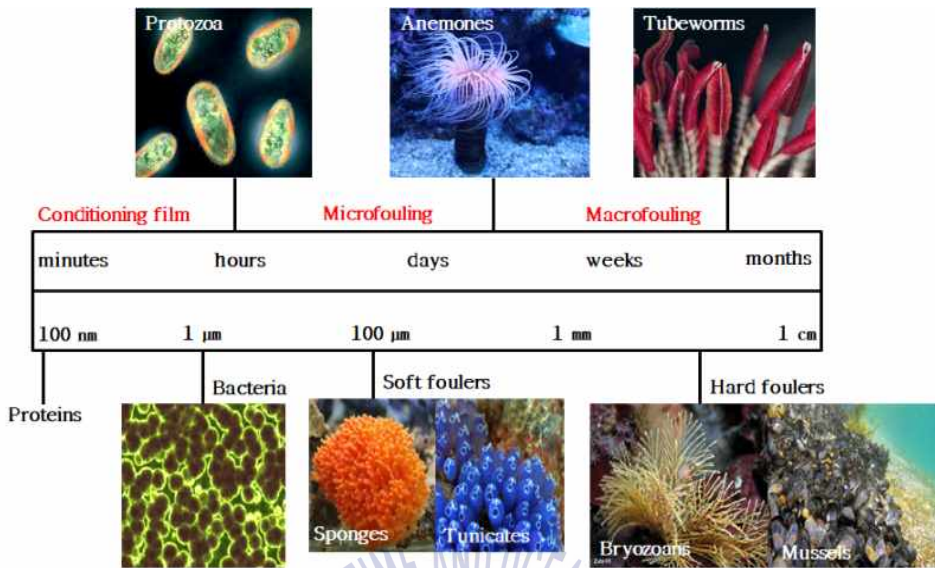


Fig 2.23 Different phases of marine biofouling: Time-line evolution and respective roughness increase

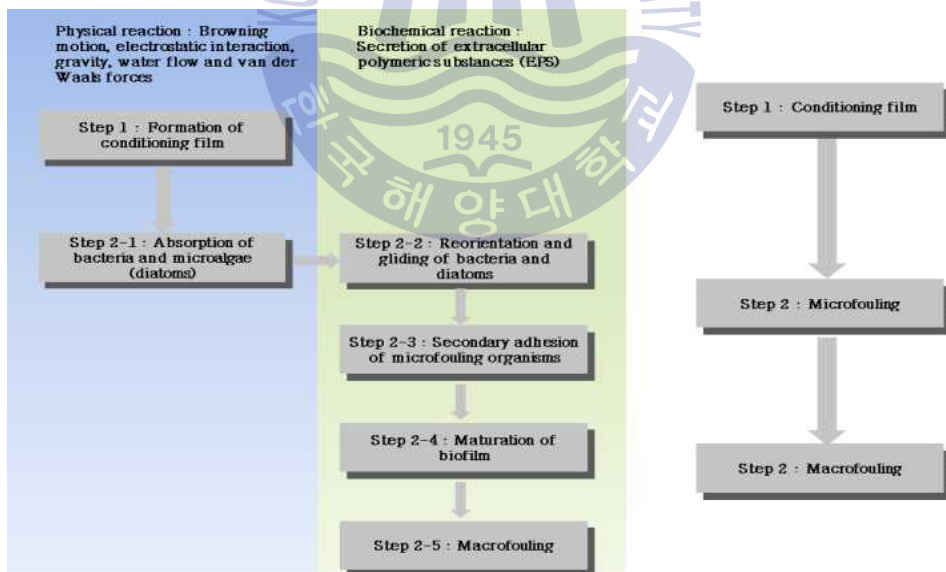


Fig 2.24 Biofouling process and the formation of biofilm

2.2.2 Biofouling control

A biofouling control system is defined as a coating, paint, surface treatment, or device that is used on a ship or marine structure to control or prevent attachment of unwanted organisms. The technologies can be subdivided into those based on the application of a coating, and those which do not. Fig 2.25 summarize many kinds of means to conduct anti-fouling²³⁾.

In the midst of methods indicated in Fig 2.25, the most economical and wide method is utilizing chlorine. Chlorine is the material used broadly in the water treatment industry and excel in preventing contamination like fouling by suppressing growth of micro-organisms, viruses and bacteria stucked to surface. In case of using chlorine of liquid or gas, however, there are problems such as storage, transportation, and utilizing. To cope with these problems, it is to generate chlorine by electrolysis of seawater. Chlorine gas made by electrolysis of seawater is directly dissolved into seawater, becoming itself chlorination phase. Hence, it is not necessary procedures such as transportation and storage. Thus, due to being able to avoid problems which are mentioned earlier, method to use chlorine made electrochemically by electrolysis of seawater is safe and economical alternative to control and prevent biofouling^{24),25),26),27)}.

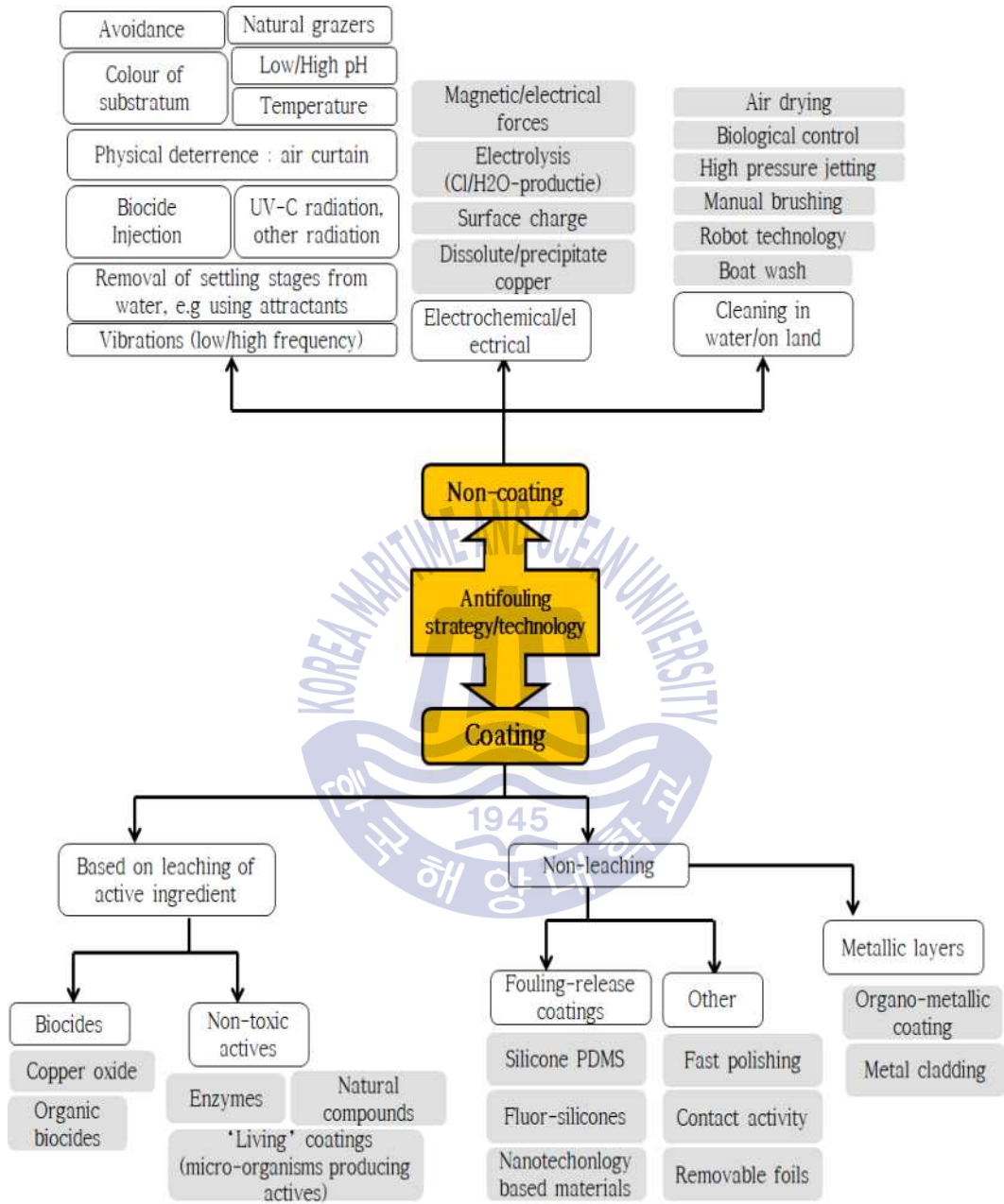


Fig 2.25 Diagram of anti-biofouling strategy/technology

(1) Characteristic of hypochlorous acid (HClO)

Hypochlorous acid (HClO) is a weak acid and a kind of antiseptic produced by the reaction of chlorine ion with water. Also, HClO produced by chlorine reacts with water dissolves in the form of hypochlorite ($pK_a=7.537$ at $25\text{ }^\circ\text{C}$) according to the formula below. The response generation equation is shown in equation 2.18²⁹).



Seawater or other water containing Cl^- may be used to generate a disinfecting solution containing chlorine by passing a direct electrical current through the solution³⁵). The main reactions of seawater electrolysis at anode and cathode are shown in Fig 2.26.

Anode:



Cathode:



Chlorine gas produced at anode fabricate HClO that act as disinfection by combining with water. Distribution of HClO, chlorine gas and hypochlorite ion for each pH level is shown in Fig 2.27. At a pH of 6.5, HClO concentration is greater than 90 %, and OCl^- is less than 10 %. For hypochlorite, pH 6 or higher dissolves and forms hypochlorite ions. At a pH of 4.5, HClO concentration and Chlorine gas is 50 % respectively, and if pH increase, HClO concentration increase and chlorine concentration gas decrease. At a pH of 7.5, HClO and OCl^- concentration is 50 % respectively, the amount of hypochlorite ion is directly proportional to pH, but HClO decrease. The oxidizing power of HClO is roughly 40 to 50 times stronger than that of hypochlorite ions, and HClO penetrates biological membrane layer and effectively kills microorganisms. Through this process, microorganisms are either killed or stunted. So, it is important to keep HClO concentration as high as possible for effective disinfection. Fig 2.27 shows that range of pH 6-7 is the optimal pH condition as it is high in HClO concentration, which is highly sterile, and has a low chlorine concentration that can cause corrosion⁴⁵⁾.

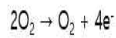
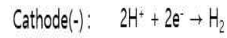
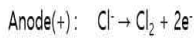
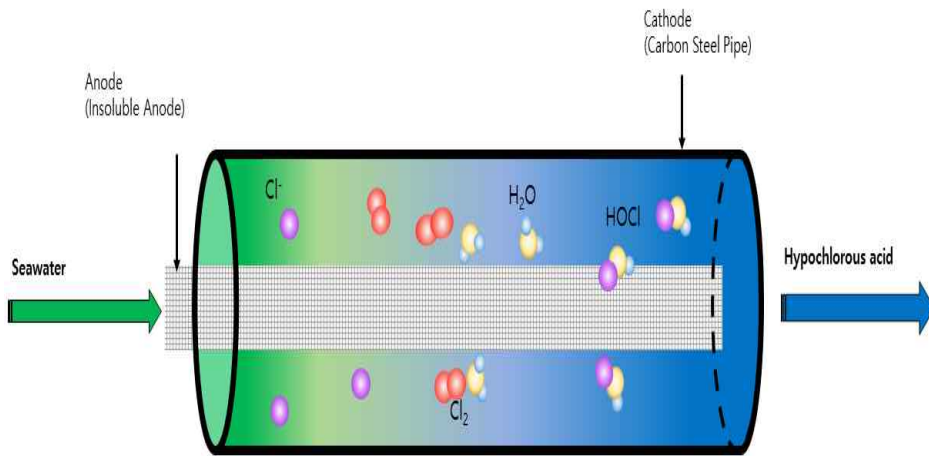


Fig 2.26 Principle of hypochlorous acid generation

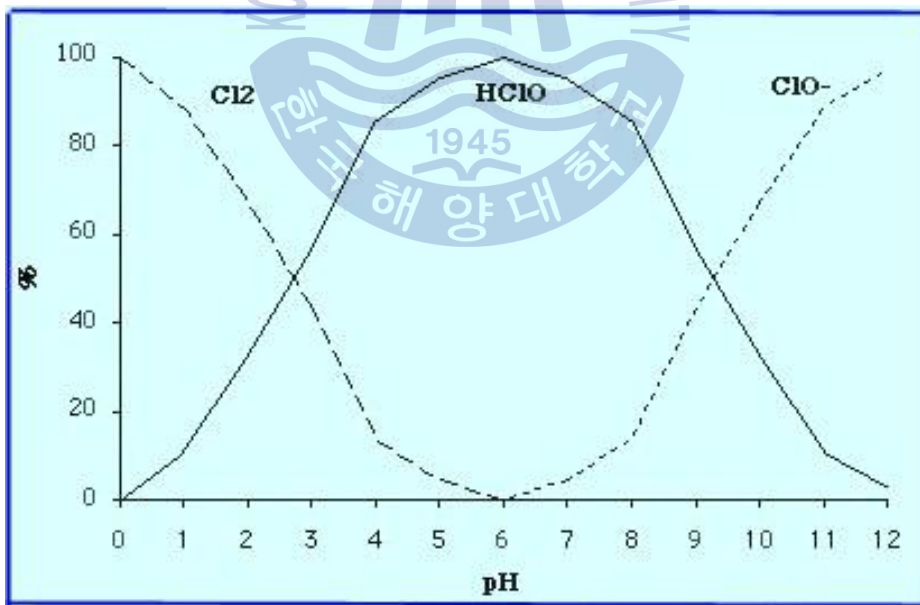


Fig 2.27 Graph of available chlorine present as HClO of varying with pH value

(2) Measuring method of hypochlorous acid

Measuring method for HClO concentration is represented in Table 2.5, and the results of investigation about measuring method is represented in Table 2.6. The evaluation results of measuring method to free chlorine is shown in Table 2.7. These results are written by expert in AWWA (The American Water Works Association). According to the results, DPD (N,N'-diethyl-p-phenylenediamine) colorimeter is the most ideal way to measure free available chlorine. DPD colorimeter is used for measuring total residual chlorine, and Pocket Colorimeter made by Hach is mostly used in these days. Pocket colorimeter and test kit is described in Fig 2.28²⁸⁾.

Table 2.5 Characteristic according to free and total chlorine measurement method

Method	Characteristic
DPD Colormetric	<ul style="list-style-type: none">- Analysis method for measuring color under neutral pH- Method for measuring both free available chlorine and total chlorine
DPD Titration	<ul style="list-style-type: none">- Similar in principle to DPD Colormetric- Free available chlorine measurement is difficult and inaccurate because of proper time
Iodometric Titration	<ul style="list-style-type: none">- Accurate analysis is impossible under 1 mg/L of concentration- Must be carried out within 1 hour using standard reducing agent for accurate analysis
Amperometric Titration	<ul style="list-style-type: none">- Electrochemical analysis method by supplying current to two electrodes- Requires specialized skills and can be applied at concentrations greater than 1 mg/L
FACTS	<ul style="list-style-type: none">- It is difficult to analyze under 0.1 mg/L of sample concentration

Table 2.6 Comparison of common analytical methods for free and total chlorine in water

Method	Analysis Range (mg/L)	DL ^{*1)}	Estimated Precision (%)	Application	Skill Level ²⁾
DPD Colormetric	0~5	0.005	1~2 %	Free & Total	1
DPD Titration	0~3	0.018	2~7 %	Free & Total	2
Idometric	up to 4	1	Not reported	Total Oxidants	2
Amperometric Titration	up to 10	0.0012	1~2 %	Free & Total	3
forward back	0.006~1.00	0.0051	2~4 %		3
FACTS	0~10	0.1	10 %	Free	1

1) * : Minimum or Estimated Detection Level

2) 1 : minimal training, 2 : moderately skilled with method, 3 : experienced.

Table 2.7 Ratings of common chlorine analytical methods vs. the ideal method

AWWA Quality Concept	DPD Colormetric	DPD Titration	Idometric	Amperometric Titration forward	Amperometric Titration back	FACTS
Specificity	7	5	2	6	2	8
Selectivity	7	7	4	5	6	7
Accuracy	8	7	5	7	6	5
No dilution required	7	8	6	8	8	8
Can automate	9	3	3	2	2	4
No special skill	9	8	8	2	1	8
Fast procedure	8	5	5	3	2	6
Cost effective	9	7	6	4	3	6

1 = does not meet quality concept

10 = meets quality concepts fully



Fig 2.28 Pocket colorimeter and Test kit

In electrolysis of seawater, it should be noted that the concentration of residual chlorine changes due to a variety of factors, such as the time of electrolysis reaction, the amount of current, pH, temperature, various organisms presented in seawater and organic matter. It is required to clean sample cell before placing the specimen in the sample cell before measuring the total residual chlorine concentration. While these DPD methods take longer time to pretreat and analyze samples, the electrochemical amperometry is simpler and faster to measure. Particularly, with the need for real-time monitoring measuring equipment, the current method was studied. Electrode sensors, which measure common residual chlorine, are the ideal method for real-time monitoring because these are easy to maintain and are not subject to small changes in chlorine concentration, sample pH, temperature, flow or pressure. However, the electrode method should be equipped with sample lines for collecting samples in real time. In addition, it should also be taken to manage and protect electrodes and equipment because electrodes are installed in environments that are highly humid and corrosive.

2.2.3 Review of previous study on biofouling control by electrochlorination

It is very attractive method that HClO which is produced through electrolysis of seawater could inhibit growth of marine organisms. That is because this method is more effective and safe than existing method. The principal objective of these studies is to evaluate disinfection effect of HClO made by electrochlorination and suppression of marine organisms.

Yang, et al.,¹⁶⁾ conducted an experiment about disinfection effect by electrolysis. Authors tried to confirm disinfection effect by performing both anodic reaction and cathodic reaction in different solutions: tap water, 3% NaCl solution, natural seawater. In case of tap water, 5 minutes after anodic reaction, viruses on the shale were observed. Conversely, in both 3% NaCl solution and natural seawater, no virus on the shale was observed (see Fig 2.29). From these results, authors confirmed that HClO made by electrolysis of solution containing salt could be an attractive antiseptic.

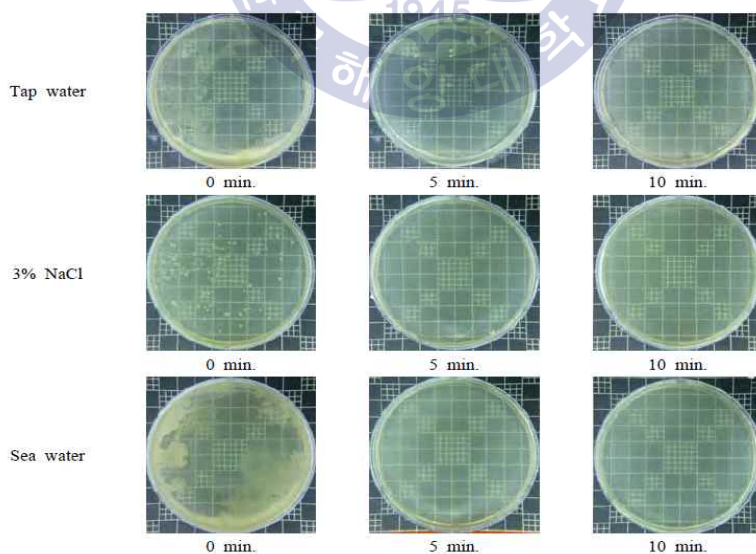


Fig 2.29 The results of pathogen culture for each solution

Muhammad Saleem¹⁷⁾ searched how much HClO produced by electrochlorination have impacts on either bacteria or protozoa. It affected viruses and fungi as well as bacteria (see Table 2.8). Moreover, in 1 mg/L of residual chlorination concentration, authors figured out that it also influenced with protozoa (see Table 2.9).

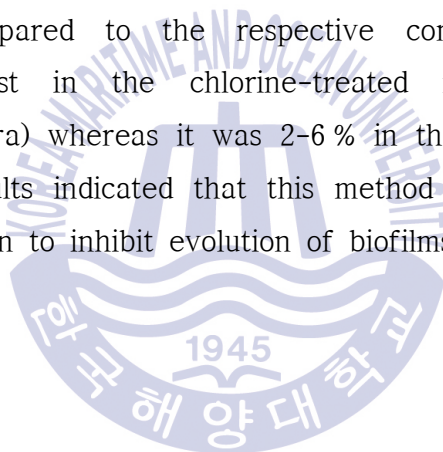
Table 2.8 Effect of chlorination on inactivating selected bacteria

Bacteria	Cl ₂ Residual (mg/L)	Temp (°C)	pH	Contact Time (min.)	Reduction (%)
<i>Campylobacter jejuni</i>	0.1	25	8.0	5	99.99
<i>Escherichia coli</i>	0.2	25	7.0	15	99.99
<i>Legionella pneumophila</i>	0.25	21	7.6–8.0	60–90	99
<i>Mycobacterium chelonae</i>	0.7	25	7.0	60	99.95
<i>Mycobacterium fortuitum</i>	1.0	20	7.0	30	99.4
<i>Mycobacterium intracellulare</i>	0.15	25	7.0	60	70
<i>Pasteurella tularensis</i>	0.5–1.0	10	7.0	5	99.6–100
<i>Salmonella Typhi</i>	0.5	20	7.0	6	99
<i>Shigella dysenteriae</i>	0.05	20–29	7.0	10	99.6–100
<i>Staphylococcus aureus</i>	0.8	25	7.2	0.5	100
<i>Vibrio cholerae</i> (smooth strain)	1.0	20	7.0	<1	100

Table 2.9 Effect of chlorination on inactivating selected protozoa

Protozoa	Cl ₂ Residual (mg/L)	Temp (°C)	pH	Contact Time (min.)	Reduction (%)
<i>Cryptosporidium parvum</i>	80	25	7.0	90	90
<i>Entamoeba histolytica</i>	1.0	22–25	7.0	50	100
<i>Giardia lamblia</i>	1.5	25	6.0–8.0	10	100
<i>Naegleria fowleri</i>	0.5–1.0	25	7.3–7.4	60	99.99

Jagadish S. Patil, et al.,¹⁸⁾ figured out antifouling efficiency of commonly available chlorine at different concentrations (0.5 %, 1 % and 2 %) and exposure time (0.5 min, 1 min, 5 min and 15 min). After chlorination, it observed that growth of diatoms from the mono-species and multiple species were inhibited and that in case of Navicula, Amphora and natural biofilms, the decline in cell densities was 67 %, 64 % and 40 % respectively (see Fig 2.30). In addition, the results of the chlorophyll analysis of control and chlorine-treated biofilms figured out that chlorine at all concentration and exposure time resulted in a considerable reduction in the biofilm chlorophyll concentrations as compared to non chlorine-treated biofilms. When compared to the respective controls only 1-8 % of chlorophyll was exist in the chlorine-treated mono-species biofilms (Navicula and Amphora) whereas it was 2-6 % in the natural biofilms (see Fig 2.31). These results indicated that this method could be regarded as the way of disinfection to inhibit evolution of biofilms.



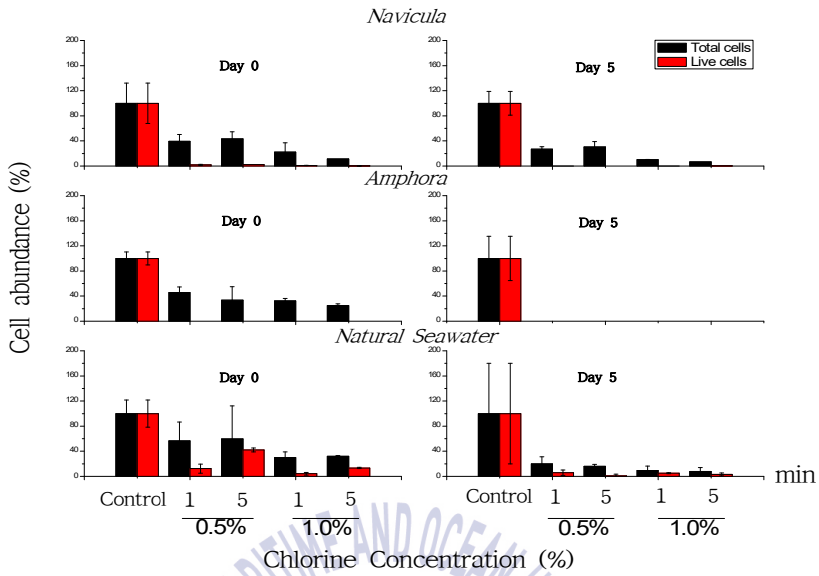


Fig 2.30 Effect of chlorine concentration and exposure time on the growth of mono-species (*Amphora* and *Navicula*) and natural biofilms

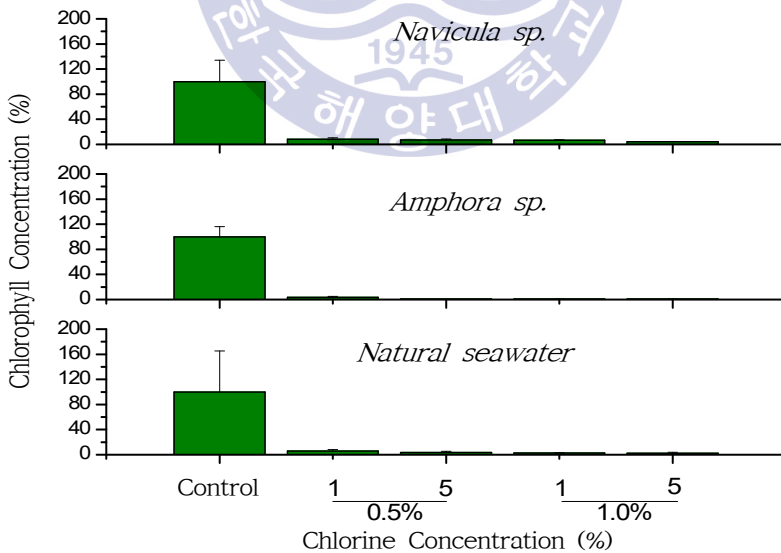


Fig 2.31 Effect of chlorine concentration and exposure time on concentration of chlorophyll 'a' in mono-species and natural biofilms

Henk A. Jenner, et al.,¹⁹⁾ figured out effectiveness of residual chlorine to marine species. In the case of the bacteria slime, it turned out that only concentration of residual chlorine at 0.1 mg/L enables bacteria slime to become extinct. Also, roughly 95 % of Zebra Mussels were eliminated at concentration of residual chlorine at 0.5 mg/L. However, at low temperature which is 0 to 4 °C, effects were only partially identified (see Table 2.10).



Table 2.10 Mortality of adult and juvenile zebra mussels exposed to continuous low-level chlorination

Experimental conditions	TRC (mg/L)	Exposure time : t (days) Mortality rate ; M (%)
Thames River, Adults T= 10°C T= 10°C T= 10°C T= 21°C T= 21°C T= 21°C	0.5 2.0 5.0 0.25 0.5 2.0	t = 7 d M = 5 % t = 7 d M = 20 % t = 7 d M = 40 % t = 7 d M = 40 % t = 7 d M = 70 % t = 7 d M = 100 %
Meuse river, Adults T = 14.5°C	0.3 1.1 1.5	t = 44 d M = 0 % t = 41 d M = 65 % t = 35 d M = 83 %
The Netherlands Adults T = 12 to 15 °C	0.25 0.5 1.0	t = 21 d M = 90 % t = 16 d M = 93 % t = 14 d M = 95 %
Niagara river. Adults T = 9.0 to 15.0 °C T = 9.0 to 15.0 °C T = 9.0 to 15.0 °C T = 18.0 to 21 °C	0.2 0.5 1.0 0.5	t = 27 d M = 50 % t = 27 d M = 50-70 % t = 27 d M = 100 % t = 9 d M = 100 %
Shell length : 10-15 mm T = 12 to 15 °C T = 12 to 15 °C T = 17 to 27 °C T = 17 to 27 °C T = 17 to 27 °C	0.5 1.0 0.5 0.9 3.0	t = 17 d M = 93 % t = 15 d M = 95 % t = 9 d M = 100 % t = 5 d M = 100 % t = 6 d M = 100 %
Shell length : 14-16 mm T = 7.2 to 17.5 °C T = 7.2 to 17.5 °C T = 4.8 to 9.5 °C T = 4.8 to 9.5 °C T = 4.8 to 9.5 °C	0.32 0.62 1.74 4.3 9.02	t = 54 d M = 50 % t = 32 d M = 50 % t = 17 d M = 50 % t = 25 d M = 50 % t = 20 d M = 50 %
Shell length : 2-6 mm T = 20 to 22 °C T = 20 to 22 °C T = 20 to 22 °C T = 20 to 22 °C	0.5 1.0 2.5 5.0	t = 20 d M = 7 % t = 13 d M = 100 % t = 9 d M = 100 % t = 7 d M = 100 %
Shell length : 2-5 mm T = 8 to 12 °C T = 10 to 11.5 °C T = 21.5 to 24 °C	1.0 0.6 ± 0.2 0.6 ± 0.2	t = 28 d M = 70 % t = 15 d M = 40 % t = 8 d M = 100 %
Shell length : 0.75-2.0 mm T = 8 to 12 °C	1.0	t = 25 d M = 100 %
Lake Erie. Adults T = 0 to 4 °C	0.3 to 0.5	t = 27 d M = 30 %

2.3 Technology to control corrosion and biofouling

2.3.1 Current technology to control corrosion and biofouling

A cathodic protection device, ICCP (Impressed Current Cathodic Protection), has been used to protect the outer surface of structures such as ships and marine structures from corrosion (see Fig 2.32). However, this device can protect only the outer surface, not the inner surface. Therefore, available devices cannot effectively protect the inner surface of the seawater pipes from corrosion. In addition, the coating technology has been used for protect the inner and outer surface from corrosion; however, coating could crack and thus become unable to reduce corrosion rate or prevent degradation of surfaces during their exposure to corrosive environment.

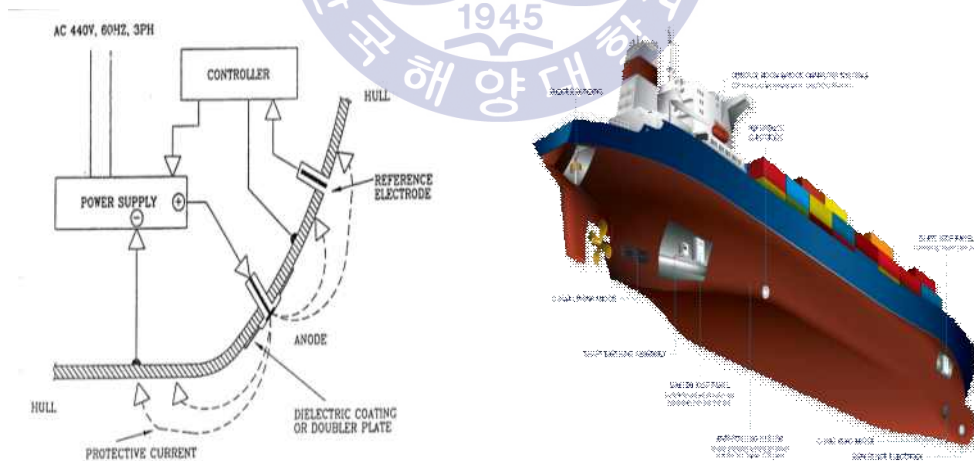


Fig 2.32 Principle of ICCP for ship's hull corrosion protection

MGPS (Marine Growth Preventing System) that dissolves copper anodes and electrolyzes seawater to suppress marine organisms has been used as a marine growth suppressing device for ships (see Fig 2.33). Previous equipment, which dissolves copper anodes, is not suitable for the facilities such as, LNGC (Liquified Natural Gas Carrier), power plants, and ocean offshore plants, which use coolants in large quantities. In comparison, even though HClO sprays have an outstanding effect on contamination in large area, corrosion can occur on the cooling piping system whenever the HClO concentration increases. Therefore, the available technology cannot effectively prevent the problems caused by corrosion damage and biofouling in the piping system.



Fig 2.33 Schematic drawing of the MGPS

MGPS made by Cathelco is the facility that adjusts and provides direct current with both MG (Marine Growth: Cu) to suppress marine organisms and TC (Trap Corrosion: Al) to avoid corrosion. However, due to the increased DC power supply required to completely decimate marine organisms, the consumption rate of the anode and, accordingly, the cost of facility management, quickly increase. Furthermore, the effect of the TC anode installed to prevent galvanic corrosion is insufficient and more and more pipes get damaged by galvanic corrosion. In the case of the chlorination facilities, even if marine organisms cannot be become extinct or are decimated, the high HClO concentration can affect marine environment, since the K.C. Ltd chlorination facility, which produces HClO and injects it to the seawater intake (see Fig 2.34), simply does not take into consideration the supply current. Consequently, until now, facilities equipped with a combined control system that would be able to both prevent the corrosion of the inner surface of pipes and inhibit biofouling, are still lacking.

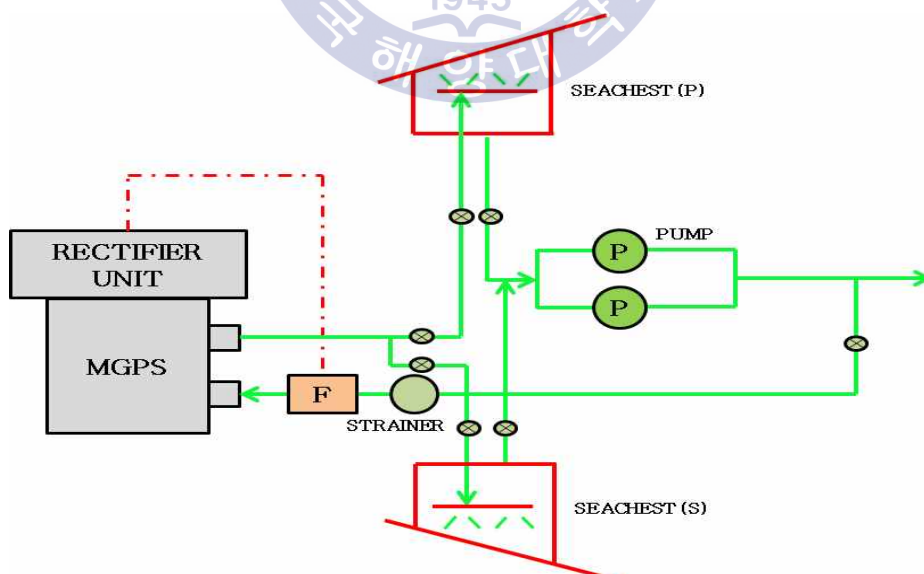


Fig 2.34 Schematic piping diagram of the chlorination type MGPS

2.3.2 Hybrid technology for cathodic protection and electrochlorination

Connecting an insoluble anode to the positive pole of the DC power unit and a negative pole to the piping to apply cathodic protection current to the inner surface of pipe prevents corrosion and creates an environment where marine organisms can hardly grow due to HClO produced by cathodic protection current. However, since the novel hybrid technology is too low HClO concentration only produced by cathodic protection current to decimate marine organisms, an additional DC power unit and the insoluble anode and cathode to electrolyze large quantities of seawater into the cooling water piping system need to be installed (see Fig 2.25). The system provides sufficient HClO concentration for the entire system by adding HClO generated by the cathodic protection current and electrochlorination system while preventing the inner surface of pipe from corrosion. Novel technology can not only prevent the corrosion of the inner surface of pipe by measuring the cathodic protection potential and by applying the cathodic protection current, but also monitor the HClO concentration in real time to maintain minimum HClO concentration.

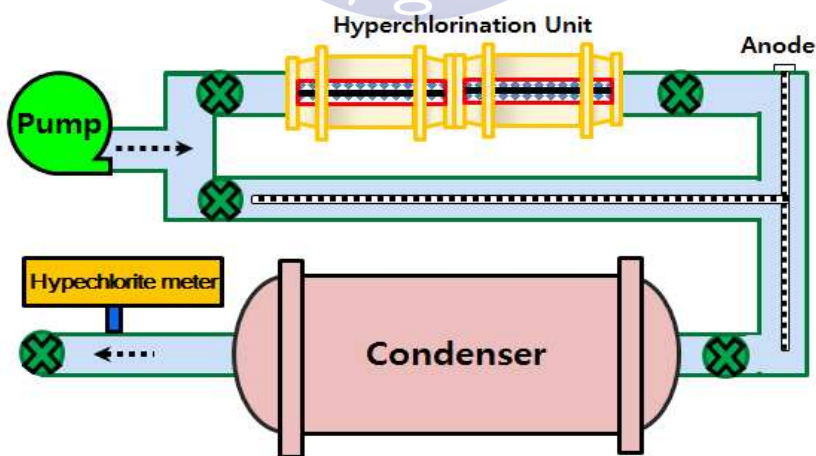


Fig 2.35 Schematic piping diagram of hybrid technology for cathodic protection and HClO generation

Chapter III

EXPERIMENTAL METHOD

3.1 Test outlines

The test of this study consists of the following four major tasks:

- (1) Electrochemical polarization test is to provide a baseline for the investigation and characterization of different environmental variables, such as temperature, flow rate, fresh water, and seawater.
- (2) Cathodic protection test in the beaker is to verify the effective of cathodic protection on small carbon steel specimens and the cathodic protection current density in different solutions and flows.
- (3) Cathodic protection test in the cistern is to verify feasibility and effectiveness of cathodic protection on the inner surface of pipe in different solutions and flows.
- (4) Cathodic protection and electrochlorination test in engine room is to verify the effectiveness of cathodic protection on the inner surface of pipe and whether or not hypochlorous acid concentration could be produced and adjusted while preventing pipe from corrosion.

3.2 Laboratory tests

3.2.1 Materials and specimens

(1) Materials

The material under study was carbon steel that have been used for piping system in usual and broad manner. In addition, to verify galvanic corrosion repercussion by connecting with dissimilar metals, copper alloy was used. The elemental composition for these specimen is shown in Table 3.1.

Table 3.1 Chemical composition of specimen

Material \ Elements	C	Si	Mn	P	S	Fe
KS D 3507	0.07	0.01	0.4	0.014	0.007	Bal.

Material \ Elements	Fe	Ni	Pb	Zn	Mn	Cu
C70600	1.0~1.8	9.0~11.0	≤0.05	≤1.0	≤1.0	Bal.

(2) Specimens

1) Electrochemical polarization test

General carbon steel normally used for seawater pipe was selected as the research material. The specimen was processed into rectangular blocks of the following dimensions length × height × width = 50 × 25 × 5 (in mm). Copper wire was connected and then coated with insulation tape and glue to seal other parts, leaving the working surface so that the corrosion surface of the area of 2.25 cm² was exposed to the solution. The appearance of specimen is shown in Fig 3.1.

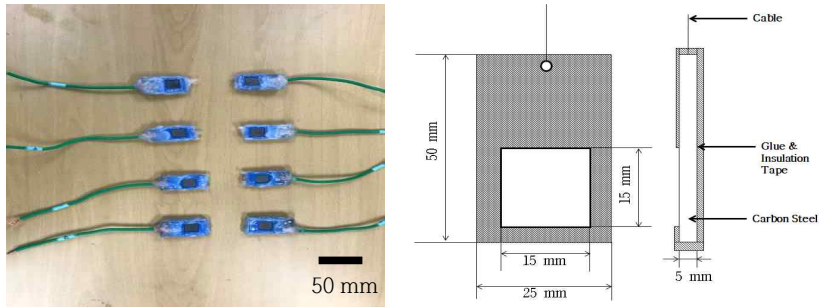


Fig 3.1 Photograph and schematic diagram of specimen for electrochemical polarization test

2) Cathodic protection test in the beaker

General carbon steel normally used for seawater pipe was selected as the research material. The specimen was processed into rectangular blocks of the following dimensions length \times height \times width = 25 \times 25 \times 5 (in mm). Copper wire was connected and then coated with insulation tape and glue to seal other parts, leaving the working surface so that the corrosion surface of the area of 2.25 cm² was exposed to the solution. The appearance of specimen is shown in Fig 3.2.

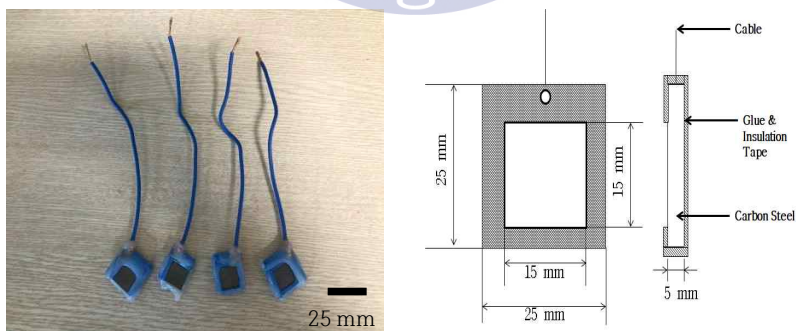


Fig 3.2 Photograph and schematic diagram of carbon steel specimen for cathodic protection test in the beaker

3) Cathodic protection test in the cistern

Specimens that were used for cathodic protection test in the cistern and a schematic diagram of specimen are shown in Fig 3.3. The kinds of specimens were as follows : carbon steel, copper alloy and the size of specimens was as follows: 100 mm × 100 mm × 5 mm. The hole to electrically connect each specimen was made on the one side of the exposed specimen.

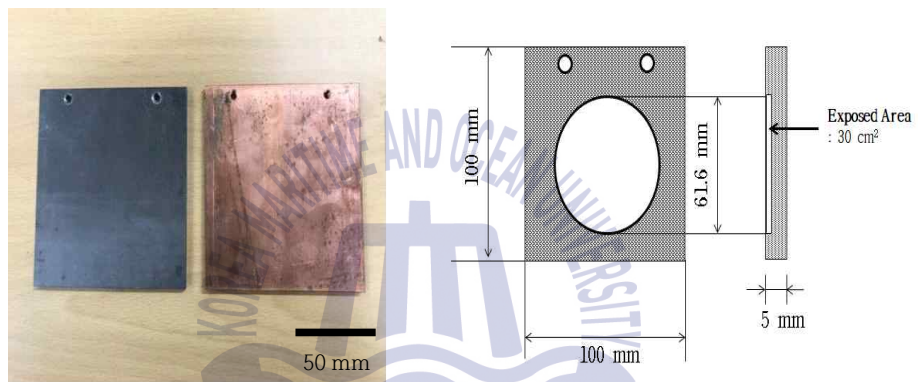


Fig 3.3 Photograph and schematic diagram of specimen for cathodic protection test in the cistern

3.2.2 Test apparatus

(1) Electrochemical polarization test

A schematic diagram of electrochemical polarization test and the overall appearance of the test apparatus are shown in Fig 3.4. The experiments focused on the electrochemical polarization characteristics according to various factors, such as fresh water, seawater, flow rate and, temperature were performed. To adjust both the flow rate and the solution temperature, a hot plate stirrer was used. The silver-silver/chlorine electrode was used as the standard electrode, and a platinum electrode was used for the counter electrode. Electrochemical polarization test was performed by a potentiostat (Gamry Instrument, Reference 600).

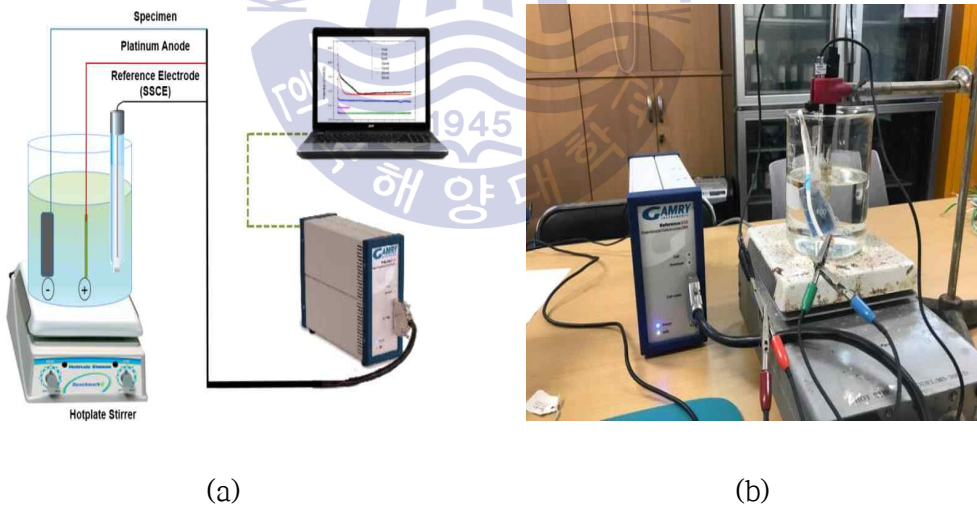
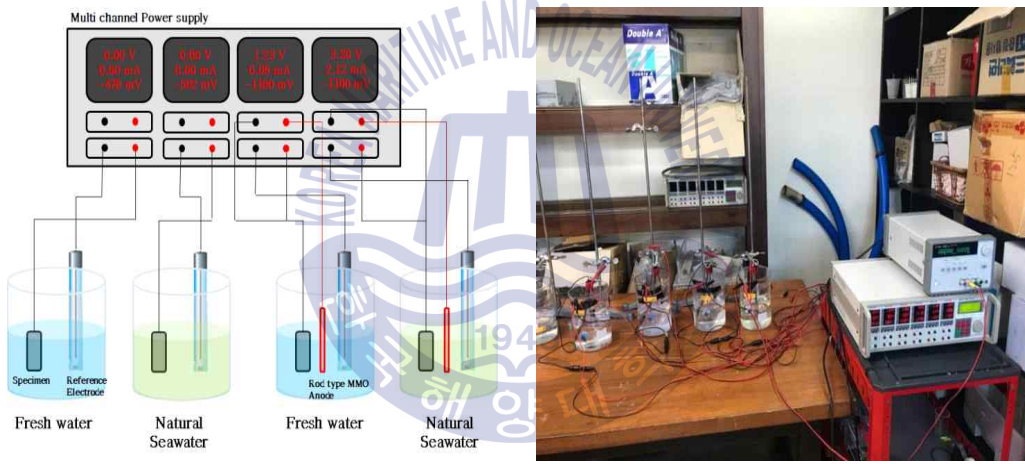


Fig 3.4 Test apparatus for electrochemical polarization test, (a): Schematic diagram, (b): Overall appearance

(2) Cathodic protection test in the beaker

A schematic diagram and the overall appearance of the test apparatus for cathodic protection test in the beaker are shown in Fig 3.5. Test apparatus was prepared using a beaker filled with fresh water and seawater (about 1 L). The silver-silver/chlorine electrode was used as the standard electrode and the rod type MMO (mixed metal oxide) anode was used as the anode. By using the multi channel power supply, we measured potential and applied current in each specimen.



(a)

(b)

Fig 3.5 Test apparatus for cathodic protection in the beaker, (a): Schematic diagram, (b): Overall appearance

(3) Cathodic protection test in the cistern

A schematic diagram and the overall appearance of the test apparatus for cathodic protection test in the cistern are shown in Fig 3.6. The cistern is shown in Fig 3.7. A cistern is a tank with the basic dimension of 1550 mm × 150 mm and the height of 160 mm. five holes of 61.6 mm in the diameter were made on the upper part of tank to expose certain part of specimens to the solution. The size of this part was 30 cm². After the installation of the specimen with the same size of holes, two cisterns were connected with a flexible hose. The auxiliary test apparatus included the rod type MMO anode, the device to control corrosion, the standard reference electrode, and device to measure potential (see Fig 3.8). The MMO anode was installed inside of the tank, and the multi channel power supply was used for both measuring the potential and applying the cathodic protection current.

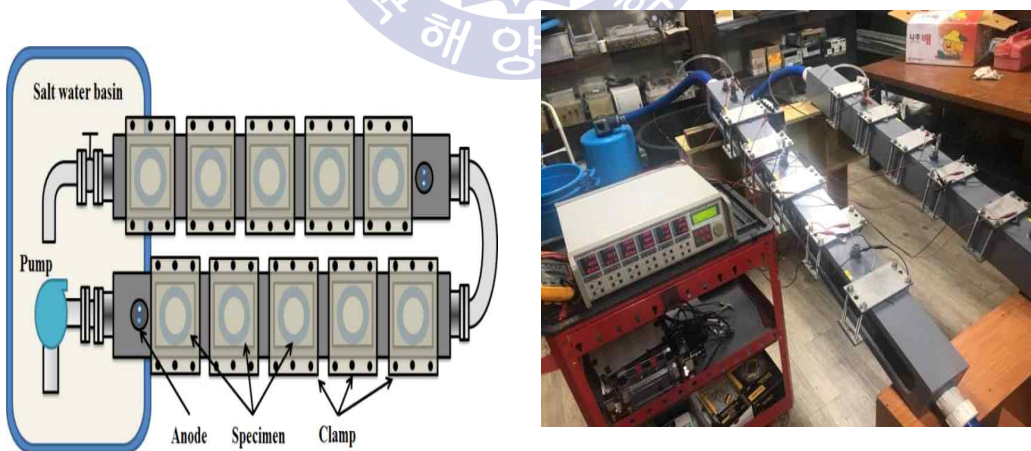


Fig 3.6 Test apparatus for cathodic protection in the cistern, (a): Schematic diagram, (b): Overall appearance

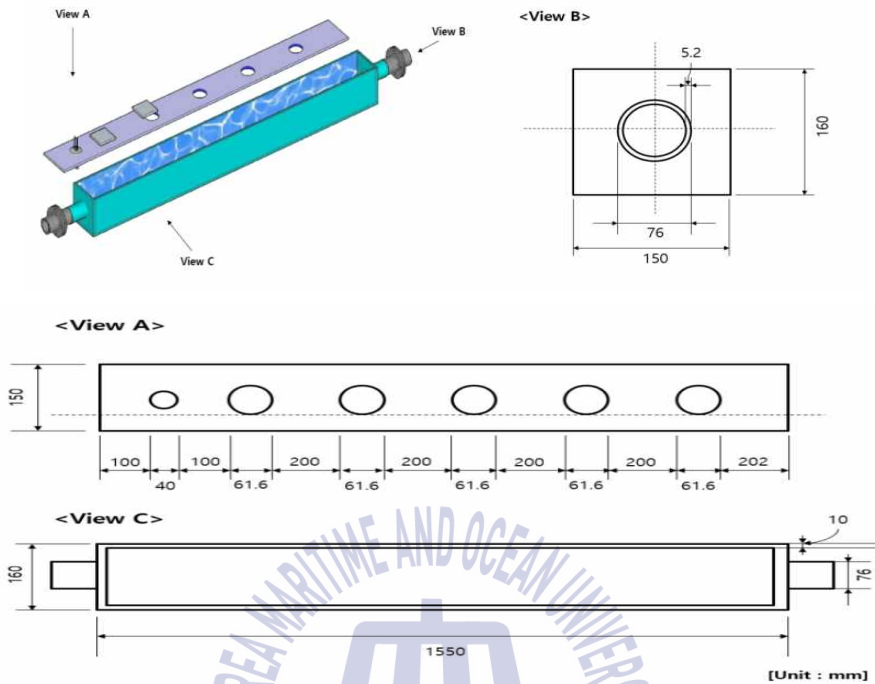


Fig 3.7 Drawing of cistern for cathodic protection test in the cistern



Fig 3.8 Auxiliary test apparatus for cathodic protection in the cistern, (a): Silver-silver/chlorine electrode, (b): Rod type MMO anode

3.2.3 Procedures

(1) Electrochemical polarization test

Fresh water and seawater were used for the experimental solution. Fresh water was general tap water, and seawater containing about 3.5 % of chlorine concentration was taken from the coastal area of the harbor located in Korea Maritime and Ocean University. Experimental temperature was maintained at 25 and 35 °C by putting the beaker containing the solution on a hot plate. The flow rate was set at 20 % output (360 RPM) and 50 % output (900 RPM) of the stirrer. Through this experiment, electrochemical polarization characteristics in specific conditions, such as temperature, salinity, and flow rate, were observed. Each environmental condition and symbol is shown in Table 3.2. The experiment types included anodic polarization, cathodic polarization, polarization resistance, and potentiostatic polarization. Experimental condition of each test is shown in Table 3.3.

Table 3.2 Symbol list of electrochemical polarization test according to conditions

Solution	Temperature	Flow rate	Symbol
Fresh water	25 °C	Static	FW Static 25 °C
		20 % Stirrer	FW 20 % Stir 25 °C
		50 % Stirrer	FW 50 % Stir 25 °C
	35 °C	Static	FW Static 35 °C
		20 % Stirrer	FW 20 % Stir 35 °C
		50 % Stirrer	FW 50 % Stir 35 °C
Seawater	25 °C	Static	SW Static 25 °C
		20 % Stirrer	SW 20 % Stir 25 °C
		50 % Stirrer	SW 50 % Stir 25 °C
	35 °C	Static	SW Static 35 °C
		20 % Stirrer	SW 20 % Stir 35 °C
		50 % Stirrer	SW 50 % Stir 35 °C

Table 3.3 Experimental set up of electrochemical polarization test

Anodic Polarization		Cathodic Polarization	
Initial E (V) vs. Eoc	-0.1	Initial E (V) vs. Eoc	0
Final E (V) vs. Eoc	1.5	Final E (V) vs. Eoc	-1.5
Scan Rate (mV/s)	5	Scan Rate (mV/s)	5
Sample Period (s)	1	Sample Period (s)	1
Sample Area (cm ²)	2.25	Sample Area (cm ²)	2.25
Initial Delay	300 Time (s) 0.0001 Stability (mV/s)	Initial Delay	300 Time (s) 0.0001 Stability (mV/s)

Polarization Resistance		Potentiostatic Scan	
Initial E (V) vs. Eoc	-0.02	Initial E (V) vs. Eoc	0
Final E (V) vs. Eoc	0.02	Initial Time (s)	10
Scan Rate (mV/s)	0.167	Final E (V) vs. Eref	-1.1
Sample Period (s)	1	Final Time (s)	600
Sample Area (cm ²)	2.25	Limit I (mA/cm ²)	25
Initial Delay	300 Time (s) 0.1 Stability (mV/s)	Sample Period (s)	1
		Sample Area (cm ²)	2.25
		Initial Delay	300 Time(s) 0.001 Stability (mV/s)

(2) Cathodic protection test in the beaker

The test was conducted for 7 days. Potential change of specimens that were put in the solutions was measured, and the surface state of specimen was inspected. Two specimens were set in corrosion condition. By contrast, in the other two specimens, cathodic protection current was applied to maintain the cathodic protection potential at $-1,100$ mV/SSCE. In addition, to verify the effect of the flow rates, Each solution was agitated with 20 % output of stirrer. Every 24 hours, the surface state of the specimen was observed. Experimental set up for cathodic protection test in beaker is shown in Table 3.4.

Table 3.4 Experimental set up of cathodic protection test in the beaker

Parameter	Value
Solution	Fresh water / Seawater
Temperature (°C)	25
Flow rate	Static / 20% Stir
Running time (day)	7
Potential setting for cathodic protection (mV/SSCE)	-1,100
Kinds of specimens	Carbon steel

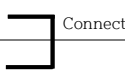
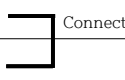
(3) Cathodic protection test in the cistern

The galvanic corrosion caused by connecting with dissimilar metals, such as valves, can be resolved by maintaining the potential at -900 mV/SSCE . Furthermore, it is effective to protect the interior of pipe from corrosion if potential is maintained in the range mostly between $-1,300 \text{ mV/SSCE}$ and $-1,200 \text{ mV/SSCE}^{12}$). Specimens No.1-5 were applied for cathodic protection. By contrast, specimens No.6~10 were set to the natural corrosion condition. Furthermore, to verify the effect of the galvanic corrosion current, specimens No.4 and 10 were set in the galvanic corrosion condition by connecting the carbon steel specimen with the copper alloy specimen. In a test specimen that applied for cathodic protection, the cathodic protection potential was maintained at $-1,100 \text{ mV/SSCE}$; in other cases, in order to compare the results, the specimens were allowed to corrode. Fresh water and seawater were used as experimental conditions. Additionally, to verify the effect of the flow rate, the condition of the non-flow and the flow were created. tests in each condition were conducted for 7 days. Experimental condition is shown in Table 3.5 and arrangement of specimen and anode is shown in Table 3.6.

Table 3.5 Experimental set up of cathodic protection test in the cistern

Parameter	Value
Specimen size (cm)	10 (W) × 10 (H) × 0.5 (D)
Source of water	Tap water / Seawater
Temperature (°C)	25
Running time (day)	7
Flow rate of circulation (L/H)	3400
Kinds of specimens	Carbon steel Copper alloy

Table 3.6 Arrangement of installed specimen and anode

No.	Material	Experimental Condition
	General	
1	CS	Cathodic protection
2	CS	
3	CS	
4	CO 	Cathodic protection (Galvanic condition)
5	CS	
6	CS	Corrosion
7	CS	
8	CS	
9	CO 	Corrosion (Galvanic condition)
10	CS	

CS : Carbon steel, CO : Copper alloy

3.3 Field test

(1) Cathodic protection and electrochlorination test

1) Test apparatus

The experiments using cathodic protection and electrochlorination were conducted by installing experimental equipment to the seawater pipe located in engine room of the training ship *Hanbada* of Korea Maritime and Ocean University. A carbon steel pipe normally used for the engine room seawater pipe was used. The diameter of the pipe was 40 mm and it was cut every 300 mm and welded with flange taking into account its workability. Insulated flange was made to set up the reference electrode to measure the potential of the pipe and the insoluble anode for cathodic protection. Moreover, insulated flange had not only the air venting valve, but also the sampling valve to get rid of the air in the cooling seawater pipe (see Fig 3.9).

Fig 3.10 shows a schematic diagram and appearance of the anode installed in the pipe. An electric cable and the anode were connected and covered by using epoxy and hardener, and electric cable was extracted through the hole located on the insulation flange. By using the cable tie, the anode was held in order to avoid its touching the pipes that played the role of the cathode.

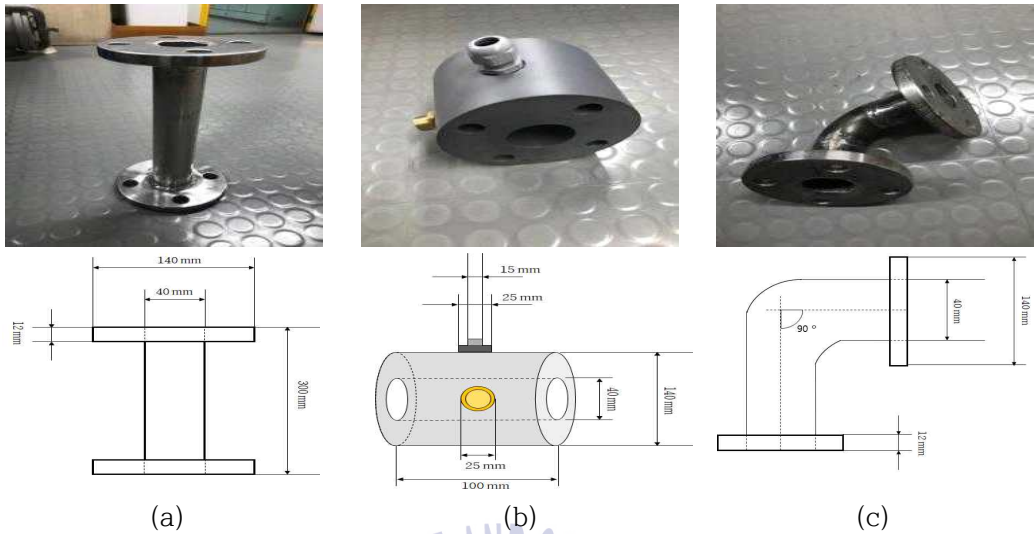
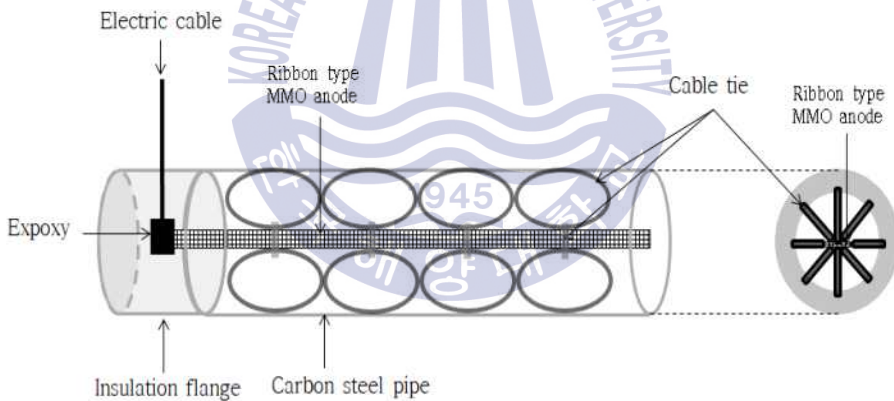


Fig 3.9 Pipe specimens for cathodic protection and electrochlorination, (a): Pipe with flange, (b): Insulation flange with hole, (c): Elbow with flange



(a) Connection anode with electric cable



(b) Cable tie installed on anode



(c) Installing & holding of anode

Fig 3.10 Schematic diagram and appearance of anode installed in the pipe

By using the fabricated carbon steel piping parts, the experiment was structured (see Fig 3.11). The test apparatus was connected to the inlet and outlet lines of the low temperature cooler in the engine room. Fig 3.12 shows the test apparatus. The inlet and outlet lines were equipped with a valve to regulate the influx of seawater and a flexible hose which is for connection with the equipment. At the entrance, the electrochlorination facility was installed, and insulated flanges were installed in front and behind the facility. The MMO ribbon anode was used for the anode of electrochlorination; a carbon steel pipe manufactured for the cathode was used. Three carbon steel pipes and one elbow for the cathodic protection experiment were then connected in a series, and an isolated flange with a standard electrode was installed. Then, one elbow and three carbon steel pipe were connected in a series. In addition, the insulated flange installed air vent valve was connected, and the flexible hose and the valve were installed to connect to the outlet.

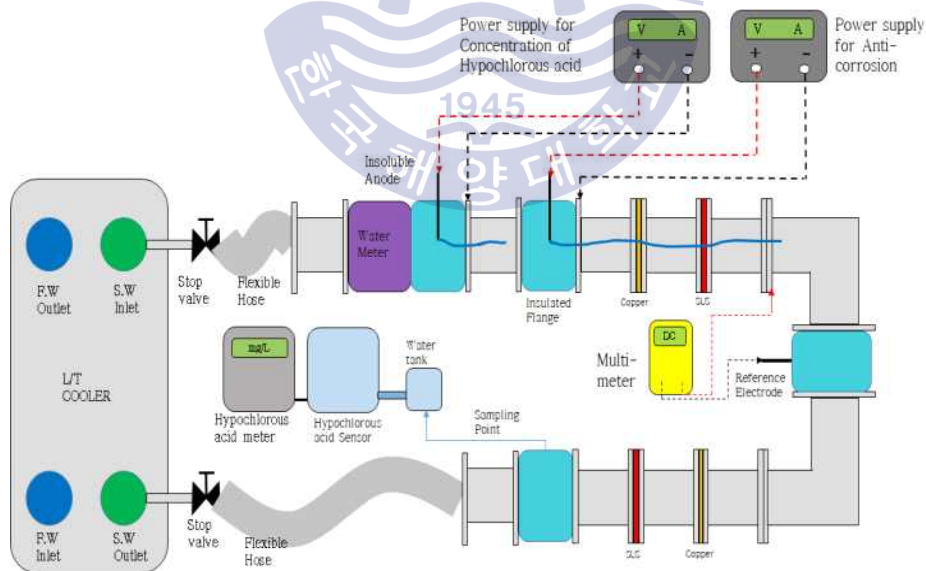


Fig 3.11 Configuration of test apparatus connected to seawater pipe in engine room of T/S Hanbada



(a)



(b)

Fig 3.12 Photograph of test apparatus for cathodic protection and electrochlorination, (a): Appearance of pipe, (b): Appearance of flexible hose connected with seawater pipe

The auxiliary test apparatus is illustrated in Fig 3.13. A flow meter was installed to measure the flow rate. The flow meter is accurate and durable-product that could perform measurement in the range from 1 to 30 m³/h. A power supply was used to supply external power for cathodic protection and electrochlorination. A Fluke multi meter was used to measure potential. In addition, a portable chlorine tester made by Hach was used to measure the HClO concentration.



Fig 3.13 Auxiliary test apparatus for cathodic protection and electrochlorination, (a): Flow meter for measuring flow rate, (b): Power supply for cathodic protection and electrochlorination, (c): Fluke multi meter (d) : Portable chlorine tester made by Hach

Aqua2000-FCL (Suntech engineering, South Korea) was used to measure HClO produced by electrochlorination in real-time. Specification of the residual chlorine sensor is shown in Table 3.7 and the appearance of the residual chlorine sensor is shown in Fig 3.14. In addition, the electrode sensor is shown in Fig 3.15.



Fig 3.14 Appearance of free chlorine meter

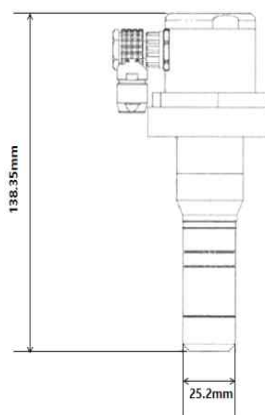


Fig 3.15 Photograph and schematic diagram of chlorine sensor

Table 3.7 Specification of chlorine sensor

Chlorine Sensor Specification	
Measurement System Performance	
Type of measurement	: Polarograph Amperometric : pH, Auto compensation of water temperature
Range	: 0 to 2/5/10/20 mg/L (User setting)
Minimum detection limit	: 0.01 mg/L
Accuracy	: ± 0.01 mg/L
Unit of measurement	: Chlorine (mg/L, Free chlorine), Water temperature($^{\circ}$ C), Potential of hydrogen(pH)
Response time	: 90 %, in 90 seconds
Cleaning method	: Auto cleaning by draining
Measurement option	: If pH sensor is added together, the correlation curve between HOCl ⁻ and OCl ⁻ is calculated by pH calibration
Construction	
Structure of electrode	: Protected by membrane cap
Material	: Electrode - Gold Cathode, Silver Anode : Temperature electrode - Platinum(PT1000 Ω)
	: Membrane - High intensity Teflon
	: O-rings - Viton
	: Measurement unit - Acrylic, Black ABS(Optional)
	: Body - CPVC
Construction	: Water proof(IP68), Corrosion resistance, Chemical resistance
Operational Environment	
Temperature range	: 0 to 70 $^{\circ}$ C (Water), -20 to 70 $^{\circ}$ C (Atmosphere)
Maximum pressure	: 15 psig @ 45 $^{\circ}$ C
Maximum flow rate	: 200 to 500 mL/min

2) Procedure

The experiment was conducted to verify the HClO concentration by electrochlorination in the vicinity of the anode by the DC current while applying the current using the external power applied for cathodic protection. To verify the performance of the external power cathodic protection and the electrochlorination facility under various flow rates, the flow rate was altered step by step. The cathodic protection potential, which is the difference between the standard electrode and the potential of the pipe, was measured by a Fluke multi meter. The HClO concentration was measured by the DPD (N,N' -diethyl-p-phenylenediamine) method using a Hach Pocket Colorimeter, and a sample was taken from the sampling line installed at the outlet of the experimental apparatus. Moreover, free chlorine meter, which is an electrochemical measurement method by the electrode, was used to monitor the HClO variation, as the measurement method by the DPD method had limitations in terms of measuring the HClO of the sample in real-time. Experimental condition is shown in Table 3.8.

Table 3.8 Experimental set up of cathodic protection and electrochlorination

Parameter	Value
Solution	Seawater
Temperature (°C)	12.6 to 13.2
pH	8.20 to 8.25
Running time (day)	30
Flow rate (m ³ /h)	3
	6
	9
	11
	15
Potential setting for cathodic protection (mV/SSCE)	-900
	-1,000
	-1,100
	-1,200

Chapter IV

RESULTS AND DISCUSSION

4.1 Test results of corrosion control

Fig 4.1 shows the results of the polarization resistance test of specimens in fresh water and seawater. Polarization resistance test was performed in the range of ± 20 mV/SSCE without any change of factors, such as the flow rate and temperature. Typically, the slope of polarization curve, defined as polarization resistance, is inversely proportional to the corrosion rate. In this test, the slope of the polarization resistance curve in fresh water was larger than in seawater, suggesting that the corrosion rate in fresh water is smaller than in seawater. This result was calculated into the corrosion rate and the corrosion current density (see Fig 4.2).

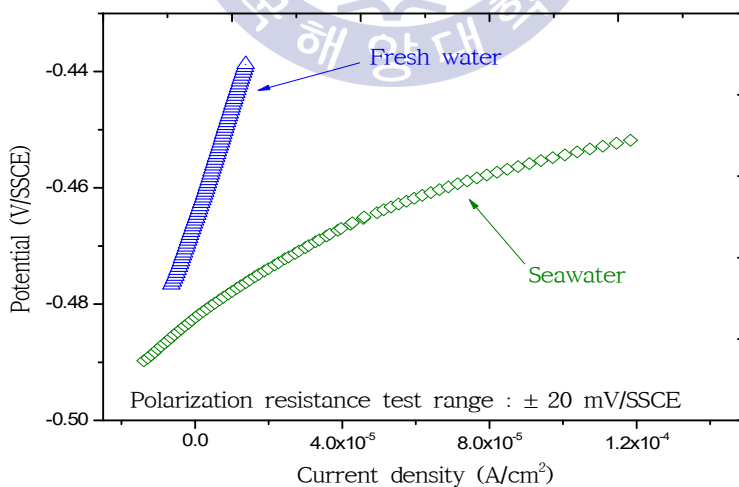
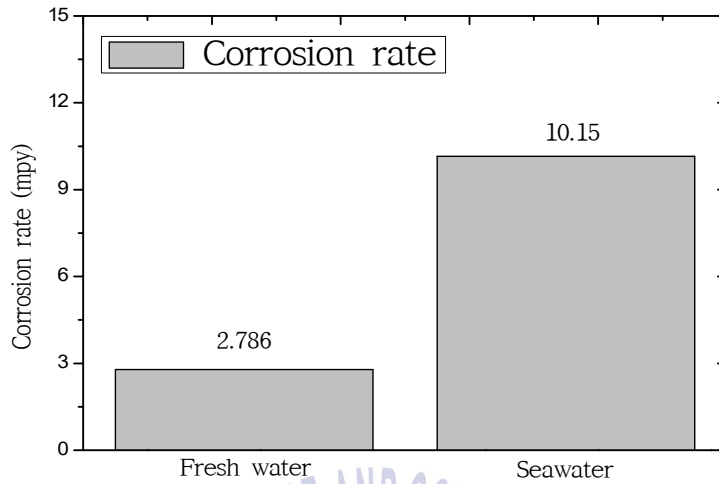
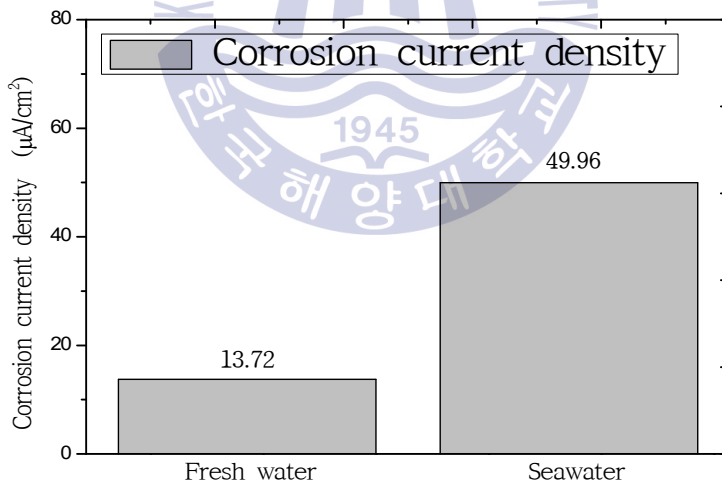


Fig 4.1 Polarization resistance test results of carbon steel specimen in fresh water and seawater with the range of ± 20 mV/SSCE

Based on the results of polarization resistance, the corrosion rate and corrosion current density in fresh water and seawater were calculated (see Fig 4.2). Specifically, the corrosion rate in 25 °C fresh water was 2.789 mpy (milis penetration per year), while that in 25 °C seawater was 10.15 mpy. Therefore, the corrosion rate in seawater is approximately 3.6-fold higher than in fresh water. In addition, corrosion current density in 25 °C fresh water was 13.72 $\mu\text{A}/\text{cm}^2$, while in seawater, it amounted 49.96 $\mu\text{A}/\text{cm}^2$. Thus, the corrosion current density in seawater is approximately 3.6-fold higher than in fresh water. According to previous researches, Ahmad Royani⁴⁷⁾ et al. reported that the corrosion rates of various carbon steels in raw water for cooling system are 4.219–6.805 mpy at 32°C. In addition, according to R.Winston revie⁴⁶⁾, the average corrosion rate of steel in static air-saturated soft waters at ordinary temperatures is roughly 4 mpy. These results are roughly similar to the results of our test. With respect to seawater, overall corrosion rates of steel continuously immersed in quiescent seawater at many locations throughout the world for periods from <1 year to 40 years collected from various literature are in range from 0.8–14.6 mpy, and the average rate is 4 mpy. Furthermore, the corrosion rate of carbon steel in seawater averages 2 mpy for the first 20 years, then drops to 1 mpy. The decrease of corrosion rate with time has been more clearly shown in corrosion test in which steel was continuously immersed in seawater⁴⁶⁾. Therefore, in terms of long period, it seems that the corrosion rate of fresh water and seawater is nearly the equal level. However, our test results in seawater are slightly higher than the results previously reported by many authors. It seems that this is because the test was performed for an extremely short time.



(a)



(b)

Fig 4.2 Comparison of corrosion rate and corrosion current density calculated from polarization resistance test result in fresh water and seawater, (a): Corrosion rate, (b): Corrosion current density

Fig 4.3 shows the results of the anodic polarization test in 25 °C and 35 °C fresh water and seawater. The corrosion potential in seawater, which contains many corrosive factors, was slightly lower than in fresh water. With an increase of the temperature increases of both solutions, a higher current density was observed in both. The current density in 25 °C seawater was 150-fold higher than in 25 °C fresh water. This is because Cl^- , which is adsorbed to the metal surface, causes the exchange current density for the anode dissolution to increase, accelerating activation dissolution reaction while reducing overpotential³⁹). The current density in 35 °C fresh water was 3-fold higher than in 25 °C fresh water. Furthermore, the current density in 35 °C seawater was 3-fold higher than in 25 °C seawater. These results are similar to the results previously reported by Kim³⁷) and Lee¹²). With an increase of temperature, current density and corrosion rate also increase since the level of activity for ions that participate in the reaction increases by altering free energy. Therefore, when performing anodic polarization, we could verify that the current density increases in seawater rather than in fresh water, and at higher temperatures as the potential rises.

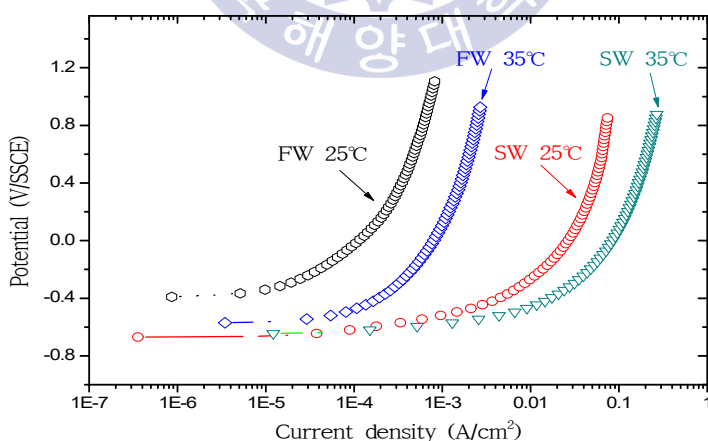


Fig 4.3 Variation of anodic polarization as a function of different solutions and temperatures

Fig 4.4 shows the results of the cathodic polarization test conducted in fresh water and seawater at 25 °C and 35 °C. In the cathodic polarization curves of fresh water, activation and concentration polarization by the reduction of dissolved oxygen appeared. In the cathodic polarization curves of seawater, concentration polarization by the reduction of dissolved oxygen and activation polarization by generating hydrogen gas appeared. The results of the experiment in both conditions demonstrated that the potential in seawater that contains a lot of corrosive factors was slightly lower than in fresh water. In the division of activation polarization, the current density in 25 °C seawater was 2-fold higher than in fresh water. In comparison of fresh water at 25 °C and at 35 °C, the current density in the latter was 3-fold higher than in the former. Furthermore, the current density of seawater at 35 °C was 3-fold higher than at 25 °C. Concentration polarization is an electrochemical reaction governed by diffusion of ions in solution; the phenomenon of polarization is caused by the concentration difference between the electrolyzed solution and the polarized surface. In this division, the increase of current density is stagnant, because the reduction rate of oxygen on the surface of the electrode increases, consuming oxygen ions that are close to the metal surface. In addition, the concentration polarization gap was reported to narrow due to the reduction of dissolved oxygen levels due to the increase of seawater temperature³⁷. In the present study, in our comparison of the divisions in concentration polarization, at 25 °C, the current density in seawater was 40-fold higher than in fresh water of the same temperature. Furthermore, in the comparison of fresh water at 25 °C and at 35 °C fresh water, the current density in the latter was 3-fold higher than in the former. Therefore, as suggested by our results, the lower potential, the greater difference in current density. When compared to difference of temperature, a slight increase in current density was observed in high temperature environments. This means that limit diffusion current density increases due to a rise of the level of activity of ions in high temperature environments. Combined results of anodic and cathodic polarization curves are shown in Fig 4.5.

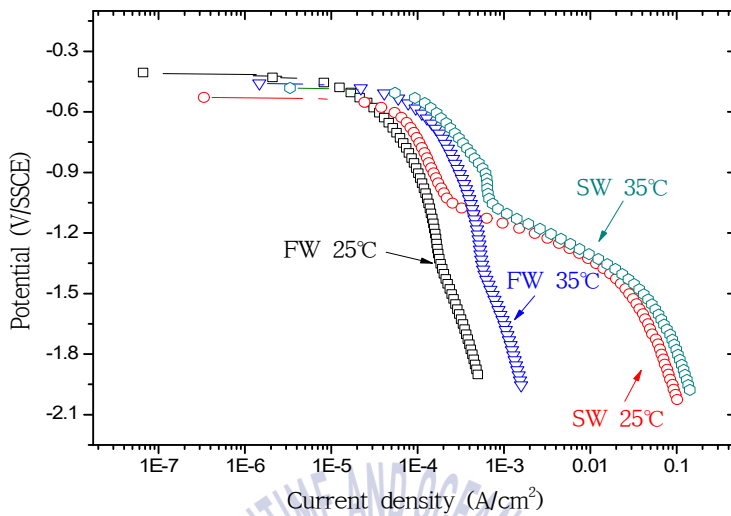


Fig 4.4 Variation of cathodic polarization as a function of different solutions and temperatures

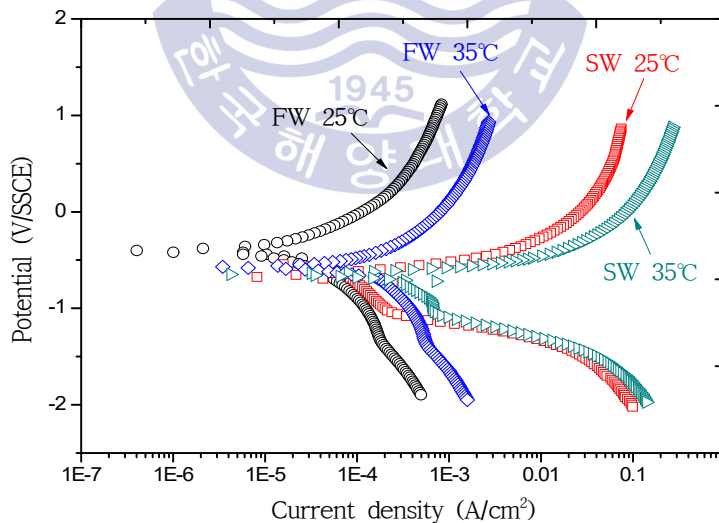


Fig 4.5 Polarization curve for carbon steel specimens as a function of different solutions and temperatures

Fig 4.6 compares the results of potentiostatic polarization test with the changes in temperature and the flow rate in fresh water. Potential was set at $-1,100\text{ mV/SSCE}$. In all conditions, at the beginning of the test, there was a general tendency for a high cathodic protection current density, while its current density gradually decreased over time. The magnitude of current density also increased with an increase of the temperature and flow rate. Because increased flow at the surface and temperature could change the limiting current density, resulting in that the corrosion rate increases. It has a massive effect on the degree of protection when cathodic current is held constant. Therefore, to compensate for the greater limiting current density, applied current also increased. The lowest current density of approximately $70\ \mu\text{A}/\text{cm}^2$ was observed in $25\ ^\circ\text{C}$ static fresh water. The highest current density of approximately $370\ \mu\text{A}/\text{cm}^2$ was observed in $35\ ^\circ\text{C}$ 50 % stir fresh water. The difference between the highest and lowest value was almost 4.3-fold.

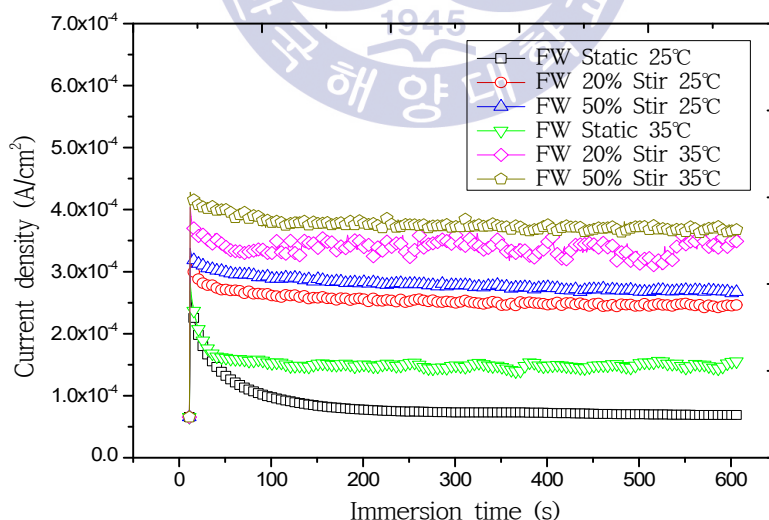


Fig 4.6 Variation of potentiostatic polarization as a function of various environments of fresh water

Fig 4.7 compares the results of the potentiostatic polarization test with the changes in the temperature and flow rate in seawater. Potential was set at $-1,100\text{ mV/SSCE}$. In all conditions, at the beginning of the test, there was a general tendency for a high cathodic protection current density, while its current density gradually decreased over time. The magnitude of current density also increased with an increase of temperature and flow. These tendencies are similar to the results in fresh water. Unlike the test in fresh water, the graph of 35°C static seawater was the third highest in current density. It can be seen that the diffusion coefficient for oxygen increases with temperature, resulting in that corrosion rate increases, and with an increase of temperature, corrosive factor in seawater, which is adsorbed to the metal surface, additionally causes the exchange current density for the anode dissolution to increase, accelerating corrosion rate. Therefore, this finding suggests that, in seawater, the influence of temperature is larger rather than that of flow rate.

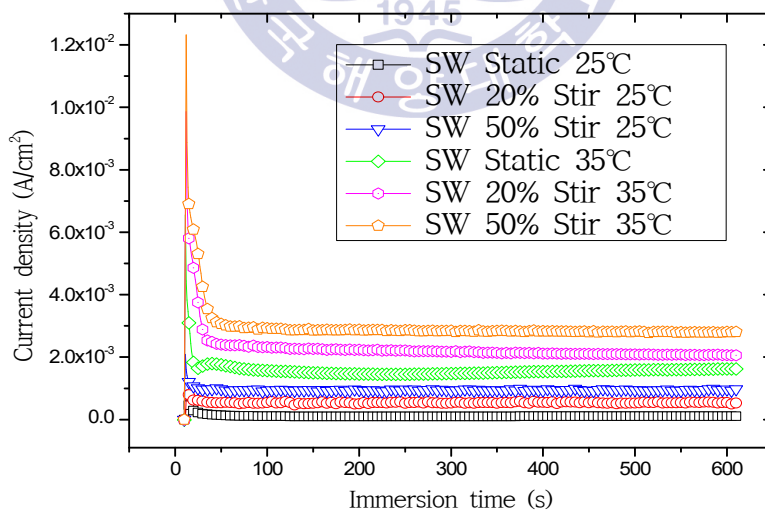


Fig 4.7 Variation of potentiostatic polarization as a function of various environments of seawater

Fig 4.8 compares the results of the potentiostatic polarization test with the various conditions in fresh water and seawater for 600 seconds. Potential was set at $-1,100$ mV/SSCE. In all conditions, at the beginning of test, there was a general tendency for a high cathodic protection current density, while its current density gradually decreased over time. The magnitude of current density was the highest at 35°C 50 % stir seawater, followed by 35°C 20 % stir seawater, 25°C 50 % stir seawater, 25°C 50 % stir fresh water, and 25°C static fresh water. The lowest current density of $70 \mu\text{A}/\text{cm}^2$ was observed in 25°C static fresh water, and the highest current density of $2.8 \text{ mA}/\text{cm}^2$ was observed in 35°C 50 % stir seawater. There was a difference between the highest and lowest value up to 40-fold. Therefore, our results suggest that the higher temperature and flow rate in both fresh water and seawater, the more current density to maintain cathodic protection potential appeared. This means that the higher temperature and flow rate, the higher activity of ions and diffusion coefficient of oxygen. These results are similar to the results previously reported by Kim³⁷.

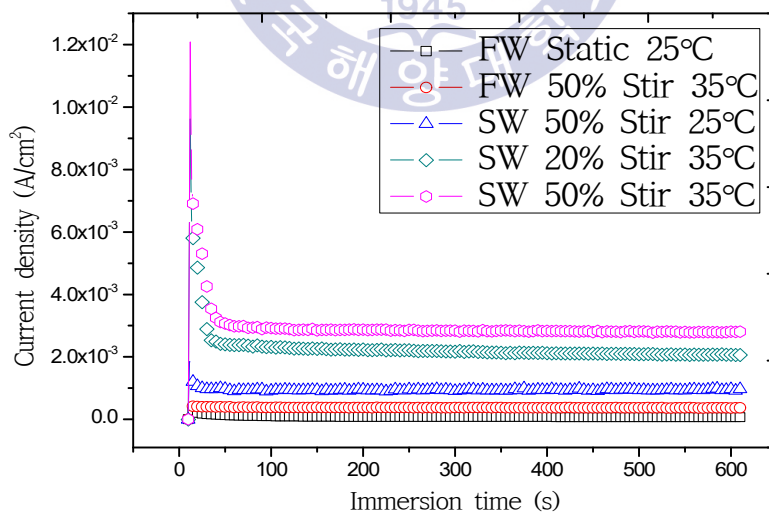


Fig 4.8 Variation of potentiostatic polarization as a function of fresh water and seawater in different flow rates and temperatures

Fig 4.9 shows the results of open-circuit potential in different solutions (e.g. fresh water and seawater) and flow rates (e.g. static and 20 % stir). As can be seen in the figure, the open-circuit potentials of fresh water were more noble than that of seawater at all time points. Open-circuit potential of specimen in static fresh water was -468 mV/SSCE, which gradually decreased to -603 mV/SSCE. In addition, open-circuit potential of specimen in static seawater was -511 mV/SSCE, which gradually decreased to -658 mV/SSCE. As time passed by, the open-circuit potential of specimens in all conditions decreased and tended to become stable. It seems that corrosion byproducts which are chemically stable covered the reacting surface, leading to a decrease of the reacting surface areas. As a result, stable potential behavior was appeared, although the open-circuit potential moved rapidly towards active direction in the beginning period³⁷⁾. In addition, in the seawater, Cl^- which is dissolved with seawater destroys the oxidation layer and adheres to the metal surface, leading to an increase of exchange current density and decrease the overpotential³⁷⁾. Furthermore, open-circuit potentials of solutions with flow were more noble than that of static solutions. Open-circuit potential of specimen in fresh water with flow (20 % stir) was -400 mV/SSCE, which gradually decreased to -600 mV/SSCE. In addition, open-circuit potential of specimen in seawater with flow (20 % stir) was -448 mV/SSCE, which gradually decreased to -660 mV/SSCE. This is because with an increase of the flow rate, the diffusion rate of the depolarization agents such as H^+ increase. Consequently, the rate of cathodic depolarization increases, the consumption of electrons increases, and the negative charge formed on the double layer reduces. These result are in agreement with researches previously reported by Zhen Li⁴⁸⁾ and Qingwei Niu⁴⁹⁾. In all cases, 4 days after, open-circuit potentials become stable. This means that open-circuit potentials of specimen approached corrosion potential that is the mixed potential at which the rate of anodic dissolution of the electrode equals the rate of cathodic reactions and there is no net current flowing in or out of the electrode.

Fig 4.10 shows the amount of current density when carrying out cathodic protection by setting the potential at $-1,100$ mV/SSCE in different solutions (fresh water and seawater) and flow rates (e.g. static and 20% stir). In all cases, the applied current was the maximum in the beginning period, and had tendency to decrease over time. Comparing fresh water with seawater, a higher current was generally applied in seawater. Seawater was initially applied the current of 0.20 mA/cm², which gradually decreased to 0.142 mA/cm². In the case of fresh water, the current of 0.03 mA/cm² was initially applied, which later decreased to 0.004 mA/cm². The results confirmed that the demand for a higher current was necessary to maintain a lower potential in seawater which contains more corrosive factors as compared to fresh water. Comparing solution with flow rate and without flow rate, a higher current was generally applied in solution with flow rate. Seawater with flow rate was initially applied the current of 0.404 mA/cm², which gradually decreased to 0.24 mA/cm². In the case of fresh water with flow, the current of 0.08 mA/cm² was initially applied, which later decreased to 0.013 mA/cm². This also means that the demand for a higher current was necessary to maintain a lower potential in flowing condition. Because increased flow rate cause limit diffusion current to increase, resulting in increase of applied current for cathodic protection. This trend is similar to the our results of potentiostatic polarization test. Furthermore, in the case of cathodic protection in seawater, our results confirmed that the deposited form on the surface through cathodic protection acted as the coating layer, leading to a decrease of the current density³⁸).

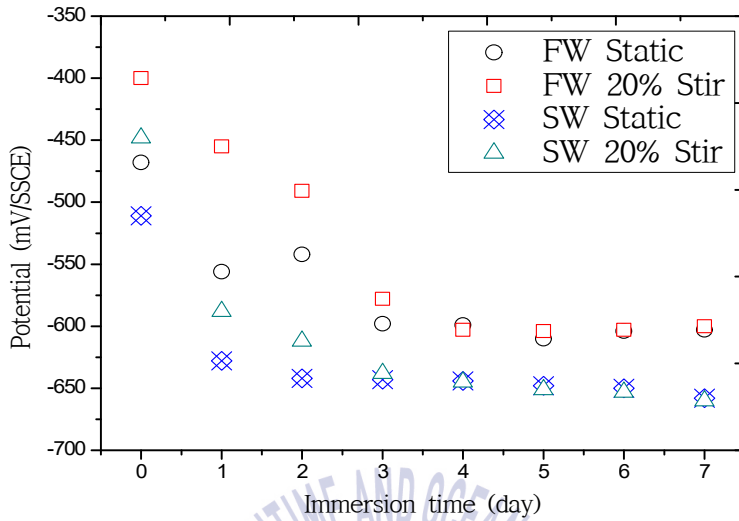


Fig 4.9 Variation curves of open-circuit potential with time at different solutions and flow rates

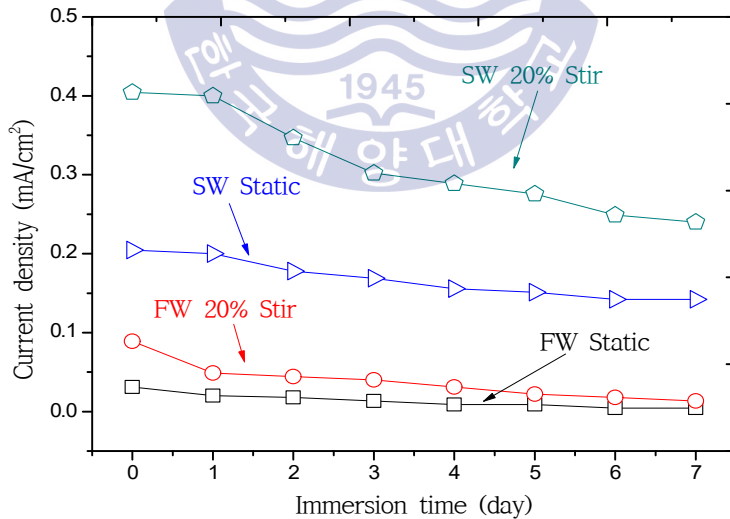


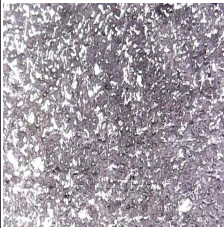
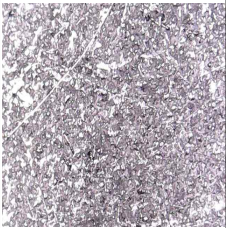
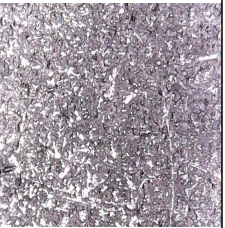
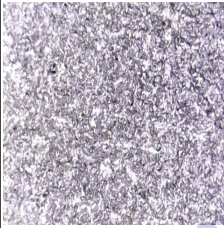
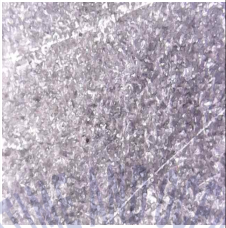
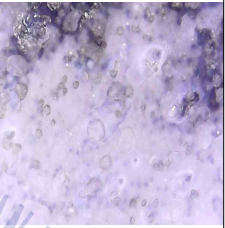
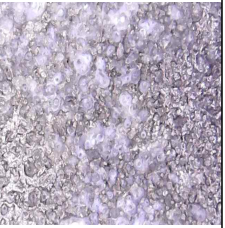
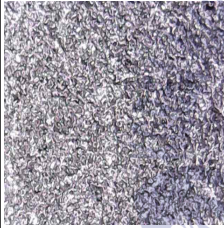
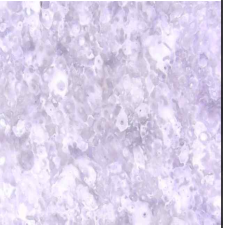
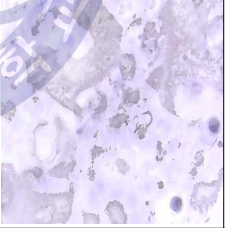
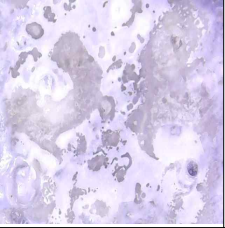
Fig 4.10 Current density maintaining -1,100 mV/SSCE for 7 days in each condition of the beaker

Fig 4.11 shows the appearances of both natural corroded specimens and protected specimens over time in different solutions and flow rates. Natural corroded specimens had corrosive byproducts on the surface after 1 day. As time passed by, the corrosive area expanded, and the amount of corrosive byproducts increased. A more severe corrosion appeared on the surface in seawater than in fresh water. Corroded surface of specimens has the corrosive byproducts (initial rust), which is a result of the reaction of the oxidation of the steel and the reduction of oxygen, which, in turn, is the result of conversion to complex iron oxide through oxidation processes due to the effects of the surrounding environment over time. In protected specimens, the initial surface was maintained over time, and no corrosion on the surface was observed. 2 days after, white crystals began to appear on the surface of specimens that were adopted to cathodic protection in seawater. This is because when cathodic protection is applied, cathodic protection current causes dissolved oxygen reduction, generating hydroxyl ions and carbonate ions. These ions combine with magnesium and calcium ions, which are dissolved in seawater, forming an inorganic layer whose principal component is calcium carbonate. This layer functions as a barrier against the corrosive environment, leading to a decrease of the current demand³⁸⁾ (see Fig 4.12). As can be seen in Fig 4.12, in 20 % stir seawater, calcareous deposit was partially cracked on day 6. This is because the effect of flow rate causes calcareous deposit to be detached from the surface. Therefore, overall thickness of calcareous deposit in 20 % stir seawater was thinner than in static seawater. Fig 4.13 shows macro-photographs of corroded and protected specimens in each conditions after scrubbing.

Solution		Fresh water				Seawater			
Condition		Corrosion		Protection		Corrosion		Protection	
Flow rate		Static	20 % Stir	Static	20 % Stir	Static	20 % Stir	Static	20 % Stir
Time (day)	0								
	1								
	2								
	3								
	4								
	5								
	6								
	7								

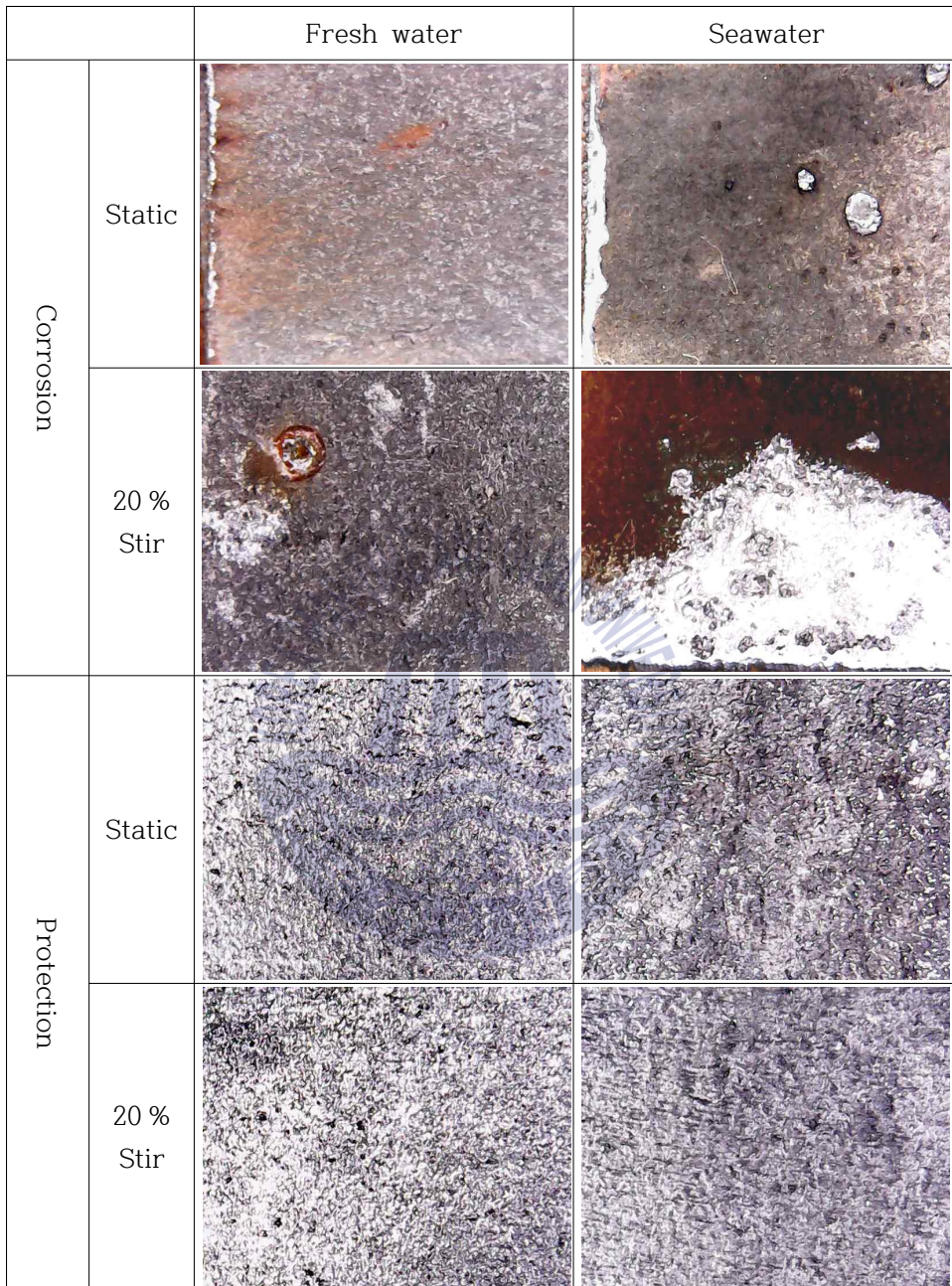
10 mm

Fig 4.11 Comparison of photographs between corroded specimens and protected specimens in different solutions and flow rates for 7 days

Condition		FW Static	FW 20 % Stir	SW Static	SW 20 % Stir
Time (day)	0				
	2				
	4				
	6				
	7				

5 mm

Fig 4.12 Macro-photographs of protected specimens' surface in each condition over time



—
1 mm

Fig 4.13 Macro-photographs of corroded and protected specimen after scrubbing in fresh water with different flows

Fig 4.14 compares the cathodic protection current density under 4 experimental conditions while maintaining a potential at $-1,100 \text{ mV/SSCE}$ with three carbon steel specimens connected electrically. In fresh water without flow, 0.04 mA/cm^2 was initially applied, but decreased to 0.02 mA/cm^2 on day 7. In fresh water with flow, 0.12 mA/cm^2 was initially applied, but decreased to 0.10 mA/cm^2 on day 7. In seawater without flow, 0.47 mA/cm^2 was initially applied, but decreased to 0.43 mA/cm^2 on day 7. In seawater with flow, 0.58 mA/cm^2 was initially applied, but decreased to 0.56 mA/cm^2 on day 7. These current trend are similar to the results of our potentiostatic test. Current was applied 5-fold higher in fresh water with flow than without flow, and 1.3-fold higher in seawater with flow than without flow. Comparing fresh water with seawater, In the environment without flow, the difference of current was about 22-fold and, in the environment with flow, 6-fold difference was observed. We also observed a 29-fold difference between the non-flowing fresh water (-the lowest amount of current) and the flowing seawater (-the largest amount of current). These results suggest that applied current to maintain certain potential was much higher in seawater than in fresh water. In addition, as reported in a previous study, increased relative movement between the metal surface and the electrolyte produced by the flow reduced the thickness of the diffuse layer barrier adjoining the metal surface and increased the movement of the response⁴⁰. Therefore, we reasoned that, if the flow increased, applied current to maintain cathodic protection potential for surface would also increases.

Fig 4.15 compares the cathodic protection current density with the galvanic corrosion condition by electrically connecting two carbon steel specimens with one copper specimen under 4 experimental conditions while maintaining a potential at $-1,100$ mV/SSCE. In fresh water without flow, 0.03 mA/cm² was initially applied, but decreased to 0.02 mA/cm² on day 7. In fresh water with flow, 0.13 mA/cm² was initially applied, but decreased to 0.08 mA/cm² on day 7. In seawater without flow, 0.31 mA/cm² was initially applied, but decreased to 0.28 mA/cm² on day 7. In seawater with flow, 0.44 mA/cm² was initially applied, but decreased to 0.31 mA/cm² on day 7. These current trends are similar to the results of our potentiostatic test and general corrosion test in the cistern. Current was applied 4-fold higher in fresh water with flow than without flow, 1.1-fold higher in seawater with flow than without flow. Comparing fresh water with seawater, in an environment with no flow, the difference of current was about 14.8-fold, and in an environment with flow, 4-fold difference of current was observed. We also observed a 16-fold difference between non-flowing fresh water (-the lowest amount of current) and flowing seawater (-the largest amount of current). Similarly to the general corrosion environment, in the galvanic corrosion environment, the current applied more in seawater was higher than in fresh water, regardless of the repercussion of galvanic currents. Our results also demonstrated that a higher current was applied in the non-flowing environment than in the flowing one. With two results of current density in the cistern, we could observe that current density trend for the inner surface of pipe is similar to general cathodic protection.

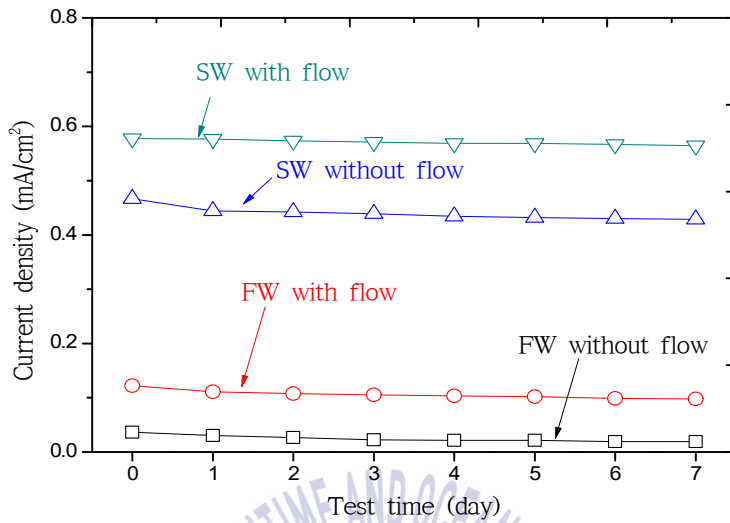


Fig 4.14 Current density maintaining $-1,100$ mV/SSCE for 7 days in general corrosion condition

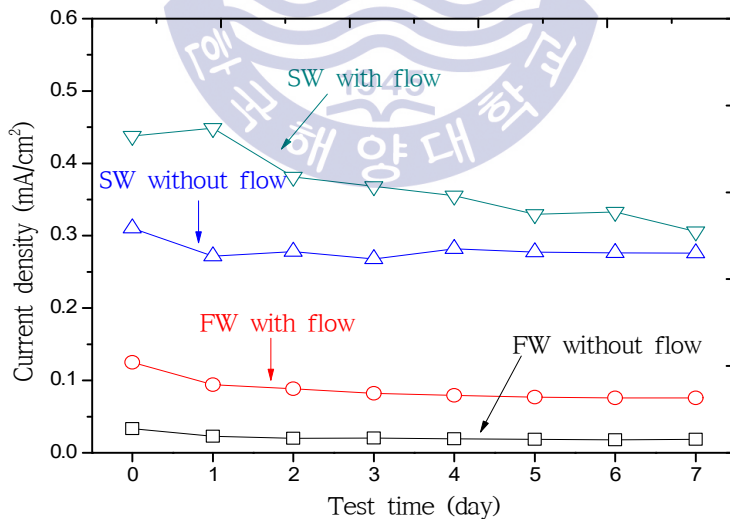


Fig 4.15 Current density maintaining $-1,100$ mV/SSCE for 7 days in galvanic corrosion condition

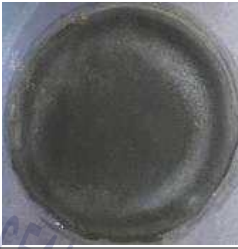
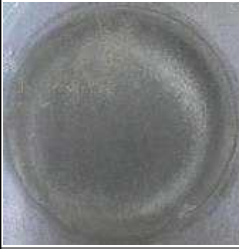
Fig 4.16 shows the specimens used in the experiment fresh water without flow. After the test was finished, corroded specimens were found to have developed corrosion in narrow areas, and their surface was damaged. In the protected specimens, no significant changes before and after the experiment were observed.

Fig 4.17 shows the specimens used in the experiment in fresh water with flow. After the test, the specimens were found to have more areas of corroded surface than in the environment without flow. The damaged specimens clearly showed the difference between the deep damaged surface and the protected surface. Therefore, we concluded that the corrosion rate increased while simultaneously affecting physical erosion due to the reduction of the thickness of mass transfer layer with an increase of the flow rate. Therefore, the damage steadily increased in the local areas³⁶). In the protected specimens, similarly to the experiment in fresh water without flow, no conspicuous changes before and after the experiment were observed.

		START	END	AFTER SCRUB
General Condition	Corrosion			
	Protection			
Galvanic Condition	Corrosion			
	Protection			

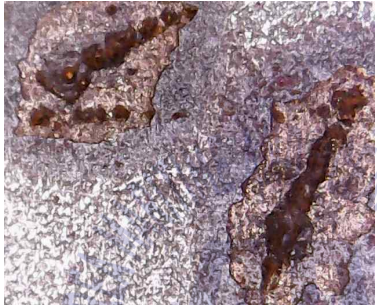
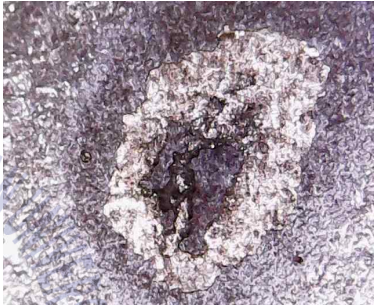
20 mm

Fig 4.16 Comparison of photographs between corroded specimens and protected specimens in fresh water without flow

		START	END	AFTER SCRUB
General Condition	Corrosion			
	Protection			
Galvanic Condition	Corrosion			
	Protection			

20 mm

Fig 4.17 Comparison of photographs between corroded specimens and protected specimens in fresh water with flow

Fresh water		General corrosion	Galvanic corrosion
Corrosion	with out flow		
	with flow		
Protection	with out flow		
	with flow		

—
1 mm

Fig 4.18 Macro-photographs of corroded and protected specimen after test in fresh water with different flows

Fig 4.19 shows the specimens used in experiment in seawater without flow. After the test, in corroded specimens, corroded areas accounted for 35 % of the total surface. In the specimens influenced by galvanic corrosion, the corroded area accounted for above 80 % of the surface of specimens. In addition, the corroded specimens showed irregular layers of surface in the areas of damage and, in particular specimens influenced by galvanic current showed obvious boundaries divided into the exposed surface and the unexposed surface. Since copper is more noble in the galvanic series, galvanic currents were applied to copper and occurred more galvanic corrosion occurred on the carbon steel, resulting in more damage. In the protected specimens, inorganic layers produced by the cathodic protection current which electrolyzed the seawater were found on the surface of specimens after the experiment. After scrubbing, no damage on the surface was observed.

Fig 4.20 shows the specimens used in the experiment in seawater with flow. After the test, the corroded specimens were found to have more areas of corroded surfaces than in the environment without flow. In seawater without flow, in protected specimens, no conspicuous changes before and after the experiment were observed. The damage increased due to the effect of seawater, which is a more corrosive environment than fresh water and physical erosion produced by flow. Furthermore, with an increase of the flow rate, the movement of reactant and limit diffusion current density increased, resulting in that more cathodic protection current was applied to the metal surface. In conclusion, owing to the energetic seawater electrolysis, the amount of product on the surface increased. We concluded that, although the thickness of the deposit layer decreases with an increase of the flow rate³²⁾, the amount of product increased due to the increase of applied current to maintain the potential.

		START	END	AFTER SCRUB
General Condition	Corrosion			
	Protection			
Galvanic Condition	Corrosion			
	Protection			

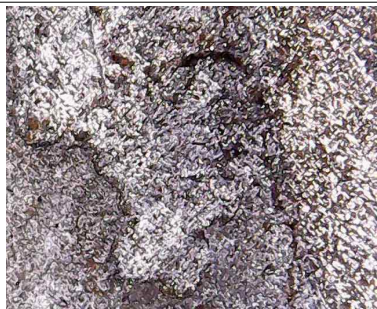
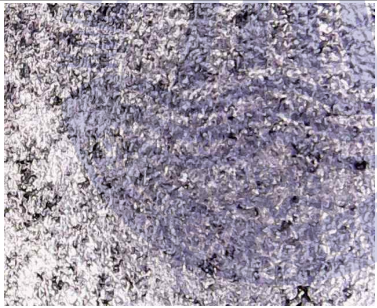
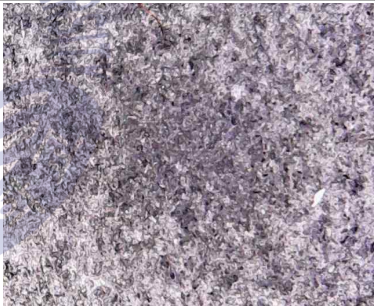
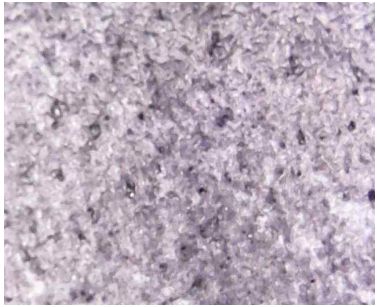
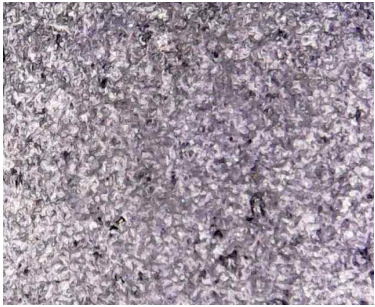
20 mm

Fig 4.19 Comparison of photographs between corroded specimens and protected specimens in seawater without flow

		START	END	AFTER SCRUB
General Condition	Corrosion			
	Protection			
Galvanic Condition	Corrosion			
	Protection			

20 mm

Fig 4.20 Comparison of photographs between corroded specimens and protected specimens in seawater with flow

Seawater		General corrosion	Galvanic corrosion
Corrosion	with out flow		
	with flow		
Protection	with out flow		
	with flow		

—
1 mm

Fig 4.21 Macro-photographs of corroded and protected specimen after test in seawater with different flows

Fig 4.22 compares current density to maintain certain cathodic protection potential in various flow rates. At -900 mV/SSCE of the cathodic protection potential, minute differences between flow rates were observed. However, with an decrease of the cathodic protection potential, the difference of current density between flow rates was augmented. At $-1,200$ mV/SSCE of the cathodic protection potential, the largest current density, 8.37 mA/cm², was identified at the flow rate of 11 m³/h.

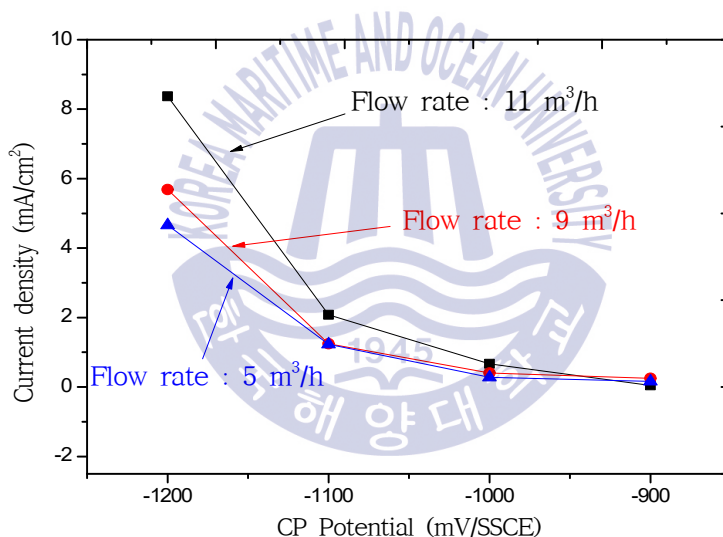


Fig 4.22 Current density at each cathodic protection potential in various flow rates

Fig 4.23 shows photographs of the inner surface of both protected pipe and corroded pipe after the experiment was performed for 30 days. According to the results, rust was found on the inner surface of the corroded pipe. By contrast, the pipes that operated by installing ribbon anode normally appeared to have deposited a film of lime, and rust which was formed when corrosion was in progress was not found. Furthermore, in the overall pipe, no marine growth or adsorption was observed. We reasoned that the phenomenon where marine growth did not proceed in the corroded pipe is due to the fact that electrochlorination facility installed at the front of the system enabled HClO that performed as antiseptic to pass through the pipe with the seawater flow. Consequently, when an anode was installed in the pipe, corrosion control in the pipe was properly performed, and the effect of marine organisms' suppression was also observed.

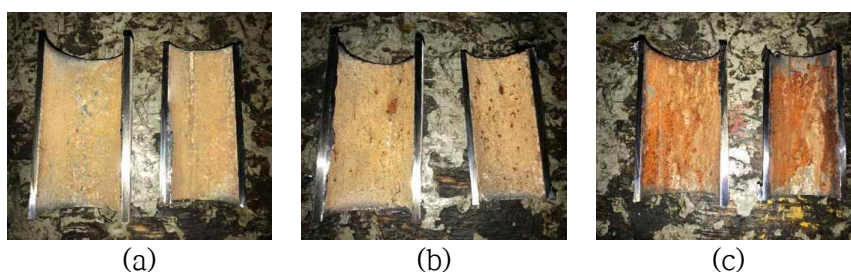
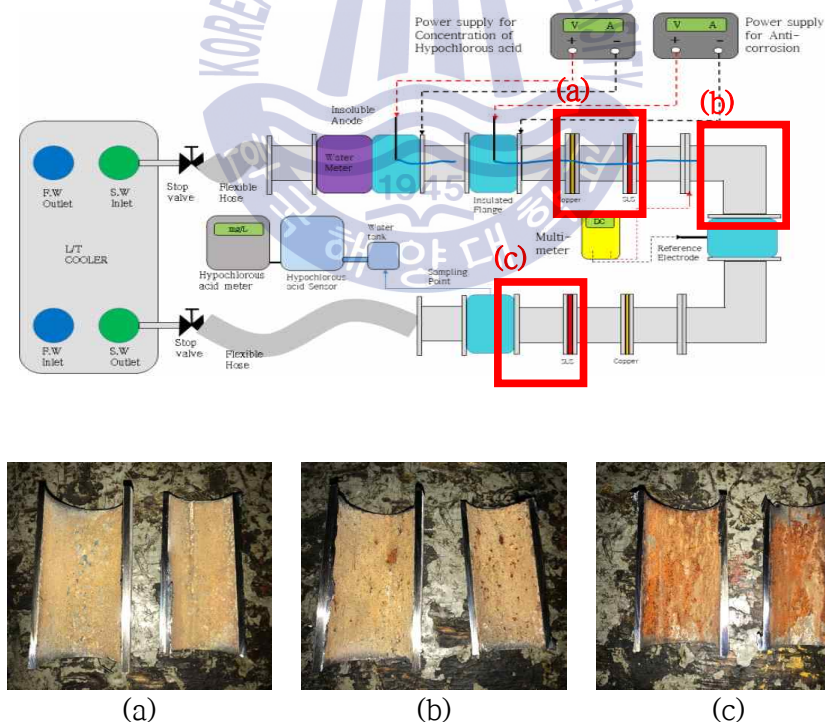


Fig 4.23 Comparison of photographs between pipes after test, (a): Protected pipe, (b): Partially protected pipe, (c): Corroded pipe

4.2 Test results of biofouling control

Fig 4.24 shows the results of HClO concentration produced by the cathodic protection current applied from an external power source for the cathodic protection system to protect the seawater pipe from corrosion. Before applying the cathodic protection current, the potential of the pipe was set at -700 mV/SSCE , and the cathodic protection current and HClO concentration were measured in the condition of -900 mV/SSCE of the cathodic protection potential. The seawater flow rate was $15\text{ m}^3/\text{h}$, and temperature during the experiment ranged from 12.6 to $13.2\text{ }^\circ\text{C}$. pH level of seawater was maintained from 8.20 to 8.24 . There was a tendency for the cathodic protection current to increase as with a decrease of the cathodic protection potential. When the cathodic protection potential was below $-1,100\text{ mV/SSCE}$, the HClO concentration amounted about 0.16 mg/L . Consequently, the HClO concentration was directly proportional to the amount of cathodic protection current.

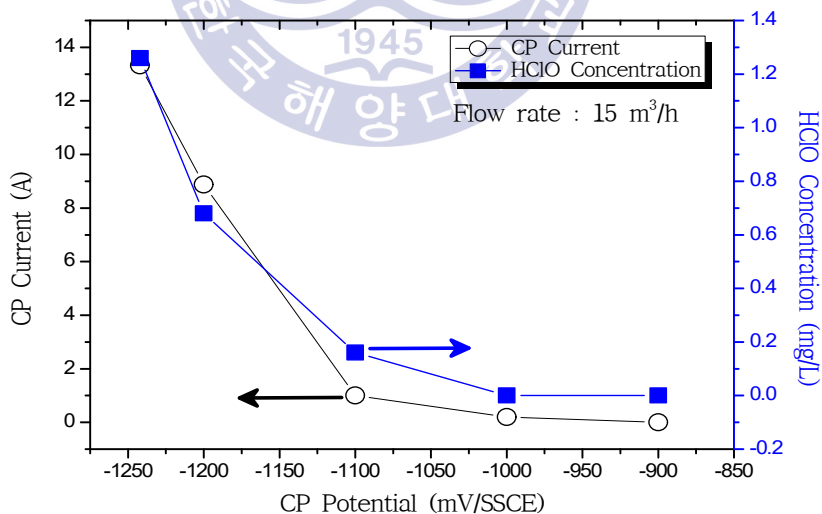
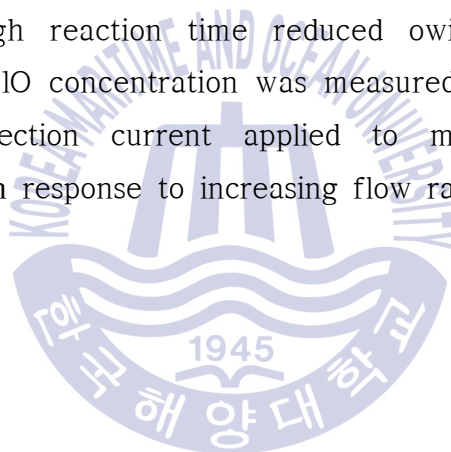


Fig 4.24 Test results of cathodic protection current and HClO concentration as a function of cathodic protection potential setting

Fig 4.25, Fig 4.26, and Fig 4.27 show the HClO concentration produced in the condition when the electrochlorination facility applied additional current while maintaining the cathodic protection potential of $-1,200$ mV/SSCE in the flow rate of 3 m³/h, 6 m³/h, and 15 m³/h respectively. The higher the total current applied (i.e. a combination cathodic protection current with electrolysis current), the higher the HClO concentration produced. When the cathodic protection potential was maintained at $-1,200$ mV/SSCE in the flow rate 3 m³/h, 6 m³/h, and 15 m³/h, the amount of applied current was 6.351 A, 6.8 A and 9.751 A respectively. In addition, 0.70 mg/L, 0.82 mg/L, and 0.92 mg/L of HClO were measured respectively. In each condition, when 6 A were added from the electrochlorination facility, the HClO concentration increased up to 2.2 mg/L, 3.76 mg/L, and 4.66 mg/L. Conversely, when additional applied current decreases, the HClO concentration also decreases. This means that HClO concentration could be adjusted by additional applied current from electrochlorination facility when the HClO concentration only produced by cathodic protection current is too low to decimate marine organisms. In addition, with an increase of flow rates, the HClO concentration increased in all conditions. This is because cathodic protection current increases of total applied current to maintain cathodic protection potential, and total applied current also increases. It seems that these increases eventually lead to an increase of the HClO concentration.

Fig 4.28 compares HClO concentration produced by both the cathodic protection current and the electrochlorination facility output current according to the flow rates while maintaining the cathodic protection potential at $-1,200$ mV/SSCE. The differences between various flow rates resulted from the fact that the high cathodic protection current was applied in order to maintain the cathodic protection potential in the increasing flow rate. Consequently, when no additional current was applied from the electrochlorination facility, there were tiny concentration differences between flow rates. In contrast, when the additional current was constantly applied, the HClO concentration differences increased considerably. Although reaction time reduced owing to the increased flow rate, a high HClO concentration was measured. This is because the large cathodic protection current applied to maintain the cathodic protection potential in response to increasing flow rates.



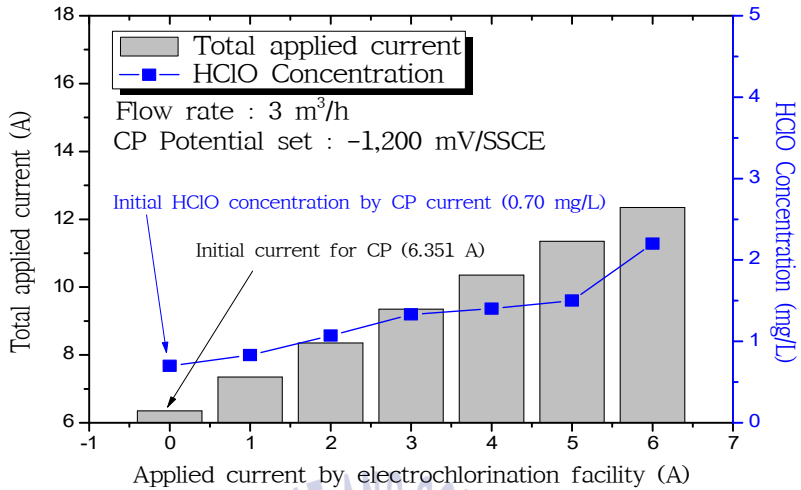


Fig 4.25 Test results of total applied current and HClO concentration at -1,200 mV/SSCE of cathodic protection potential in 3 m³/h

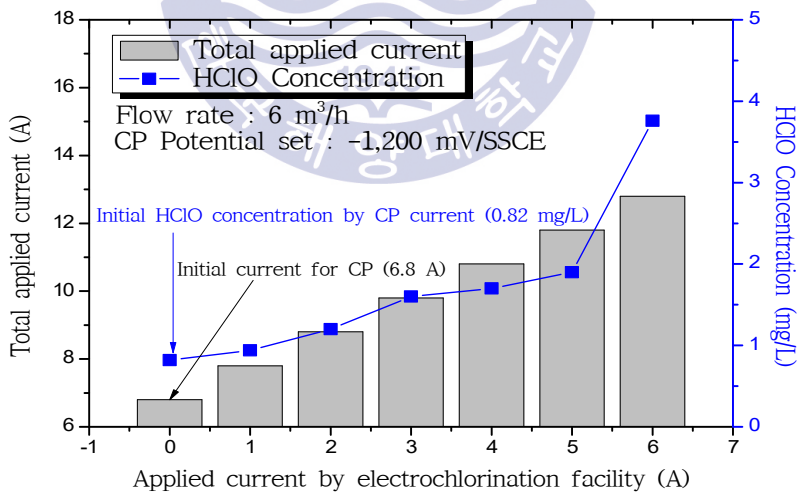


Fig 4.26 Test results of total applied current and HClO concentration at -1,200 mV/SSCE of cathodic protection potential in 6 m³/h

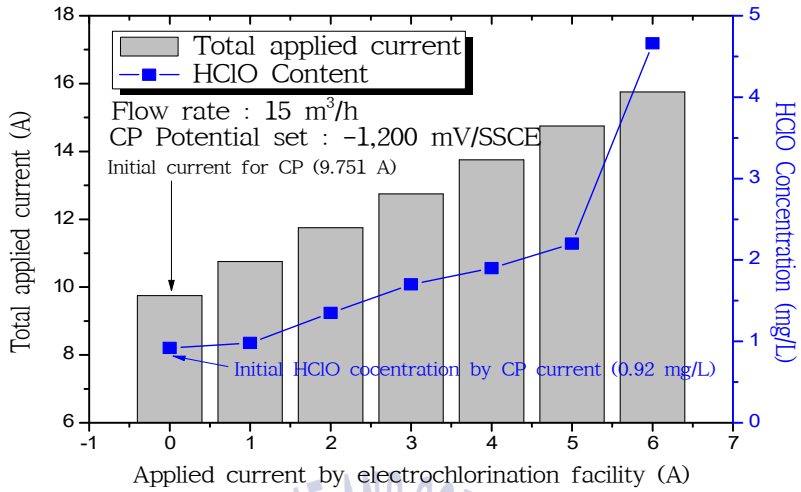


Fig 4.27 Test results of total applied current and HClO concentration at $-1,200$ mV/SSCE of cathodic protection potential in 15 m³/h

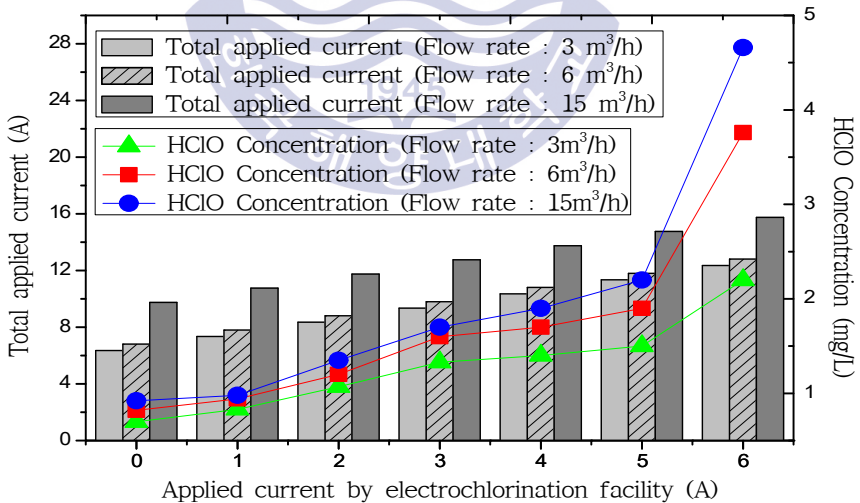


Fig 4.28 Comparisons of total applied current and HClO concentration at $-1,200$ mV/SSCE of cathodic protection potential in each flow rate

During measuring the HClO concentration, the concentration differences between FCL (Free Chlorine Meter) and DPD were observed. Therefore, to minimize the concentration differences and set calibration point of FCL properly, HClO concentration was measured by modifying calibration point of FCL, and measuring test allow us to draw the following results.

Fig 4.29, Fig 4.30, and Fig 4.31 show the difference in the measured concentration between the FCL and the DPD in a solution of equal concentration when FCL was calibrated at 0.5 mg/L, 2.0 mg/L, and 4.0 mg/L. When FCL was calibrated at 0.5 mg/L, the same level of concentration was observed at 0.5 mg/L. However, with an increase of HClO concentration, the difference also increased. When concentration was at 2.0 mg/L, a difference of 0.5 mg/L on average was observed. Whereas a concentration higher than 2.0 mg/L showed an increasing tendency. In concentration above 2.0 mg/L, the difference of 4.3 mg/L on average was observed. In addition, when FCL was calibrated at 2.0 mg/L, In the condition between 0 and 2.0 mg/L, minute difference was observed. Similarly to the calibration at 0.5 mg/L, differences in concentration above 2.0 mg/L were more likely to be greater than those at 2.0 mg/L; however, the difference in concentration above 2.0 mg/L was reduced to 1.57 mg/L on average. Compared to case when calibration was 0.5 mg/L, the difference was slightly decreased. Lastly, when FCL was calibrated at 4.0 mg/L, unlike in the results reported in previous graphs, the DPD method was measured lower than FCL in the range between 0 and 2.0 mg/L. The closer concentration was to 4.0 mg/L (i.e. the calibration value), the smaller difference was observed. In the range from 0 to 2.0 mg/L, the concentration difference was 0.55 mg/L on average. In addition, in the range above 2.0 mg/L, the concentration difference amounted to 0.31 mg/L.

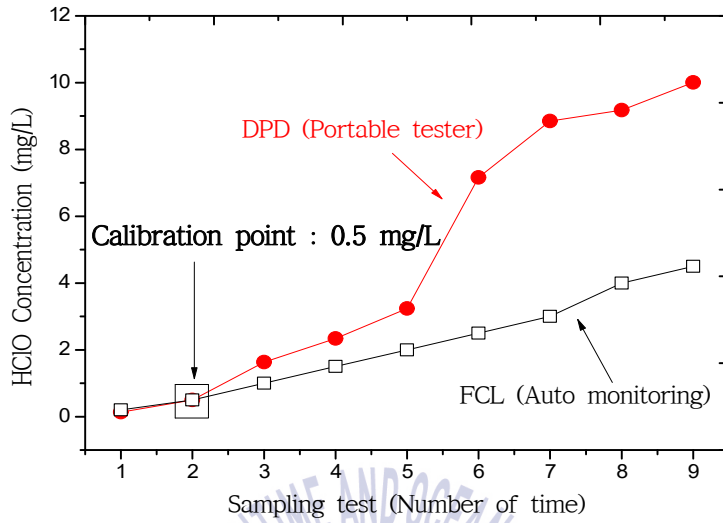


Fig 4.29 Difference of concentration between DPD and FCL calibrated at 0.5 mg/L

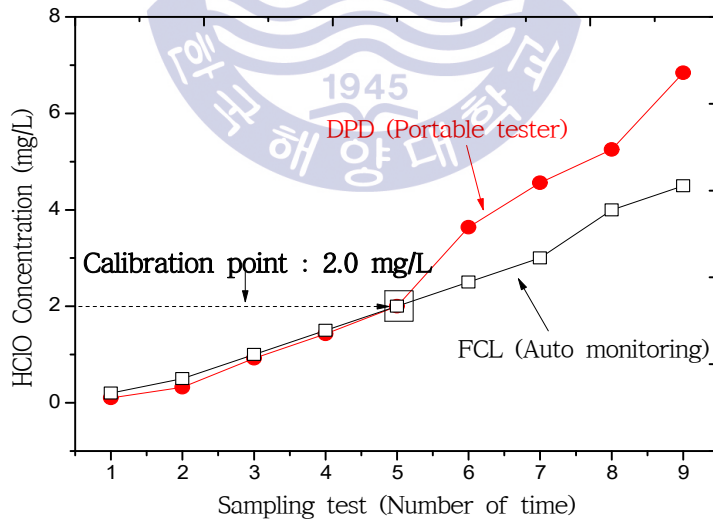


Fig 4.30 Difference of concentration between DPD and FCL calibrated at 2.0 mg/L

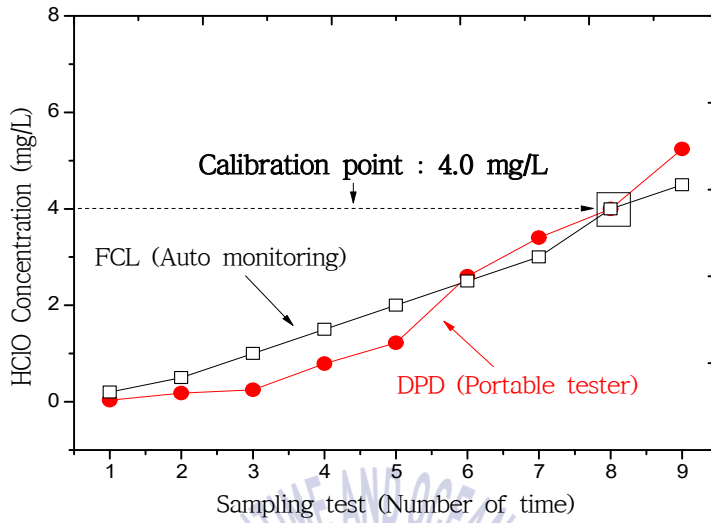


Fig 4.31 Difference of concentration between DPD and FCL calibrated at 4.0 mg/L



Chapter V

CONCLUSIONS

The results of the present study on the control of corrosion and biofouling in seawater pipe allow us to draw the following conclusions:

1. The results of the electrochemical polarization test showed that corrosion current density and corrosion rate, in anodic and cathodic polarization, were generally higher in seawater than in fresh water. Furthermore, as shown by the results of the potentiostatic polarization test, current density in seawater was normally higher than in fresh water and current density increased with an increase of temperature and flow rate in both solutions.

2. The results of cathodic protection test in the beaker showed a more active potential in seawater than in fresh water, and more currents were applied. Protected specimens in both fresh water and seawater produced no corrosive byproducts on the surface of the test specimen applied to cathodic protection as compared to the naturally corroded test specimen.

3. As shown by the results of cathodic protection in the cistern, in both general and galvanic corrosion conditions, current was applied more in seawater than in fresh water, and no repercussion of galvanic current was observed in the case of the galvanic corrosion. In addition, as shown by the results of surface observation, corrosive byproducts on the corroded specimens were observed. Whereas, in the protected specimens, no damage on the surface of specimens was observed in all experimental conditions.

4. As demonstrated by the results of cathodic protection and electrochlorination, in corrosion control aspect, the higher cathodic protection current was applied, the lower cathodic protection potential was maintained. When observing the inner surface of the pipe, no corrosive byproducts were observed. Therefore, by using cathodic protection in the pipe, we could prevent the inner surface of pipe from corrosion. Furthermore, in biofouling control aspect, with an increase of flow rate, HClO concentration increased due to the increase of cathodic protection current. when adjusting the output current of the electrochlorination facility, the HClO concentration could also be regulated. Although FCL could perform monitoring in real-time, deviation according to the range of calibration was observed. This deviation could be alleviated by calibration. Consequently, it can be seen that HClO produced by cathodic protection and electrochlorination current could control biofouling by automatically adjusting the HClO concentration.

When performing corrosion and biofouling control, given that cathodic protection condition varies depending on the diameter, shape, and flow rate of the pipe, and that the efficiency of the electrochlorination facility varies depending on the kinds of anodes and distance between the anode and the pipe (cathode), additional experiments would be needed to establish an optimal cathodic protection and electrochlorination. With these additional experiments, the results of the present this study could provide fundamental data to develop a hybrid technique to control corrosion and biofouling.

References

- 1) Ku, D.S., et al., “Analysis of defective pipings in nuclear power plants and applications of guided ultrasonic wave techniques” , Korea Atomic Energy Research Institute, pp.36-43, 2006.
- 2) Kim Y.S., “Trends in Standardization of Corrosion Methods in Domestic and Foreign” , Technology report of Korea Agency for Technology and Standards, pp.2-4, 2012.
- 3) K.K. Satpathy et al., “Biofouling and its Control in Seawater Cooled Power Plant Cooling Water System - A Review” , Nuclear Power, Pavel Tsvetkov (ED.), 2010.
- 4) Lee, S.Y., et al., “Electrochemical Evaluation of Corrosion Property of Welded Zone of Seawater Pipe by DC Shielded Metal Arc Welding with Types of Electrodes” , Journal of Ocean Engineering and Technology 27(3), June 2013, pp.78-84, 2013.
- 5) J.R. Davis, Davis & Associates, Corrosion : Understanding the Basics (#06691G), ASM International, pp.1-84, 2000.
- 6) Denny A. Jones, Principles and Prevention of Corrosion, Prentice Hall, Inc, pp.5, 1996.
- 7) E. McCafferty, Introduction to Corrosion Science, Springer, pp.17-130, 2009.
- 8) Harold V.Thurman, Alan P.Trujillo, Introductory Oceanography, Prentice Hall, Inc, pp.9-175, 2004.

- 9) Luciano Lazzari, Pietro Pedefferri, Cathodic Protection, Polipress, pp.237, 2006.
- 10) Kim, K.J., et al., “A study on the Performance Evaluation & Improvement of Sacrificial Anodes for Cathodic Protection (Comparison of Performance Test Methods for Sacrificial Anode)” , Maritime Industry Research Institute, Korea Maritime and Ocean University, 2009.
- 11) Kim, S.J., “Apparatus on Corrosion Protection and Marine Corrosion of Ship” , Journal of Korean Institute of Surface Engineering, Vol. 44, No. 3. pp.105-116, 2011.
- 12) Lee, D.H., “An experimental study on the effect of the inner surface of seawater pipe using impressed current cathodic protection” , M. S. Thesis, Korea Maritime and Ocean University, 2018.
- 13) Jin, C.K., “Tidal Effect of Hybrid Cathodic Protection System in Reinforced Concrete Structures” , M. S. Thesis, Korea Maritime and Ocean University, 2012.
- 14) Jeong, J.A., et al., “A Characteristic Study on the Electrochemical Polarization Test of the Carbon Steel in Natural Seawater” , Journal of the Korean Society of Marine Engineering, Vol. 42, No.4, pp.274-279, 2018.
- 15) Jeong, J.A., et al., “The cathodic protection using insoluble anodes by delivering protection currents to the inner surfaces of carbon steel seawater pipes” , Journal of the Korean Society of Marine Engineering, Vol. 42, No.4, pp.280-286, 2018.
- 16) Yang, J.H., et al., “Sterilization and ecofriendly neutralization of seawater using electrolysis” , Journal of the Korean Society of Marine Engineering, Vol.41, No.3, pp.276-280, 2017.

- 17) Muhammad Saleem, "Biofouling Management in the Cooling Circuit of a Power Industry Using Electrochemical Process", Journal of Chemical Society of Pakistan, Vol.33, No.3, pp.295-304, 2011.
- 18) Jagadish S.Patil et al., "Effect of chlorination on the development of marine biofilms dominated by diatoms", Biofouling, Vol.27, No.3, pp.241-254, 2011.
- 19) Henk A. Jenner et al., "Cooling water management in European power stations Biology and control of fouling", Hydroécologie Appliquée, 1-2(1), 1998.
- 20) Diego Meseguer Yebra et al., "Antifouling technology - past,present and future steps towards efficient and environmentally friendly antifouling coatings", Progress in Organic Coatings, 50, pp.75-104, 2004.
- 21) CAO Shan et al., "Progress of marine biofouling and antifouling technologies", Material Science, Vol.56, No.7, pp.598-612, 2011.
- 22) Ayda G. Nurioglu et al., "Non-toxic, non-biocide-release antifouling coatings based on molecular structure design for marine applications", Journal of Materials Chemistry B, 3, pp.6547-6570, 2015.
- 23) Lynn Jackson, "Marine Biofouling & Invasive species : Guidelines for Prevention and Management", Global Invasive Species Programme (GISP). 2008.
- 24) Q. Zhao et al., "Bacterial adhesion on the metal-polymer composite coatings", International Journal of Adhesion and Adhesives Vol.27, Issue 2, pp.85-91, 2007.
- 25) G. Kiely, Environmental Engineering, McGraw Hill International, Boston, MA, p.148, 2007.

- 26) A. Latif et al., Journal of the Chemical Society of Pakistan, Vol.32, 115, 2010.
- 27) S. Baig et al., Journal of the Chemical Society of Pakistan, Vol.31, 857, 2009.
- 28) Shin, B.K., “Residual chlorine analysis of thermal effluent by power plant” , The Korean Association of Ocean Science and Technology Societies Symposium, pp.2469-2473, 2007.
- 29) Basic Chemistry of Chlorination, hydro Instruments, BCOC Rev.7/10.
- 30) Corrosion Thermodynamics [Online] Available at : <http://www.corrosion-doctors.org/Corrosion-Thermodynamics/Corrosion-Thermodynamics.htm> [Accessed 21 Sep]
- 31) Lee, H.R., Surface Engineering, Hyeongsul publishing, pp.241-243, Seoul, 1999.
- 32) Lee, C.S., “Properties Analysis and Formation Mechanism of Environmental Friendly Electrodeposit Films in Natural Seawater” , M. S. Thesis, Korea Maritime and Ocean University, 2005.
- 33) IM, W.J. et al., Corrosion and Anti-corrosion, Wonchang publishing, Incheon, pp.56-57, 1994.
- 34) G.V. Akimov, Corrosion, 11, 515t, 1955.
- 35) Rudolf C. Matousek et al., “Electrolytic Sodium Hypochlorite System for Treatment of Ballast Water” , Journal of Ship Production, Vol.22, No.3, pp.160-171, 2006.
- 36) Lee, S.J. et al., “Effect of Flow Velocity on Corrosion Rate and Corrosion Protection Current of Marine Material” , Corrosion Science and

Technology, Vol.14, No.5, pp.226-231, 2015.

- 37) Jang, S.K. et al., “Evaluation of Corrosion Tendency for S355ML Steel with Seawater Temperature” , Corrosion Science and Technology, Vo.14, No.5, pp.232-238, 2015.
- 38) Lee, C.S. et al., “Properties analysis of environment friendly calcareous deposit films electrodeposited at various temperature conditions in natural seawater” , Journal of the Korean Society of Marine Engineering, Vol.39, No.7, pp.779-785, 2015.
- 39) Lee, H.R., Corrosion of Metals, Yeunkyung, Pusan, p.166, 2004.
- 40) Kim, K.J. et al., “A study on corrosion characteristic of steel structures in seawater” , Maritime Industry Research Institute, Korea Maritime and Ocean University, p.3, 1997.
- 41) Ko, K.H., “A study on the effect of the impressed current cathodic protection system in reinforced concrete structures.” M. S. Thesis, Korea Maritime and Ocean University, 2018.
- 42) How does an ICCP system work? [Online] Available at : <http://www.cathelco.com/iccp-overview/how-does-an-iccp-system-work/> [Accessed 23 Sep 2018]
- 43) CATHODIC PROTECTION [Online] Available at : <http://www.nstcenter.biz/navy-preservation-resources/cathodic-protection/> [Accessed 23 Sep 2018]
- 44) Marine Growth Prevention System [Online] Available at : <https://cathodicme.com/mgps-systems/marine-growth-prevention-system/> [Accessed 23 Sep 2018]

- 45) OxyChem Sodium Hypochlorite Handbook, Occidental Chemical Corporation, December 2014.
- 46) R.Winston review, Uhlig' s corrosion hand book third edition, A John Wiley & Sons, INC., Publication, pp.589-601, 2011.
- 47) Ahmad Royani et al., “Corrosion Rate of Various Carbon Steels in Raw Water for Water Cooling System at Ammonia Plant” , International Journal of Engineering Trends and Technology (IJETT), Volume 59 Issue 1, pp.51-58, 2018.
- 48) Zhen Li and Jiding Zhang “The influence of flow velocity on electrochemical reaction of metal surface” , IOP Conf. Series: Materials Science and Engineering, 274, 012098, 2017.
- 49) Qingwei Niu et al., “Effect of Flow Rate on the Corrosion Behavior of N80 Steel in Simulated Oil Field Environment Containing CO₂ and HAc” , Int. J.Electrochem. Sci., 12 p.10279-10290, 2017.

감사의 글

‘목표라는 항구를 모르는 사람에게 순풍은 불지 않는다’는 세네카의 명언을 가슴에 새기며 생활한 2년 간의 석사과정을 중 작은 목표를 향해 달려가던 저의 주변에 계셨던 많은 순풍 같은 분들 덕분에 무사히 졸업이라는 작은 결실을 맺을 수 있었습니다. 그 분들에게 짧은 글로나마 감사한 마음을 전하고자 합니다.

먼저, 저에게 새로운 길을 걸어 갈 수 있도록 기회를 열어주시고 항상 제 의견을 존중해주시며 찾아갈 때마다 마다 않고 지도해주신 정진아 지도교수님께 머리 숙여 감사의 마음을 전합니다. 또한, 논문의 아주 작은 부분까지 꼼꼼하게 심사를 해주시고 소중한 충고와 조언을 아끼지 않으신 이명훈 교수님, 윤용섭 교수님, 매 학기 수강 할 때 마다 따뜻하게 맞이해주신 최재혁 교수님, 강호근 교수님께도 깊은 감사의 마음을 전하고 싶습니다.

실습선에서 근무하면서 학업과 업무를 동시에 병행할 수 있도록 많은 배려를 해주신 한바다호 윤귀호 선생님을 비롯한 선박운항과 교수님들께도 감사한 마음을 전합니다. 그리고 항상 자신감 잃지 않게 응원해주시고 격려해주신 정승배 일항사님, 이상우, 임대원 일기사님을 비롯하여 함께 동고동락한 실습선 선후배 사관님들께도 고마운 마음을 전합니다. 또한, 기관실에서 실험을 진행하는데 많은 도움을 주신 한바다호 기관부 선생님들께도 고마운 마음을 전합니다.

유난히도 더웠던 2018년 여름, 학교 롱비치에서 해수를 채취하는 일부터 실험의 전반적인 부분에 도움과 조언을 해주시고, 매번 도움의 손길을 부탁드릴 때마다 흔쾌히 도와주신 이두형 교수님과 지칠 때마다 대화 상대가 되어주셨던 멀리서 고생하고 계신 권흠이형에게 고마운 마음을 전합니다.

그리고, 항상 제가 어디에서 무엇을 하던 응원해주고 삶의 활력소가 되어주는 한결같은 나의 소중한 친구들 윤수와 종빈이에게 심심한 감사의 마음을 전합니다.

마지막으로, 작은 아들을 항상 믿어주시고 격려해주시는 사랑하는 부모님, 저에게 큰 버팀목이 되어주는 형과 형수님, 그리고 너무나 사랑스러운 조카 소울이와 곧 태어날 둘째 조카에게도 고맙고 사랑한다고 말하고 싶습니다.

앞으로도 초심을 잃지 않고 또 다른 목표를 향해서 끊임없이 노력하고 발전하는 사람이 되도록 하겠습니다. 감사합니다.

2019년 1월

김 문 수